

Lateral Collapse Potential of Wood Pallets

by

Daniel L. Arritt

Thesis Submitted to the Faculty of the

Virginia Polytechnic and State University

in partial fulfillment of the requirements for the degree

of

MASTER OF SCIENCE

in

Forest Products

APPROVED:

T.E. McLain, Chairman

M.S. White

G. Ifju

September, 1985

Blacksburg, Virginia

Lateral Collapse Potential of Wood Pallets

by

Daniel L. Arritt

(Abstract)

Lateral collapse is a failure mode of wood pallets which most frequently occurs during transportation and handling. The study objective was to develop a simplified procedure for making relative comparisons in the lateral collapse potential of competing pallet designs.

A theoretical model was developed to predict the maximum horizontal force a pallet can sustain. A simple equilibrium of forces approach including joint rigidity was used. A lateral load test machine was built which induces and measures the amount of horizontal force required to collapse a pallet. After testing, the model was shown to be accurate when no upper deckboard bending occurred and inaccurate when bending occurred.

To account for bending, two multiple regression equations were developed to predict modification factors using a

matrix structural analysis program. A closed form solution predicts K-factors for two stringer designs. These K-factors are used to modify the resisting moments generated by the fastened joints. The modified model was shown to slightly overpredict maximum collapse load but did accurately discern differences in relative lateral collapse potential.

The ratio of the maximum horizontal load to the vertical load on the pallet provides a means of ranking the potential for lateral collapse. Those designs whose ratios fall between 0.0 and 0.6 are at high risk, from 0.6 but less than 1.0 are at medium risk, and from 1.0 to infinity are at low risk of lateral collapse. These ratios have been calibrated against documented cases of lateral collapse. The factors that influence the lateral collapse potential of a design are stringer aspect ratio, joint characteristics, unit load, and upper deck flexural rigidity.

ACKNOWLEDGEMENTS

The author wishes to extend his sincere appreciation to his committee members Drs. Thomas McLain, Marshall White, Geza Ifju, and Albert DeBonis for their leadership, advice and friendship throughout this study.

Special thanks are extended to the Cooperative Pallet Research Project funded by Va. Tech and the NWPCA for their financial support throughout this study.

Grateful acknowledgment is given to the author's employer, Timber Truss Housing Systems, Inc. of Salem, Virginia, for allowing him a leave of absence to complete this thesis.

Finally, a personal note of gratitude is extended to the author's wife, Kim, for her encouragement and sacrifices during the study, to the author's family for assisting with the basic educational opportunity and for moral support, and to Kelly Mulheren and Harold Vandivort for their invaluable assistance during this project.

TABLE OF CONTENTS

<u>TITLE</u>	<u>PAGE</u>
1. Introduction	1
2. Literature Review	4
2.1 Pallet Stability	6
2.2 Joint Characteristics	8
3. Theoretical Model Development	17
3.1 General	17
3.2 Type I Model	30
3.3 Type II Model	36
3.3.1 Three and Four Stringer Designs	38
3.3.2 Two Stringer Design	40
4. Experimental Verification	46
4.1 Introduction	46
4.2 Development of Lateral Load Test Machine	46
4.3 Model Verification: Type I	51
4.4 Model Verification: Type II	61
4.5 Experimental Verification of LCP	68
5. Design Procedures and Calibration	73
5.1 Introduction	73
5.2 Field Survey and LCP Categories	73

TABLE OF CONTENTS (continued)

<u>TITLE</u>	<u>PAGE</u>
5.3 Implementation into PDS-the Pallet Design System	75
5.4 Documented Lateral Collapse Failures	76
5.5 Variable Sensitivity	77
6. Conclusions	84
LITERATURE CITED	86
APPENDIX A	89
A1 - Machine Drawings	90
A2 - Machine Wiring	94
A3 - Machine Operation	96
A3.1 - Pre Test Calibration Procedures	97
A3.2 - Typical Test Procedures	98
APPENDIX B	100
B1 - Listing of LKAN Program	101
B2 - Analog Models	118
B3 - Pallet Designs for Computer	121
B3.1 - Three Stringer, Double-Faced Pallets Designed for K-Factor Development	122
B3.2 - Four Stringer, Double-Faced Pallets Designed for K-Factor Development	123

TABLE OF CONTENTS (continued)

<u>TITLE</u>	<u>PAGE</u>
B3.3 - Three Stringer, Single-Faced Pallets Designed for K-Factor Development	124
B3.4 - Four Stringer, Single-Faced Pallets Designed for K-Factor Development	125
APPENDIX C	126
C1 - Fastener Patterns	127
C2 - Construction Specifications and Unit Load for Type I Pallets	130
C3 - Construction Specifications for Joint Rotation Samples	132
C3.1 - Specification of Joint Rotation Samples Fastened with Nails	133
C3.2 - Specification of Joint Rotation Samples Fastened with Staples	134
C3.3 - Specification of Joint Rotation Samples for Rate of Loading Study	135
C4 - Upper Deckboard MOE by Pallet	136
C5 - Construction Specifications and Unit Load for Type II Pallets	140
C6 - Construction Specifications and Unit Load for Field Pallets	142
APPENDIX D	145
D1 - Result of Joint Rotation Tests	146
D1.1 - Test Results of Joint Rotation Samples for Nails	147

TABLE OF CONTENTS (continued)

<u>TITLE</u>	<u>PAGE</u>
D1.2 - Test Results of Joint Rotation Samples for Staples	148
D1.3 - Test Results of Joint Rotation Samples for Rate of Loading Study	149
D2 - Regression Equations for Individual Joints	150
D2.1 - K-factor Regression Equations and Corresponding R-Square Values for 3 Stringer, Single-faced Pallets	151
D2.2 - K-factor Regression Equations and Corresponding R-Square Values for 3 Stringer, Double-faced Pallets	152
D2.3 - K-factor Regression Equations and Corresponding R-Square Values for 4 Stringer, Single-faced Pallets	153
D2.4 - K-factor Regression Equations and Corresponding R-Square Values for 4 Stringer, Double-faced Pallets	154
VITA	155

List of Abbreviations

Ar	-	aspect ratio (w/d) (in./in.)
b	-	width of upper deckboards (in.)
c	-	diagonal distance of stringer cross section (in.)
CL	-	inside distance between the legs of the staple measured at the crown (in.)
C	-	compression perpendicular to the grain (lbs.)
d	-	height of stringer (in.)
E	-	modulus of elasticity (psi.)
E_t	-	combined E of upper deckboards (psi.)
FQI	-	fastener quality index
FWT	-	fastener withdrawal resistance (lbs.)
G	-	specific gravity
h	-	horizontal force applied to each stringer (lbs.)
H	-	horizontal force applied to pallet (lbs.)
H_{eq}	-	H required to maintain equilibrium of SPACEPAL analog models (lbs.)
H_{max}	-	maximum H a pallet can sustain before collapse (lbs.)
H_{tot}	-	H applied to SPACEPAL analog models (lbs.)
HD	-	head diameter of nail (in.)
HP	-	head pull-through resistance (lbs.)
HX	-	number of helix per inch of thread length
i	-	number of a stringer
I_t	-	combined moment of inertia of upper deckboards (in^4)

List of Abbreviations (continued)

- j - number of a deckboard
- K₁ - modification factor for top joint moments
- K₂ - modification factor for bottom joint moments
- K₃ - three stringer modification factor for joint moments
- K₄ - four stringer modification factor for joint moments
- ℓ - center to center distance between outer stringers (in.)
- ℓ' - deckboard overhang (in.)
- LCP - lateral collapse potential
- m₁ - resisting moments of individual top deckboard-stringer joints (in.-lb.)
- m₂ - resisting moments of individual bottom deckboard-stringer joints (in.-lb.)
- M - moment (in.-lb.)
- M₁ - sum of m₁ (in.-lb.)
- M₂ - sum of m₂ (in.-lb.)
- M₁^S - total m₁ from SPACEPAL analysis (in.-lb.)
- M₂^S - total m₂ from SPACEPAL analysis (in.-lb.)
- MC - moisture content (%)
- ND - total number of upper deckboards
- NS - total number of stringers
- P - penetration in holding member (in.)
- q - upper deckboard thickness (in.)

List of Abbreviations (continued)

- r1 - R of top deckboard-stringer joints (in.-lb./radian)
- r2 - R of bottom deckboard-stringer joints (in.-lb./radian)
- R - rotation modulus (in.-lb./radian)
- R1 - sum of r1 (in.-lb./radian)
- R2 - sum of r2 (in.-lb./radian)
- S - reaction to unit load by stringers (lbs.)
- T - thickness of fastened member (in.)
- TH - thread-crest diameter of a nail (in.)
- u - distributed unit load (lbs./in.)
- V - unit load (lbs.)
- w - width of stringer (in.)
- WD - wire diameter (in.)
- WW - diameter or width of crown (in.)
- X - horizontal displacement of stringer (in.)
- Y - vertical distance from assumed point of rotation to h_i (in.)
- Z - lever-arm distance of V (in.)
- α - angle between C and w (radians)
- α' - angle between C and horizontal plane at point A (radians)
- β_1 - opening of the upper deckboard-stringer joints for a Type II, two stringer pallet (radians)
- β_2 - opening of the lower deckboard-stringer joints for a Type II, two stringer pallet (radians)

List of Abbreviations (continued)

- ϕ - angular rotation (radians)
- ϕ_1 - ϕ of upper deckboard-joint (radians)
- ϕ_2 - ϕ of lower deckboard-joint (radians)
- λ_1 - angle between horizontal plane at point A and top deckboards due to end moments (radians)
- τ_1 - angle between horizontal plane at point A and top deckboards due to distributed load between supports (radians)
- ξ - total angular rotation between horizontal plane at point A and top deckboards due to unit load (radians)

List of Figures

<u>FIGURE</u>		<u>PAGE</u>
2.1	- An Illustration of Tests which Determine Joint Properties	10
2.2	- Typical Moment (in.-lb.)-Rotation (Radians) Curve from Joint Rotation Test	11
2.3	- Nail Nomenclature	14
2.4	- Staple Nomenclature	16
3.1	- The Effect Unit Load has on a Collapsing, Type I Pallet	19
3.2	- Load Distribution on a Two Stringer Pallet	23
3.3	- Load Distribution on a Three Stringer Pallet	24
3.4	- Load Distribution on a Four Stringer Pallet	25
3.5	- The Deckboard-Stringer Joint	28
3.6	- The Effect Unit Load has on a Collapsing, Type II Pallet	37
3.7	- The Effect Unit Load has on a Collapsing, Two Stringer, Type II Pallet	41
3.8	- An Illustration of how λ_1 and λ_2 are Calculated Utilizing the Principles of Superposition	43
4.1	- Photograph of Test Machine	48
4.2	- Plan and Profile Views of Test Machine	49
4.3	- Photograph of Collapse Test	53
4.4	- Horizontal Force (lbs.) vs. Horizontal Translation (in.) Curve from Collapse Test	54

List of Figures (continued)

<u>FIGURE</u>	<u>PAGE</u>
4.5 - The Change in Rank of $H_{2_{\max}}/V$ Versus the $H_{1_{\max}}/V$ Rank for 3 Stringer Pallets	66
4.6 - The Change in Rank of $H_{2_{\max}}/V$ Versus the $H_{1_{\max}}/V$ Rank for 4 Stringer Pallets	67
5.1 - The Effect Stringer Aspect Ratio has on H_{\max}/V	78
5.2 - The Effect Unit Load Ratio has on H_{\max}/V	80
5.3 - The Effect of Flexural Rigidity on H_{\max}/V	81
5.4 - The Effect Maximum Moment of the Joints has on H_{\max}/V	83
A1.1 - End Profile Views of Test Machine	91
A1.2 - Plan and Profile Views of Buttress-Load Head Connection	92
A1.3 - Details of LVDT Bracket	93
A2.1 - Electrical Wiring Diagram of Test Machine	95
B2.1 - Three Stringer Analog Model	119
B2.2 - Four Stringer Analog Model	120
C1.1 - Nail Patterns	128
C1.2 - Staple Patterns	129

List of Tables

<u>TABLE</u>	<u>PAGE</u>
4.1 - Actual H_{max} Versus Predicted H_{max} for Type I Tests	55
4.2 - Average M_{max} Values for Modification Factor Analysis	58
4.3 - Average R Values for Modification Factor Analysis	59
4.4 - Actual H_{max} Versus Predicted H_{max} after Reanalysis of Type I Tests	60
4.5 - Actual H_{max} Versus Predicted H_{max} for Type II Tests	71
B3.1 - Three Stringer, Double-Faced Pallets Designed for K-Factor Development	122
B3.2 - Four Stringer, Double-Faced Pallets Designed for K-Factor Development	123
B3.3 - Three Stringer, Single-Faced Pallets Designed for K-Factor Development	124
B3.4 - Four Stringer, Single-Faced Pallets Designed for K-Factor Development	125
C2 - Construction Specifications and Unit Load for Type I Pallets	131
C3.1 - Specification of Joint Rotation Samples Fastened with Nails	133
C3.2 - Specification of Joint Rotation Samples Fastened with Staples	134
C3.3 - Specification of Joint Rotation Samples for Rate of Loading Study	135
C4 - Upper Deckboard MOE by Pallet	137

List of Tables (continued)

<u>TABLE</u>	<u>PAGE</u>
C5 - Construction Specifications and Unit Load for Type II Pallets	141
C6 - Construction Specifications and Unit Load for Field Pallets	143
D1.1 - Test Results of Joint Rotation Samples for Nails	147
D1.2 - Test Results of Joint Rotation Samples for Staples	148
D1.3 - Test Results of Joint Rotation Samples for Rate of Loading Study	149
D2.1 - K-factor Regression Equations and Corresponding R-Square Values for 3 Stringer, Single-faced Pallets	151
D2.2 - K-factor Regression Equations and Corresponding R-Square Values for 3 Stringer, Double-faced Pallets	152
D2.3 - K-factor Regression Equations and Corresponding R-Square Values for 4 Stringer, Single-faced Pallets	153
D2.4 - K-factor Regression Equations and Corresponding R-Square Values for 4 Stringer, Double-faced Pallets	154

CHAPTER 1

INTRODUCTION

Pallets are an essential component of today's materials handling industry. They offer an economical, efficacious intermediary between unitized products and the lift-truck. More than 277 million wooden pallets were manufactured in the U.S. during 1980 (15) which shows the large demand for this product.

There are currently no standard design procedures for wooden pallets which would insure a minimum level of structural performance and serviceability. As a result most pallets are designed by trial and error, experience or not at all. Because of the very competitive nature of the industry the user, the manufacturer and the pallet industry as a whole suffer because there are no uniformly recognized guidelines for establishing a minimum pallet design for a specific application. In response to this void and a major concern with product liability, Virginia Polytechnic Institute and State University, the National Wooden Pallet and Container Association, and the U.S. Forest Service

entered into a cooperative Pallet Research Program (PRP). The objective of this program were to develop rational design procedures which will provide a means of assessing a pallet's durability and structural adequacy prior to manufacture.

One damaging failure mode of stringer pallets in service is lateral collapse. For the purpose of this study lateral collapse is defined as the overturning of all stringers in a pallet with a unit load as a result of in-plane vibration or load. This collapse may result from an impact load perpendicular to the wide face of the stringers or to the unit load itself. Collision between forklift tines and stringers commonly induces these lateral impact loads but other horizontal, in-plane forces may also contribute to this failure. Pallets may also experience collapse due to transverse vibration during transportation of palletized loads. Lateral collapse is known to occur during rail or truck shipment with inadequate dunnage.

There are relatively few well documented cases of lateral collapse available to researchers. However, within the industry it is a well known problem although one that many users do not necessarily report to manufacturers.

Unfortunately, analysis of the load or vibration required to cause collapse is a complicated dynamic problem made further complex by innumerable different pallet geometries, fasteners, unit load types and service conditions.

The materials handling industry will benefit if some relative measure of the potential of a pallet to collapse in "average" service could be made. Undoubtedly, this could be gained empirically, although the cost of doing so would be prohibitive. As a result, this study was initiated with the global objective of developing a method to estimate a relative measure of the Lateral Collapse Potential (LCP) of single- and double-faced, stringer pallets.

CHAPTER 2

LITERATURE REVIEW

Understanding structural collapse and its prevention is no simple task. A review of the literature is presented to help explain these topics.

During the early years of structural engineering, large building materials, such as stones and timbers were frequently used. By incorporating these large elements into their design, engineers were mostly concerned with instability, not strength (23,24).

These massive building materials were gradually replaced and were virtually eliminated early in the nineteenth century with the advent of metals. Long, slender elements could be fashioned from metal and used to build in new geometric proportions. With these designs, new buckling and stability problems arose. In the latter part of the nineteenth century Euler's equation became popular in buckling design. Since its refinement in the early twentieth century, Euler's equation has made the analysis of

buckling less a problem than overall structural stability (7). Today, economic pressures demand buildings to be constructed with less material and in more extreme proportions which may exaggerate stability problems.

The analysis of structural stability is pursued in many directions. Often the structure, the environment, and the behavior is simulated by models; however, this approach has limited practicality. Entirely theoretical analyses are useful, but rare. The most popular approach to structural analysis is semi-theoretical and empirical for example, "column curves". Quite often, all of these techniques are used in the final design (9).

Even with the most sophisticated analysis, uncertainty of the system and environment will influence design (23). It is a good engineering practice to apply a margin of safety to the analysis and the variables affecting stability. The level of safety should be in balance with other design principles: servicability, feasibility, repairability, and aesthetics (3).

In summary of the reviewed literature to this point, the stability of any structure is a function of its environment and its design (9,23,30). Included in the environmental

factors are equilibrium moisture content, snow loads, wind loads, and seismic forces. Some structural factors include material quality, fasteners, and foundations (8). Pallet behavior is governed by similar criteria.

2.1 Pallet Stability

Wallin et al. (28) suggests that the design of a pallet should consider both static and shock loads. Their investigations concluded that the two most important factors affecting impact strength are 1) the method of pallet assembly and 2) the type and quality of pallet shock. The Pallet Exchange Program (as cited by 12) recommends placing high quality shock on the periphery of a pallet to optimize its contribution to impact resistance.

The destructive vibrational forces inflicted on a structure by shock loads are resisted by damping forces (11). The damping forces come from internal friction and the friction between the structure and its support system (4). To avoid failure of pallets due to impact loads, nailed joints should not be too rigid (27). Dunmire (5) found that those pallets whose deckboards were dry and whose stringers were green during assembly were more durable against shock loads than those assembled from completely

green material. He hypothesized that as the structure dries, a large gap is formed between the deckboards and the stringers which causes greater absorption of impact energy.

In addition to horizontal impact forces, unit loads are applied to the pallet deck. A unit load is composed of materials and products that a pallet supports (19). These materials are frequently stacked individually, in boxes, or in bags. Unit loads are considered most often to be 1) uniformly distributed over the entire deck, 2) uniformly distributed over part of the deck, or 3) concentrated (6).

In summary, the loads most frequently applied to a pallet are lateral impact and unit loads. The environment of a pallet offers many types of loads that must be recognized during design to assure a semi-predictable behavior. The arrangement of materials and the quality of those materials play a significant role in structural stability.

For instance, pallet shock always exhibits variability. As a result, each pallet will behave differently in an environment. To maximize pallet durability, those stringers and deckboards that have few defects should be placed on the periphery of the structure (19,22). To assess the overall quality of the material, a grading procedure can be incorporated into the manufacturing process (19).

The typical wooden stringer manufactured in the U.S. has dimensions ranging from 1.00 x 3.00 to 2.00 x 4.00 inches (31). Gregory (7) describes the relationship between stability and geometry of rectangles and solids. He concluded that as an object's base, hinged at one corner, increases and/or its height decreases, the horizontal load applied to the top required to induce instability increases. In a pallet the stringers act similarly. For example a pallet with greater lateral strength is produced if 3 x 4 inch stringers are used instead of 2 x 4's. Similarly, a four stringer pallet will exhibit more lateral stiffness than a three stringer pallet made with the same size stringers (22).

2.2 Joint Characteristics

Pallet stringers and deckboards are most frequently connected by nails or staples. The rigidity of these connections is likely to be an important variable in pallet lateral behavior. Commonly used models to describe joint rigidity are translational stiffness, separation modulus, and rotation modulus. Translational stiffness measures the rigidity of a joint in lateral loading. Loferski (12) notes that the durability of a pallet under an impact load is

directly related to the lateral load carrying capacity. The separation modulus is "the ratio of the applied withdrawal force to the corresponding separation" (Figure 2.1). This modulus is helpful in predicting bending stiffness of a pallet (10). The third model of joint rigidity, rotation modulus, is defined by Kyokong (10) as "the ratio of the applied moment to the angular rotation", or as defined in the following equation:

$$R = M/\phi \quad (1)$$

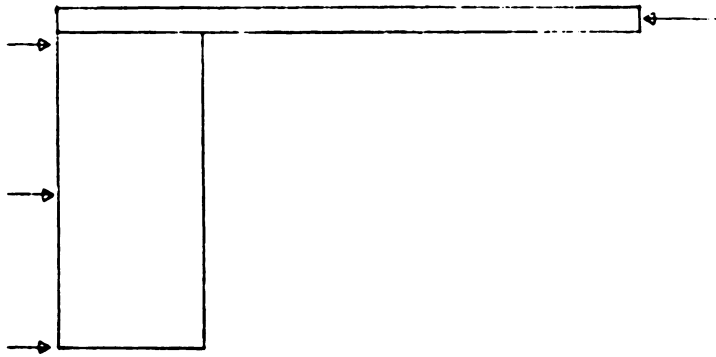
where:

R = rotation modulus (in.-lb./radian),

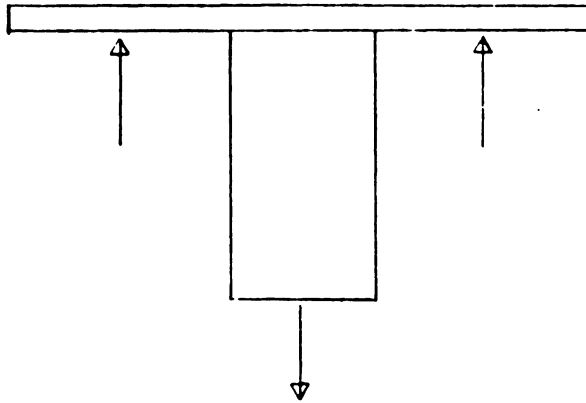
M = moment (in.-lb.), and

ϕ = angular rotation (radians).

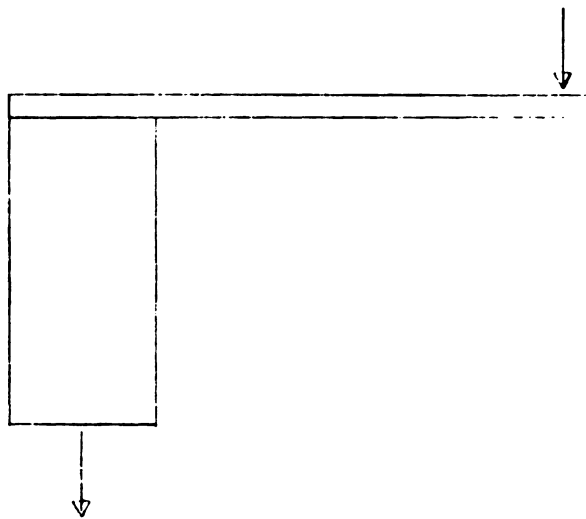
Figure 2.2 is a M- ϕ curve for a nailed joint. As illustrated, there are three distinct zones of interest along the curve. Zone 1 is the initial part of the curve where M is a linear function of ϕ . Conversely, Zone 2 is characterized by non-linear behavior of the joint. Zone 3 is joint failure. For the purpose of modeling the M- ϕ behavior the linear function which describes the secant to Zone 1 can be used until the line intersects with a horizontal line where $M = M_{\max}$.



Translational
Stiffness



Separation
Modulus



Rotation
Modulus

FIGURE 2.1 - An Illustration of Tests which Determine Joint Properties

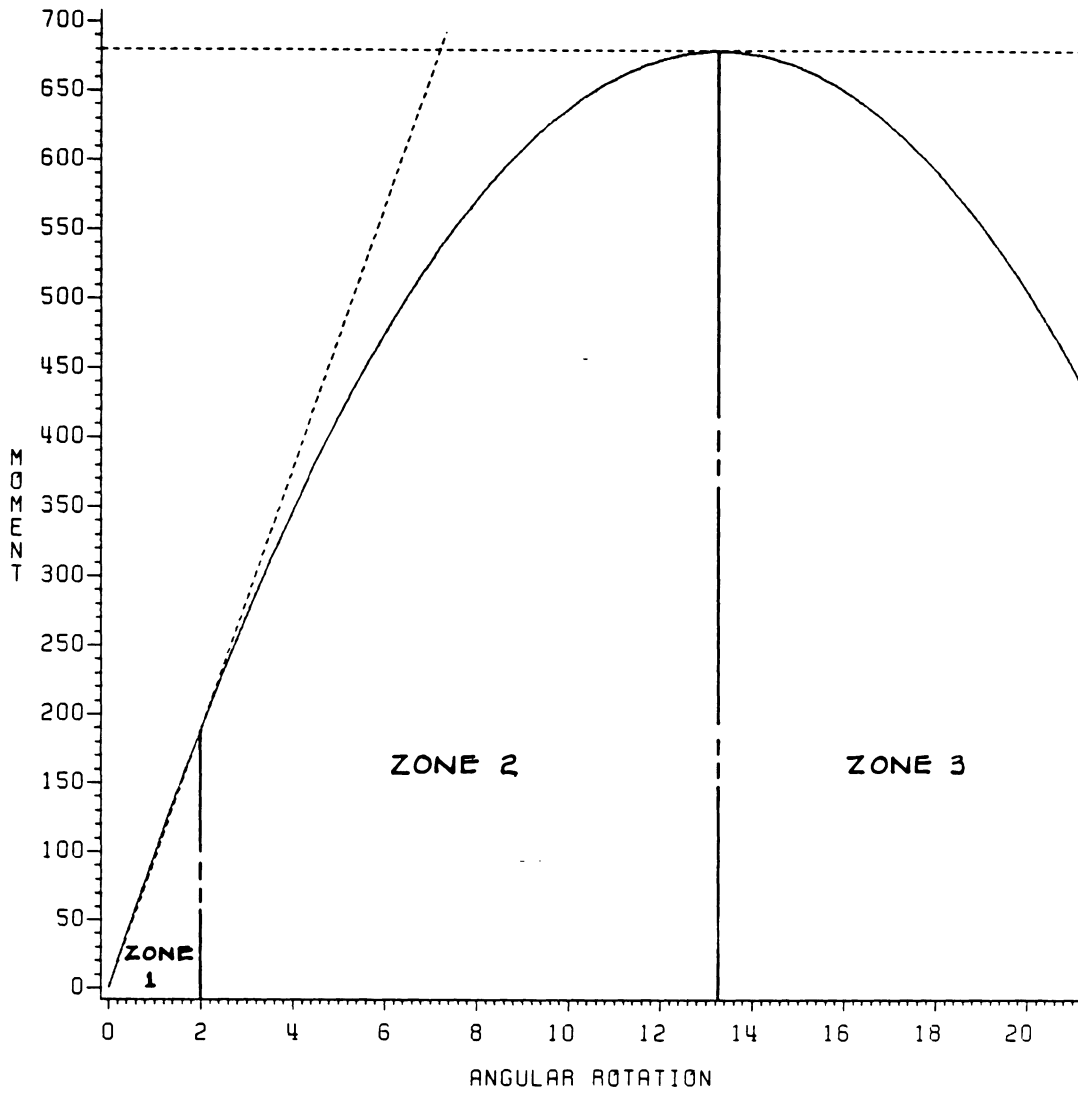


FIGURE 2.2 - TYPICAL MOMENT (IN.-LB.)-ROTATION
(RADIAN) CURVE FROM JOINT ROTATION TEST

Certainly there are numerous variables that affect the M- ϕ behavior of a joint. One such variable of a nailed joint is withdrawal resistance. Both the rotation modulus and the separation modulus are dependent on this characteristic. Withdrawal resistance is a function of several variables which include specific gravity, nail diameter, depth of penetration, type of nail shank, type of nail point, thread angle, surface coatings on the nail, wood seasoning effects, and moisture content (12,32).

Wallin and Whitenack (29) have developed an equation to estimate the withdrawal resistance of nails and staples.

First:

$$FWT = 222.2(FQI)(G^{2.25})(P)/(MC-3) \quad (2)$$

where:

FWT = Fastener Withdrawal Resistance (lbs.),

FQI = $221.24(WD) + 27.15(TD-WD)(Hx) + 1$,

WD = wire diameter (in.),

TH = thread-crest diameter (in.),

Hx = number of helix per inch of thread length,

G = specific gravity of the holding member,

P = penetration in holding member (in.), and

MC = moisture content at assembly of the holding member (%).

Equation 2 was developed to be used for either helically threaded or plain shank nails. Figure 2.3 illustrates the characteristics of a nail.

Another characteristic of nailed joints which may affect the limits of rotation and separation moduli, is the fastener-head pull-through resistance. Those factors that effect this resistance are moisture content, specific gravity, and the thickness of the fastened member. Furthermore, the head-bearing area significantly influences this resistance.

For nails, head pull-through resistance is computed using the following equation from Wallin and Whitenack (29):

$$HP = 1,250,000(HD - WD)(T)(G^{2.25})/(MC-3) \quad (3)$$

where:

HP = Head Pull-Through resistance (lbs.),

HD = head diameter (in.),

T = thickness of fastened member (in.),

G = specific gravity of fastened member, and

MC = moisture content of fastened member at assembly (%).

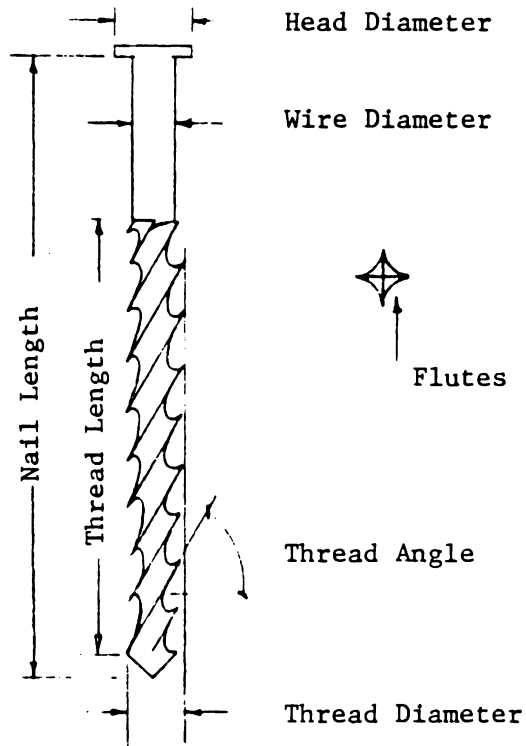


FIGURE 2.3 - Nail Nomenclature

For staples, HP is computed as:

$$HP = 1,591,550(CL)(WW)(T)(G^{2.25})/(MC-3) \quad (4)$$

where:

CL = inside distance between the legs of the staple measured at the crown (in.) and

WW = diameter or width of the crown (in.).

Figure 2.4 illustrates the characteristics of a staple.

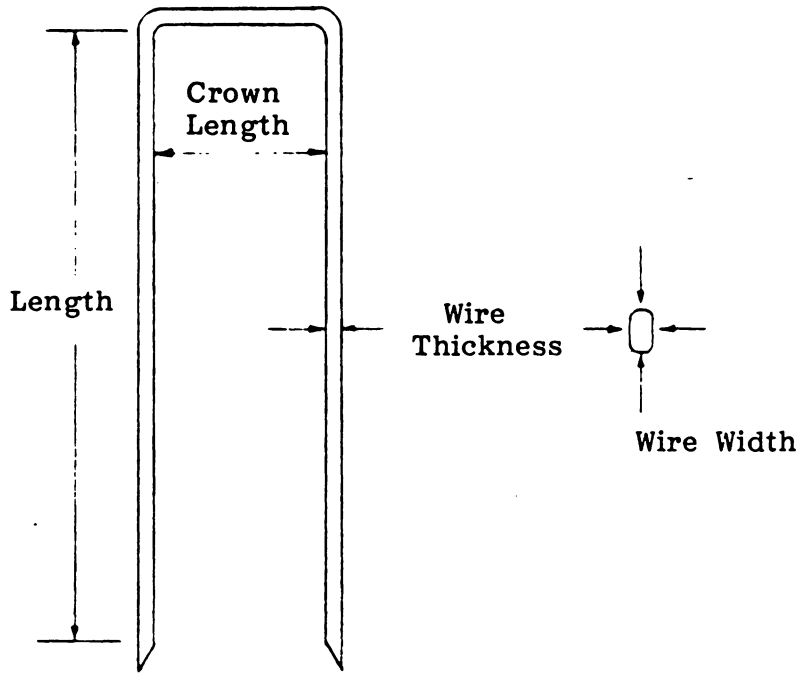


FIGURE 2.4 - Staple Nomenclature

CHAPTER 3

THEORETICAL MODEL DEVELOPMENT

3.1 General

The lateral collapse of a wood pallet is essentially a complex dynamic problem subject to many variables. Solution of this problem will require a great deal of effort and many limiting assumptions concerning the nature of the dynamic horizontal forces and/or displacements. Because of these limitations and a perceived high cost-to-benefit ratio of the necessary research for the pallet industry it seems reasonable to explore some very simplified approaches. It is understood that in taking this path any end result may lack general applicability. Nevertheless, a reasonable first step must be taken.

The underlying premise of this research is to make comparisons of stability between pallet designs and some "yardstick" or acceptance criteria. The mechanism for making this relative comparison should be sensitive to the

same variables that influence the dynamic forces causing instability. By making relative comparisons the potential problems with lateral collapse for a certain pallet design can be assessed. This technique can not identify whether a pallet will collapse under any given situation.

One simplified approach for a relative comparison is to consider a horizontal force (H) applied to a pallet in the plane of the top deckboards. This pallet may have stringers (rectangular solid elements) of varying widths but not varying height. A unit load exerts some uniformly distributed force over the top deckboard. A bottom deck may or may not be present. If H is great enough, then the top deck will translate causing the stringer to rotate as in Figure 3.1. After some critical amount of rotation, the pallet will collapse.

Two approaches to this stability problem come to mind immediately. The first is a prediction of the energy required to cause the pallet stringers to rotate 90 degrees to the fully collapsed position. The second approach is to predict a maximum horizontal force (H_{\max}) that will cause the stringer to rotate to a position of unstable equilibrium. That is, to a point where the unit load by itself will complete stringer collapse.

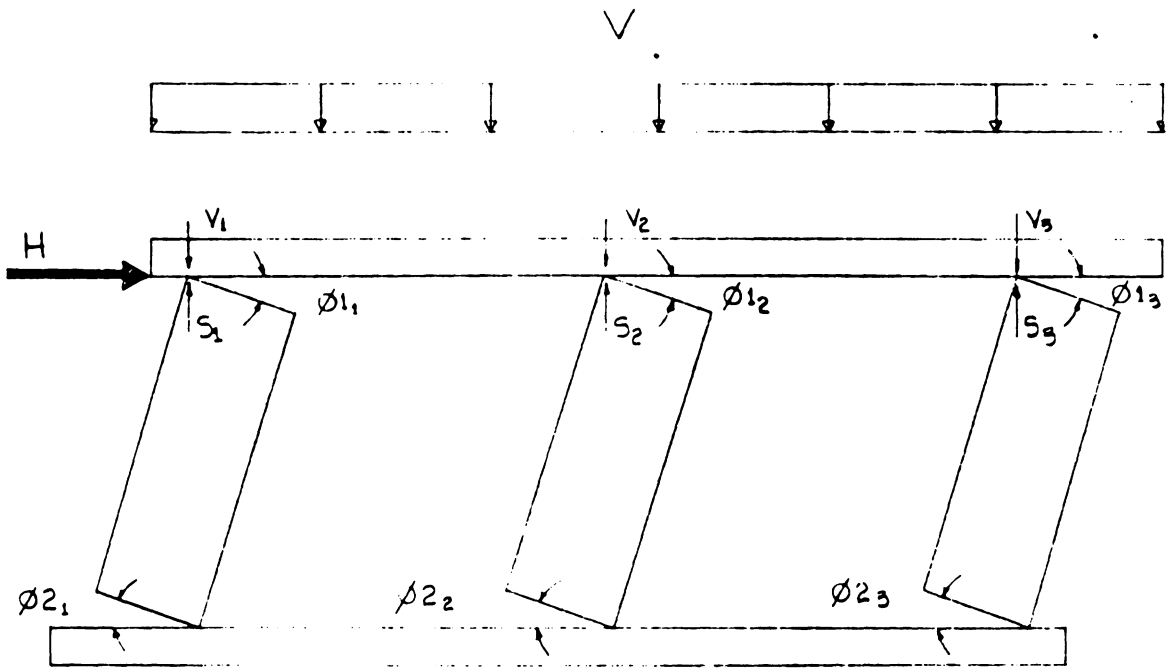


FIGURE 3.1 - The Effect Unit Load has on a Collapsing, Type I Pallet

Both approaches require simplifying assumptions concerning the geometry of failure, joint properties past the "elastic" range and the horizontal force which is a function of displacement. A clear selection of one approach over the other is not obvious to the author. However, a mitigating factor is that the procedure must be simple and must make sense when explained and used by users and manufacturers in the pallet industry. Since this group is relatively inexperienced in engineering science and the process of design, the procedure must be simple to be "solid". If the procedure is not accepted by this group, then all will have been for naught. For this reason the maximum horizontal force approach was selected as the most likely candidate.

The ratio of H_{\max} to the vertical unit load (V) a pallet can sustain provides a convenient, unitless means of comparing the lateral behavior of pallets. The boundaries of H_{\max}/V are zero and infinity. A pallet with a H_{\max}/V ratio equal to zero, requires very little horizontal load to cause collapse. Conversely, the pallet which has a H_{\max}/V ratio of infinity simply will not collapse.

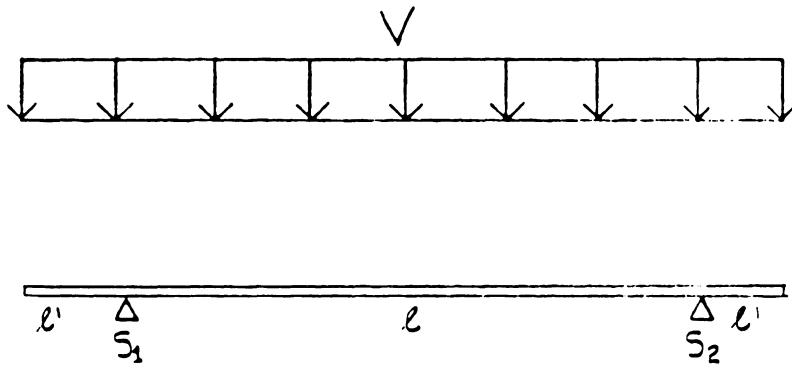
This ratio, H_{\max}/V , incorporates the unit load because comparison without this value is meaningless. To illustrate

this, compare two pallet designs using H_{\max} alone as the governing criteria. If design #1 has an H_{\max} of 8,000 lbs. and design #2 has an H_{\max} of 6,000 lbs., one is likely to conclude that design #1 has greater resistance to lateral collapse. On the other hand, if design #1 is known to support 5,000 lbs. and design #2 supports 1,000 lbs., the H_{\max}/V ratios for design #1 and #2 are 1.6 and 6, respectively. Utilizing the boundary conditions stated in the previous paragraph one concludes that design #2 is the least likely of the two designs to experience lateral collapse. This ratio can only be used as a relative, not an absolute comparison. It may well be that under some conditions both designs may collapse. To help explain the design approach, the following paragraphs describe the assumptions involved in the collapse model derivation.

First, the horizontal load applied to the pallet during collapse is considered to be applied at the lower edge of the top deckboards and perpendicular to the length of the stringers (Figure 3.1). This assumption was made so that the model would recognize various deckboard thicknesses and stringer heights. It is also assumed that the unit load does not slip on the top deckboard but maintains its relative placement.

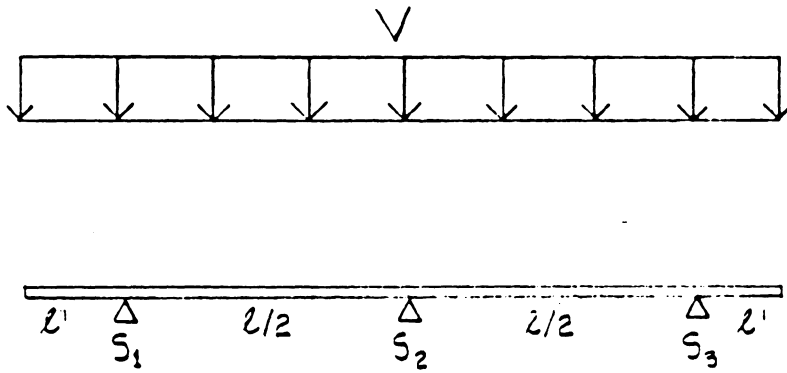
Another assumption made was that the unit load on the pallet is transmitted to the stringers in certain percentages. The load on each stringer is designated as V_i where $i=1$ to the number of stringers. The V_i s in the model are considered to act in a vertical direction on the corners of each deckboard-stringer joint. Thus, reactions S_i where $i = 1$ to the number of stringers are created at the stringers to support V . For example Figure 3.2 shows S_1 and S_2 of a two stringer pallet equals 50% of V . For the three and four stringer pallets (Figures 3.3 and 3.4) equations are given which are used to compute the reactions. For example, if a 3 stringer pallet that had 48" deckboards, where $l' = 4"$ and $l = 40"$, and $V=1000$ lbs., then $S_1=S_3=292$ lbs. and $S_2=708$ lbs.

The slight rounding of the stringer's edges that occurs during collapse because of the compression perpendicular to grain (C_{\perp}) of wood is not recognized in the model. This assumption was made because the extreme variability of C_{\perp} among species would have made it extremely difficult to account for in the model. Furthermore, the rounding effect results in only a small change in the location of V_i that the overall effect on H_{\max} is negligible.



$$S_1 = S_2 = \frac{V}{2}$$

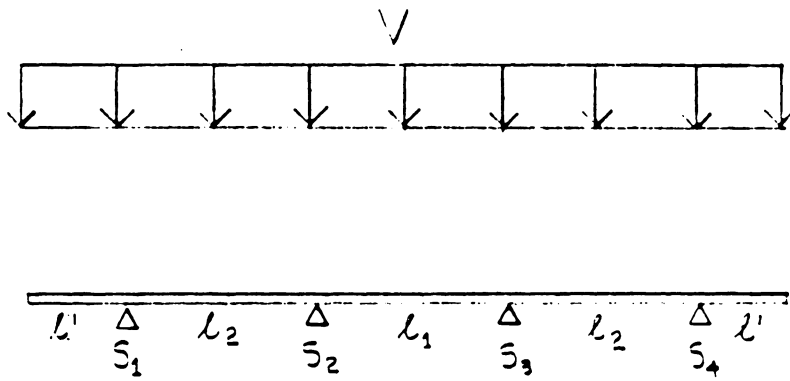
FIGURE 3.2 - Load Distribution on a Two Stringer Pallet



$$S_1 = S_3 = (V) \left(\frac{l' + l/4}{2l' + l} \right)$$

$$S_2 = (V) \left(\frac{l/2}{2l' + l} \right)$$

FIGURE 3.3 - Load Distribution on a Three Stringer Pallet



$$S_1 = S_4 = (V) \left(\frac{l' + l_2/2}{2l' + 2l_2 + l_1} \right)$$

$$S_2 = S_3 = (V) \left(\frac{l_1/2 + l_2/2}{2l' + 2l_2 + l_1} \right)$$

FIGURE 3.4 - Load Distribution on a Four Stringer Pallet

The assumptions presented have dealt with the external forces that may act on a pallet. An internal characteristic considered is the nailed or stapled deckboard-stringer joints which causes resisting moments to collapse as a horizontal force is applied. These moments are denoted by m_{ij} where $i=1$ to the number of stringers (NS) and $j=1$ to the number of deckboards (ND) along each stringer. The value of each moment is a function of all the material and geometric parameters as well as the amount of rotation the joints experience. For example, if there are six upper deckboards on a pallet, then m_{i1}, \dots, m_{i6} resisting moments occur along each stringer. Summation of these moments yields the total resisting moments for each stringer. The total moment for the top joints are denoted by $M1_i = \sum_{j=1}^{ND} m1_{ij}$. And the total bottom moment is $M2_i = \sum_{j=1}^{ND} m2_{ij}$.

Additionally, define a weighted average of the upper deckboards' moduli of elasticity as:

$$E_t = \frac{1}{\sum_{j=1}^{ND} b_j} \left(\sum_{j=1}^{ND} (b_j)(E_j) \right) \quad (5)$$

where:

E_t = combined modulus of elasticity of upper deckboards (psi),

b_j = width of the j^{th} upper deckboard (in.),

E_j = modulus of elasticity of j^{th} upper deckboard (psi), and

ND = number of upper deckboards.

Similarly, the moment of inertia of the upper deckboards is calculated as:

$$I_t = (q^3 \sum_{j=1}^{ND} b_j^3) / 12 \quad (6)$$

where:

I_t = combined moment of inertia of upper deckboards (in.^4) and

q = upper deckboard thickness (in.).

A typical pallet deckboard-stringer joint is modeled as shown in Figure 3.5 where:

X_i = horizontal displacement of point A on stringer i (in.) from initial rest position,

Y_i = vertical distance from assumed point of rotation (o) to h_i on stringer i (in.),

V_i = vertical load assumed to be transmitted to stringer i (lbs.) at point A,

h_i = horizontal disturbing force on stringer i (lbs.),

d_i = height of stringer i (in.),

w_i = width of stringer i (in.),

ϕ_{1_i} = angular opening of upper deckboard-stringer i joint (radians),

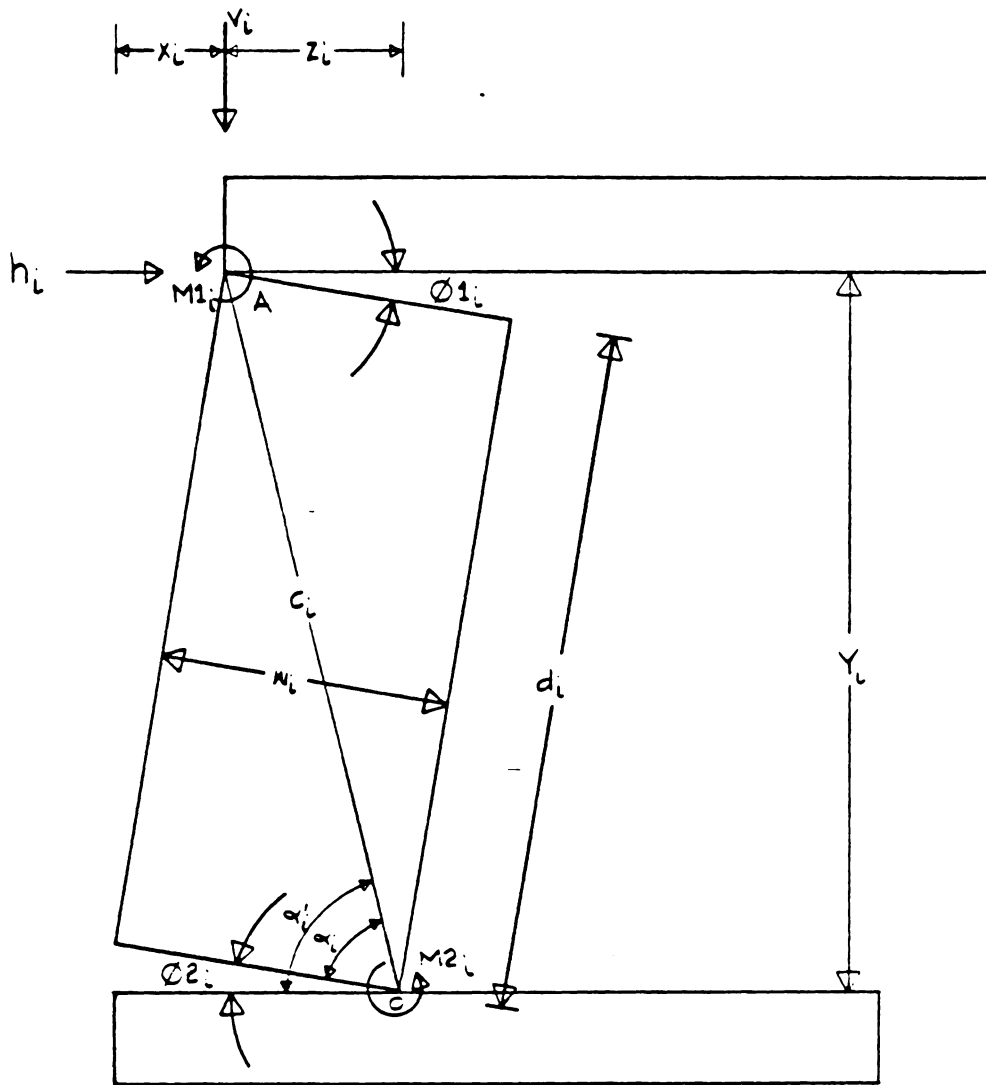


FIGURE 3.5 - The Deckboard-Stringer Joint

ϕ_{2_i} = angular opening of lower deckboard-stringer i joint (radians),

$M1_i$ = sum of the resisting moments from the joints along the top of stringer i (in.-lb./radian), and

$M2_i$ = sum of the resisting moments from the joints along the top of stringer i (in.-lb./radian).

Finally, a very important criterion is the inter-relationship between $E_t I_t / l^3$ (l =distance between stringers) of the upper deckboards and the unit load on the pallet. Each plays a significant role in the amount of bending of the upper deckboards. For this study two pallet responses are recognized: Type I where negligible bending occurs in the top deck and Type II where the upper deckboards significantly bend under load. The reason bending plays a role in lateral collapse is that it influences joint behavior during collapse. When no bending occurs in the upper-deckboards each joint has the same amount of rotation for a given top deck translation. Therefore, by using the $M-\phi$ curve all joint m_{ij} 's can be determined and solving for H_{\max} is a linear problem.

On the otherhand, deckboard bending during collapse causes the joints to open by unequal amounts. As a result, the moment generated in each joint is different making the determination of H_{\max} a complex non-linear problem.

3.2 Type I Model

Type I pallets experience no bending in the upper deckboards; therefore, the angular rotation, ϕ_{1_i} and ϕ_{2_i} , are equal. This is true for two, three, and four stringer pallets. It is the purpose of this section to present the theory used to develop the model which predicts H_{\max} for the Type I pallet.

The model is based on stability concepts described by Gregory (7). Consider the diagram of an individual stringer as illustrated in Figure 3.5, after some significant rotation has occurred. Summing moments about point o yields:

$$\Sigma M_o = 0 = h_i(Y_i) - V_i(w_i - X_i) - M1_i - M2_i \quad (7)$$

Rearranging equation (7) gives:

$$h_i = (V_i(w_i - X_i) + M1_i + M2_i) / Y_i \quad (8)$$

Before using equation (8) to calculate H_{\max} an explanation of each variable is in order. .

In Figure 3.5, V_i is located on the uppermost corner of the stringer and has a leverarm distance (Z_i) with respect to point o:

$$Z_i = w_i - X_i \quad (9)$$

As the force h_i is applied to the structure its lever-arm distance, Y_i , increases (Figure 3.5). This is true until $Y_i = C_i$ where:

$$C_i = \sqrt{d_i^2 + w_i^2} \quad (10)$$

where:

C_i = diagonal distance of stringer i cross-section (in.).

Since Z_i and C_i are known, the lever-arm distance of h_i is:

$$Y_i = \sqrt{C_i^2 - Z_i^2} \quad (11)$$

where:

Y_i = lever-arm distance of h_i (in.).

At this point all external rotational moments acting on a pallet can be evaluated by multiplying force times lever-arm distance. A method to calculate the internal resistance to collapse was required to complete the model.

During collapse the resisting moments $M1_i$ and $M2_i$ are generated by the fasteners used to hold the joints together. As explained in Chapter 2 the resisting moment of a joint can be described by the $M-\phi$ curve (Figure 2.2). For simplification, the joint rotation is assumed to be perfectly elasto-plastic with the secant to Zone 1 as the linear initial portion of the curve. To calculate $M1_i$ and $M2_i$, ϕ must be computed in the following manner:

$$\alpha_i = \tan^{-1} (d_i/w_i) \quad (12)$$

where:

$$\alpha_i = \text{angle between } C_i \text{ and } w_i \text{ (radians).}$$

And:

$$\alpha_i' = \sin^{-1} (Y_i/C_i) \quad (13)$$

where:

$$\alpha_i' = \text{angle between } C_i \text{ and the horizontal plane at point A (radians).}$$

The angle through which the bottom joints rotate is then:

$$\phi_{2_i} = \alpha_i' - \alpha_i \quad (14)$$

where:

ϕ_{2_i} = angular opening of lower deckboard- i^{th} stringer joint (radians).

Because of the definition of the Type I response it is known that $\phi_{1_i} = \phi_{2_i}$. Thus:

$$M_{1_i} = (\phi_{1_i})(R_{1_i}) \quad (15)$$

where:

M_{1_i} = sum of the resisting moments from the joints along the top of stringer i (in.-lb.),

R_{1_i} = sum of rotational moduli of top deckboard- i^{th} joints (in.-lb./radian).

Similarly:

$$M_{2_i} = (\phi_{2_i})(R_{2_i}) \quad (16)$$

where:

M_{2_i} = sum of the resisting moments from the joints along the bottom of the stringer i (in.-lb.) and

R_{2_i} = sum of rotational moduli of bottom deckboard- i^{th} stringer joints (in.-lb./radian).

Equations (15) and (16) are misleading by implying that as long as ϕ increases, so does M . The results of actual joint tests show that M does increase up to a maximum M_{\max} . $M1_{i,\max}$ and $M2_{i,\max}$ are computed with:

$$M1_{i,\max} = \sum_{j=1}^{ND} m1_{ij,\max} \quad (17)$$

$$M2_{i,\max} = \sum_{j=1}^{ND} m2_{ij,\max} \quad (18)$$

where:

$M1_{i,\max}$; $M2_{i,\max}$ = sum of maximum moments of joints along top or bottom of stringer i (in.-lb.) and

$m1_{ij,\max}$; $m2_{ij,\max}$ = maximum moments of individual joints along top or bottom of stringer i (in.-lb.).

The $R1_i$ and $R2_i$ used in equation (15) and (16) are the sums of the rotational moduli along each stringer where:

$$R1_i = \sum_{j=1}^{ND} rml_{ij} \quad R2_i = \sum_{j=1}^{ND} rm2_{ij} \quad (19;20)$$

where:

$R1_i$; $R2_i$ = sum of rotational moduli of the joints along the top or bottom of stringer i (in.-lb./radian) and

rml_{ij} ; $rm2_{ij}$ = rotational moduli of individual deckboard-stringer joint along top or bottom of stringer (in.-lb./radian).

Knowing the joint moments as a function of rotation (or horizontal displacement, X) it is possible to solve equation (8) for h_i . However, the computed h_i is only the amount of force necessary to cause an amount of displacement in stringer i . The total horizontal force necessary to cause the total amount of displacement is found using:

$$H = \sum_{i=1}^{NS} h_i \quad (21)$$

The H_{\max} a pallet can sustain is determined by incrementing X until H is maximized. Generally, H_{\max} occurs before X = 2 inches in actual tests of typical pallets. To help minimize the error in estimating H_{\max} the size of the increments of X should not exceed 0.1 inch.

In summary, the solution to finding the H_{\max} for a Type I pallet is as follows:

1. determine the load distributed to each stringer (V_i),
2. determine the constants which describe each joint type (R_{ij} and $M_{ij,\max}$),
3. introduce a small horizontal displacement (X),
4. determine $M1_i$ and $M2_i$ for each stringer by summing the proper m_{ij} 's,
5. compute h_i for each stringer using equation (8),
6. sum the h_i 's (equation 21) to give the total H at that increment, and

7. repeat steps three through six until H is maximized (H_{\max}).

3.3 Type II Model

Type II pallets experience upper deckboard deflection during collapse, and therefore, $\phi_{1_i} \neq \phi_{2_i}$. Figure 3.6 shows that bending of the top deckboard cause the stringers to experience different amounts of horizontal translations due to geometric non-linearity. Since each stringer may translate differently, $\phi_{1_i} \neq \phi_{2_i}$.

As a result of this non-linearity, the moments generated in the joints during collapse are not equal as they are in the Type I pallet; therefore, the moments in equation (8) must be modified. Another possibility is that the deckboards will behave as combined bending and axial force members and may buckle. For pallets with very low top deck flexural stiffness, $E_t I_t$, this mechanism may predominate over a reduced joint moment contribution. However the end fixity conditions are typically more rigid than pins and are not easily determined. Since a beam column analysis approach would add greatly to the complexity of the solution

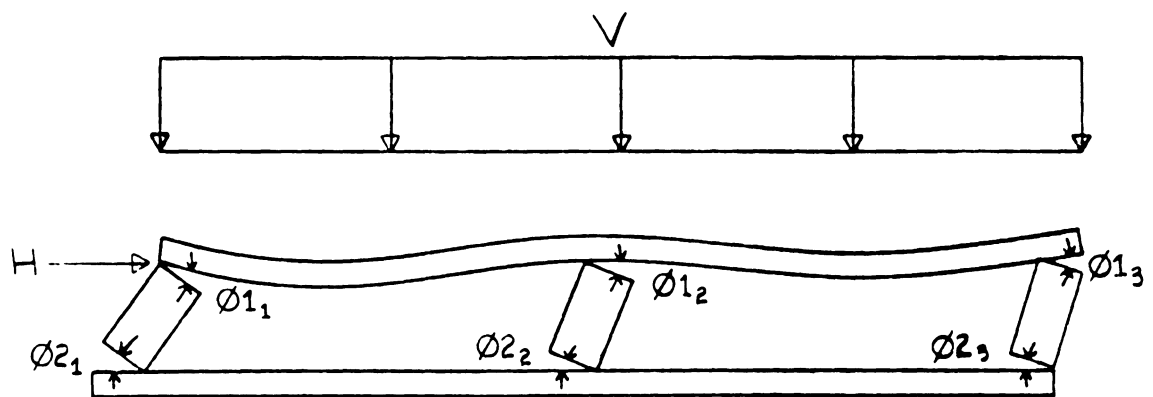


FIGURE 3.6 - The Effect Unit Load has on a Collapsing, Type II Pallet

with no readily identifiable significant benefit, it was not pursued. The experimental results of a wide variety of pallets and sections failed to demonstrate a significant combined bending - axial force influence on collapse. However, this does not mean that this mode could not be prevail in some circumstances.

3.3.1 Three and Four Stringer Designs

The purpose of this section is to describe how the modification factors for the joint moments in three and four stringer pallets were developed for the Type II model. Physically testing the influence of unit loads, stringer dimensions, deckboard properties, and nail properties on lateral collapse in this mode would be immensely time consuming and expensive. This testing was reduced by utilizing a computer program, SPACEPAL (17), which is capable of analyzing structures using the stiffness method of matrix structural analyses. SPACEPAL was used to model a wide variety of pallet designs subjected to various horizontal and unit loads. The resulting theoretical top and bottom moments along each stringer ($M1^S_i$ and $M2^S_i$) were evaluated. These analyses are described in Chapter 4.

If $M1_i^S$ and $M2_i^S$ from SPACEPAL tests which accounts for Type II behavior and $M1_i$ and $M2_i$ from the Type I model are known, then a modification factor can be computed for each joint of all test pallets using:

$$K1_i = \frac{M1_i^S}{M1_i} \quad ; \quad K2_i = \frac{M2_i^S}{M2_i} \quad (22;23)$$

where:

$K1_i$; $K2_i$ = modification factors for top
and bottom joint moments,

$M1_i^S$; $M2_i^S$ = upper and lower deckboard-stringer
moments resulting from SPACEPAL
analysis on pallets (in.-lb./radian)
and

$M1_i$; $M2_i$ = moments from equations
(15) and (16).

$K1_i$ and $K2_i$ values were computed for a wide variety of different types of pallets. Multiple regression relationships were then developed to estimate $K1_i$ and $K2_i$ utilizing unit loads, stringer dimensions, deckboard dimensions, deckboard MOE's, and fastener properties as the variables. These estimated K-factors are multiplied by the moments determined in a Type I analysis ($M1_i$ or $M2_i$) and the product is an estimate of the moments in a Type II pallet. One constraint imposed on the K-factors was that they fall

in a range $0 < K\text{-factor} < 1$. This assumes that the moment is not less than zero or greater than M_{\max} . Therefore, if $K > 1$, then $K=1$ or if $K < 0$, then $K=0$.

Equation (8) for h_i now becomes:

$$h_i = \frac{V_i (w_i - X_i) + K1_i (M1_i) + K2_i (M2_i)}{Y_i} \quad (24)$$

3.3.2 Two Stringer Design

The relative simplicity of the two stringer pallet allowed the development of a closed form solution to compute $K1_i$ and $K2_i$. Utilizing the principle of superposition the actual structure (Figure 3.7) was modeled as both a simply supported beam with a uniform load and a simply supported beam with end moments.

In Figure 3.7, $\tau1_1$ and $\tau1_2$ are computed with:

$$\tau1_1 = \frac{(-u)(l)}{24(E_t)(I_t)} ; \tau1_2 = \frac{(u)(l)}{24(E_t)(I_t)} \quad (25;26)$$

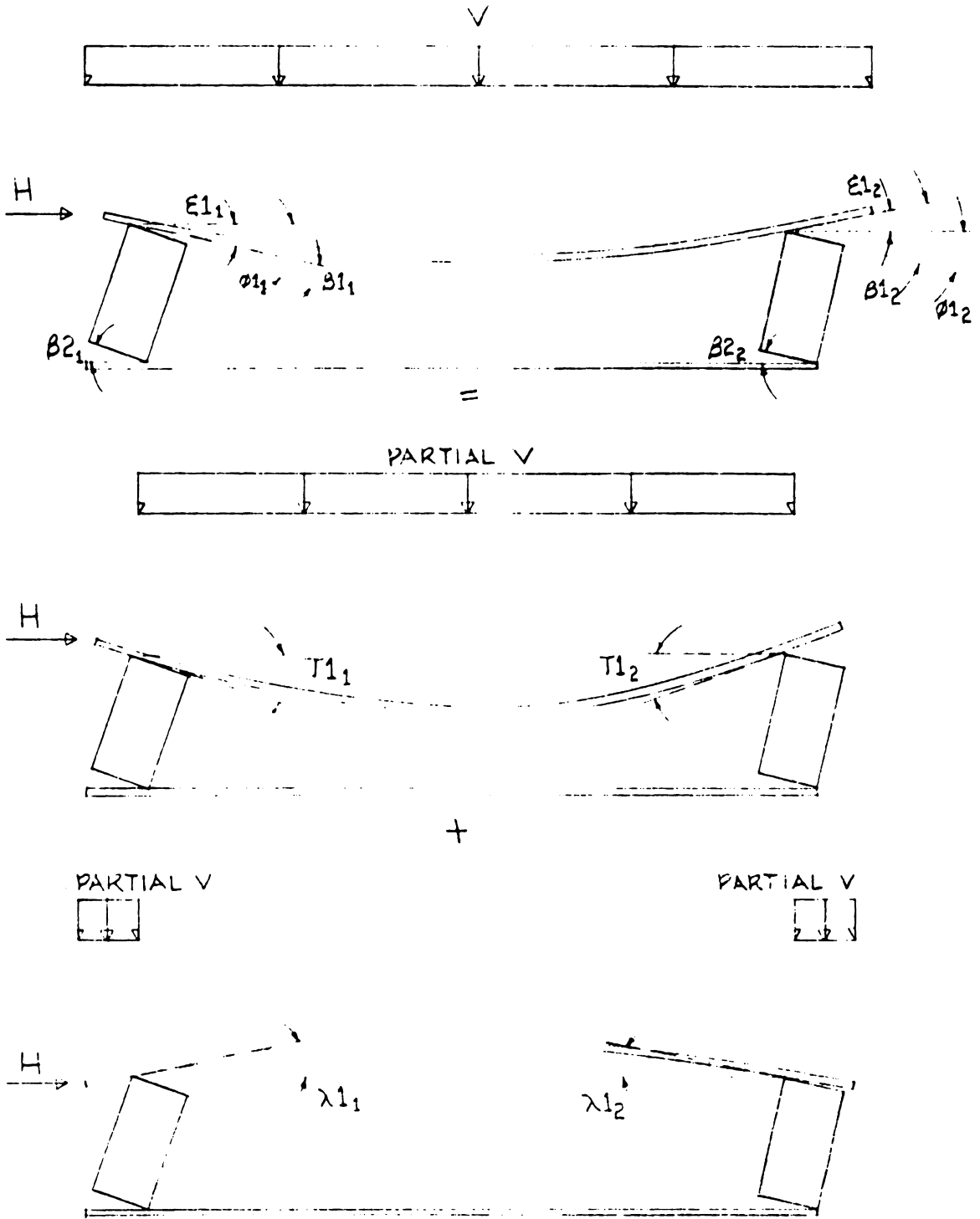


FIGURE 3.7 - The Effect Unit Load has on a Collapsing, Two-Stringer, Type II Pallet

where:

τl_1 ; τl_2 = angle between horizontal plane and upper deckboard at the i^{th} support point due to distributed load between supports (clockwise negative) (radians) and

u = distributed load (lb./in.).

Looking at Figure 3.7 it is apparent that τl_1 and τl_2 are equal in magnitude but opposite in direction for the assumed symmetrical loads.

The end moments produced by the uniform load (Figure 3.7) on the overhang of the deck are calculated as:

$$M_o = (-u)(l'^2)/2 \quad (27)$$

where:

M_o = moment at support point (in.-lb.).

Furthermore, Figure 3.8 shows the necessary equations used to calculate the angles, λl_1 and λl_2 due to the applied end moments:

$$\lambda l_1 = \frac{(u)(l'^2)(1)}{4(E_t)(I_t)} \quad (28)$$

$$\lambda l_2 = \frac{(-u)(l'^2)(1)}{4(E_t)(I_t)} \quad (29)$$

$$\lambda_1 = \frac{(-M_o)(l)}{(3)(E_t)(I_t)} \quad \begin{array}{c} M_o \\ \curvearrowright \\ \Delta \end{array} \quad \begin{array}{c} \lambda_1 \\ \downarrow \end{array} \quad \begin{array}{c} \lambda_2 \\ \downarrow \end{array} \quad \begin{array}{c} \lambda_2 = \frac{(M_o)(l)}{(6)(E_t)(I_t)} \\ \downarrow \end{array} \quad \Delta$$

+

$$\lambda_1 = \frac{(-M_o)(l)}{(6)(E_t)(I_t)} \quad \begin{array}{c} \lambda_1 \\ \downarrow \end{array} \quad \begin{array}{c} \lambda_2 \\ \downarrow \end{array} \quad \begin{array}{c} M_c \\ \curvearrowright \\ \Delta \end{array} \quad \lambda_2 = \frac{(M_o)(l)}{(3)(E_t)(I_t)}$$

=

$$\lambda_1 = \frac{(-M_o)(l)}{(2)(E_t)(I_t)} \quad \begin{array}{c} M_o \\ \curvearrowright \\ \Delta \end{array} \quad \begin{array}{c} \lambda_1 \\ \downarrow \end{array} \quad \begin{array}{c} \lambda_2 \\ \downarrow \end{array} \quad \begin{array}{c} M_o \\ \curvearrowright \\ \Delta \end{array} \quad \lambda_2 = \frac{(M_o)(l)}{(2)(E_t)(I_t)}$$

FIGURE 3.8 - An Illustration of how λ_1 and λ_2 are Calculated Utilizing the Principles of Superposition

where:

$\lambda 1_1 ; \lambda 1_2$ = angle between horizontal plane
and top deckboard due to end moment
(radians).

Since $\tau 1_i$ and $\lambda 1_i$ can be computed, then the total angular rotation due to loading (Figure 3.7) can be computed from:

$$\xi 1_i = \tau 1_i + \lambda 1_i \quad (30)$$

In the Type I model $\phi 1_1$ and $\phi 1_2$ are assumed equal. With this in mind:

$$\beta 1_1 = \phi 1_1 - \xi 1_1 = \phi 1_1 - \frac{(u)(l) \left(\left(\frac{l^2}{6} \right) - l' \right)}{4(E_t)(I_t)} \quad (31)$$

$$\beta 1_2 = \phi 1_2 - \xi 1_2 = \phi 1_2 + \frac{(u)(l) \left(\left(\frac{l^2}{6} \right) - l' \right)}{4(E)(I)} \quad (32)$$

where:

$\beta 1_i$ = total opening of the upper deckboard- i^{th}
stringer joint (Figure 11) for a Type II, 2.
stringer pallet (radians).

Equations (30) and (31) or (32) supply enough information to compute:

$$\beta 2_i = \xi 1_i + \beta 1_i \quad (33)$$

where:

β_{2_i} = total opening of the lower deckboard-
 i^{th} stringer joint for a Type II, 2 stringer
 pallet.

Since all angles of the 2 stringer collapse specimen (Figure 3.7) can be computed, a K-factor can be calculated from:

$$K1_i = \frac{\beta_{1_i}}{\phi_{1_i}} \quad ; \quad K2_i = \frac{\beta_{2_i}}{\phi_{2_i}} \quad (34;35)$$

where the K-factor is again based on the angular rotation of a Type I pallet. These K-factors are used in equation (24) to compute h_i .

CHAPTER 4

Experimental Verification

4.1 Introduction

Experimental verification of the ability of the model to predict H_{\max} was necessary to justify its use in design. Without strong support from experimental data the model will not be an accepted tool. This Chapter describes each step taken to verify the model.

4.2 Development of a Lateral Load Test Machine

To physically measure the H_{\max} of a full-size pallet a test machine was designed and constructed. The machine was capable of testing pallet sections with dimensions as small as 8" x 30" and full-size pallets with dimensions as large as 72" x 72". Furthermore, the machine accomodates realistic unit loads and is capable of inducing a uniformly distributed horizontal load on the leading stringer of a test specimen. For simplification and consistency with the limitation of the theoretical model, the horizontal load was quasi-static in nature, rather than dynamic.

Figure 4.1 is a photograph of the test machine. The backbone of this machine (Figure 4.2) is made of three 4" wideflange I-beams each 12' long. These lay on a concrete floor and are interconnected by one piece of 2.5" angle iron at each end. Holes are drilled every 4" throughout the length of the angle irons. The center I-beam always remains stationary unlike the two outer beams which are connected by bolts to the angle iron. This enables them to be moved to accomodate pallets whose stringers range from 8" to 72" in length.

Fastened perpendicular to the base I-beams is a 6" wide-flange I-beam. This beam acts as a buttress for the load head. It is attached to the base I-beams by bolts which allow spacer blocks to be placed beneath the buttress I-beam, thereby, allowing vertical adjustment.

A 10,000 lb. hydraulic cylinder is attached by a swivel connection to the buttress I-beam. The controls and motor for the cylinder are stationed beside the test machine. A 4" x 2.75", I-beam which is 72" long, is connected to the hydraulic piston. Teflon coated slider blocks are mounted underneath the load head which rests on the two outboard base I-beams. Necessary vertical adjustments to the load

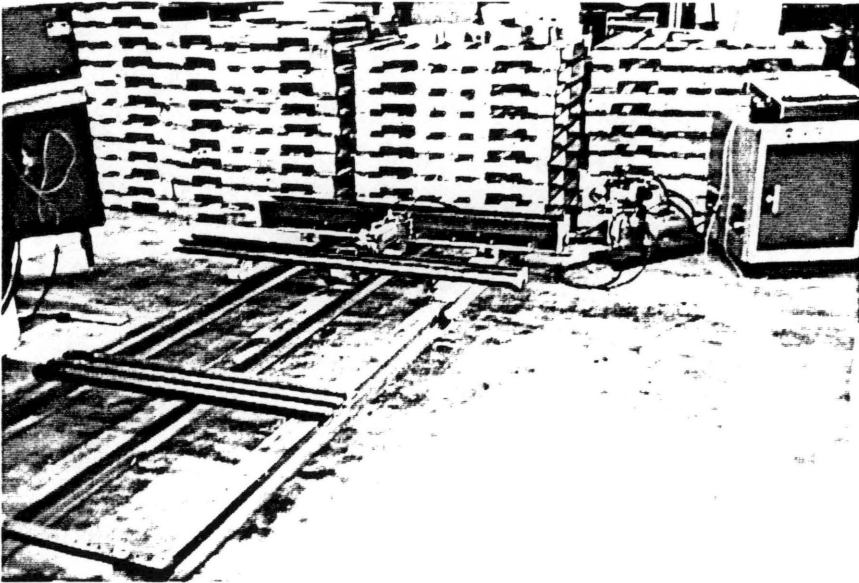


FIGURE 4.1 - Photograph of Test Machine

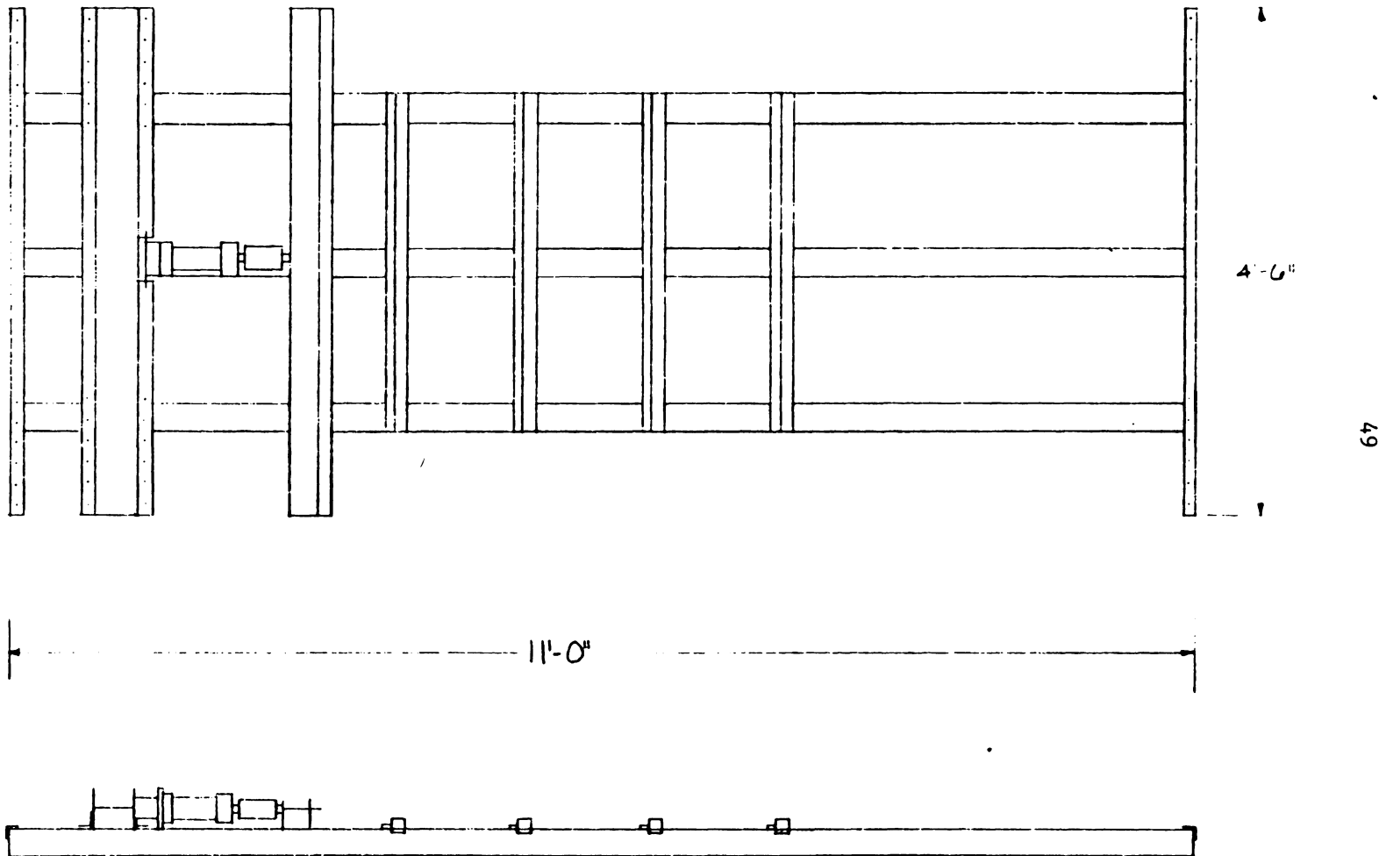


FIGURE 4.2 - Plan and Profile Views of Test Machine

head are made by placing wood spacers beneath the slider blocks.

Finally, to prevent the test specimen from sliding when the horizontal load is applied, four restraining bars are attached to the machine. These bars are mounted perpendicular to the base I-beams and can be adjusted to any position parallel to the base. When testing skids, a restraining bar may be placed behind each stringer if desired. For testing double-faced pallets, a bar may be placed behind the last stringer to prevent specimen sliding.

A 10,000 lb. BLH type U3G2-S load cell was mounted in series between the hydraulic cylinder and the load head. A Vishay amplifier sends an electronic signal from the load cell to a Hewlett Packard model 7044A X-Y recorder.

The Y-coordinate of the recorder plots horizontal translation of the upper deckboards of a test specimen. This is accomplished with two LVDT's which are mounted along any channel of the base I-beams. Two T-shaped brackets are attached to the upper deckboards of the test specimen and bear against the plunger of the LVDT's. For complete machine drawings, wiring, and operation see Appendix A. With the test machine complete, actual testing was ready to commence.

4.3 Model Verification: Type I

The objective of this section is to describe the experimental design and the analysis techniques used to determine the validity of the Type I model.

First, a computer program entitled "LCAN" (an acronym for Lateral Collapse ANalysis) was developed to calculate H_{\max} using the Type I model. LCAN is written in the Fortran IV language, and is presented in Appendix B. The input parameters required to run this program are the geometric properties of the deckboards and stringers, the unit load applied to the structure, and the rotation modulus and maximum moment of each joint in the pallet. Once this data is entered and the program run, the output echoes the input data, the moments generated along each stringer, a predicted H_{\max} , and a H_{\max}/V ratio.

To determine the accuracy of LCAN five full-size pallets, eight pallet sections, and eighteen joint rotation samples were built. All stringers and deckboards were oak (Quercus spp.) and had moisture contents above 30%. The fasteners used were 2-1/4 inch long, helically threaded, low-carbon steel nails. They contained 4 flutes at 68 degrees with an

average thread crest diameter of 0.126 inches. The average MIBANT (25) angle of the nail was 46 degrees. All nails were meticulously placed in the patterns illustrated in Appendix C1.

The pallets built were expected to behave as the Type I model. Refer to Appendix C2 for construction specifications and for the unit load applied to test pallets. Testing was conducted on the lateral load machine with a cross-head rate of approximately 4 inches per minute. Figure 4.3 is a photograph of a test in progress. During each test a horizontal force (H) versus upper deckboard translation (X) curve was plotted (Figure 4.4). H_{\max} was then determined from each curve for the test specimens (Table 4.1).

After testing the pallets, joint rotation samples were fabricated as described and to the dimensions specified in Table D1.1 of the Appendix. These samples were built to provide an estimate of M_{\max} and R was for use in LCAN. The joints were tested on a Tinius Olsen test machine with a cross-head rate of 0.015 inches per minute. During each test, a load-deflection curve was recorded and from it the M_{\max} and rotation modulus were determined (Appendix D1.1). After each test, the MC and G were determined for the

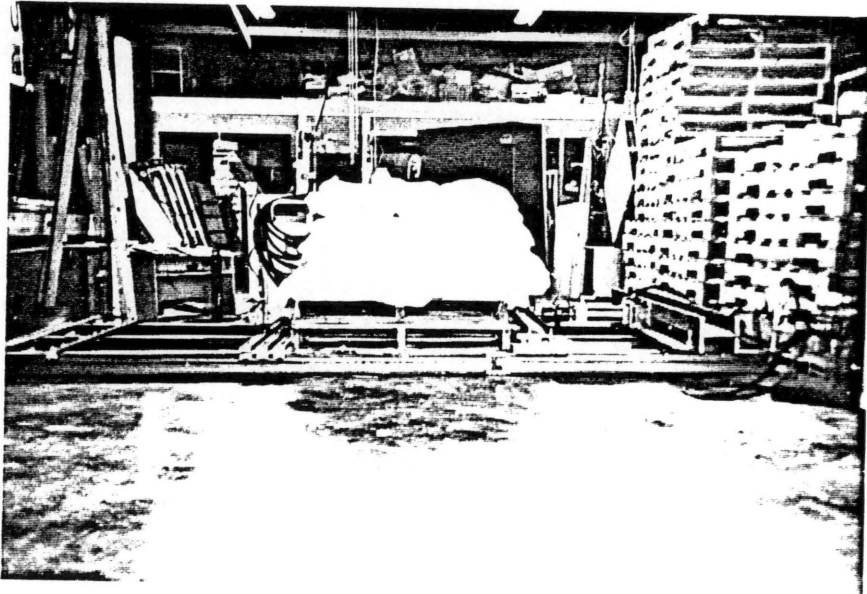


FIGURE 4.3 - Photograph of Collapse Test

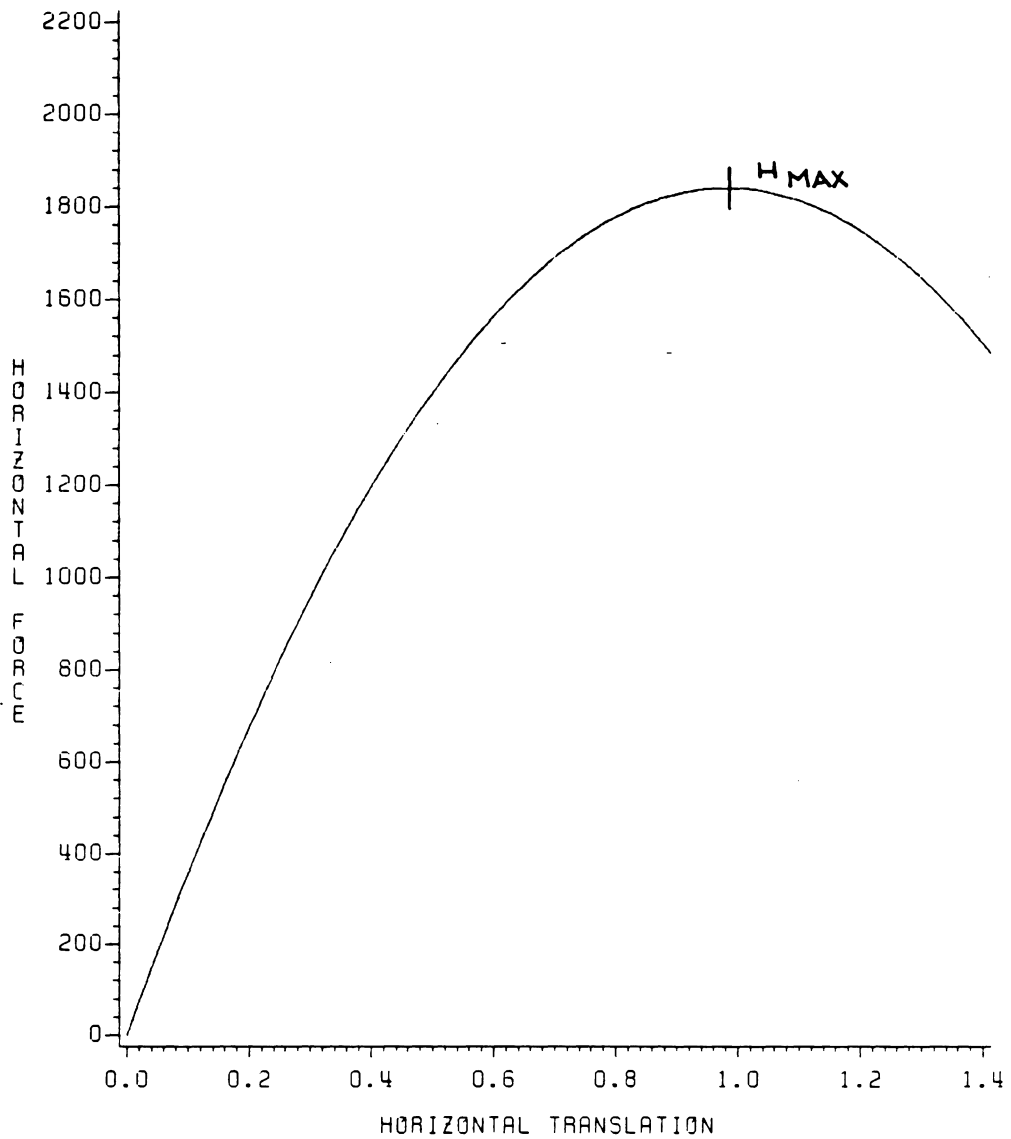


FIGURE 4.4 - HORIZONTAL FORCE (LBS.) VS. HORIZONTAL TRANSLATION (IN.) CURVE FROM COLLAPSE TEST

Table 4.1 Actual H_{\max} Versus Predicted H_{\max} for
Type I Tests

Specimen No.	Actual H_{\max} (lb.)	Predicted H_{\max} (lb.)
1	1188	760
2	1200	760
3	1525	811
4	1563	811
5	738	1165
6	2575	2245
7	2375	2428
8	2825	2484
9	4200	2985
10	4200	2985
11	5300	3957
12	4725	3957
13	6880	6468
Average	3022	2443

deckboard and stringer components according to ASTM D-143 standards (1).

Once the testing was complete, each design was run through LKAN to predict H_{\max} . Table 4.1 shows those values of H_{\max} . It is apparent from the illustration that the model tends to under estimate H_{\max} by an average of 579 lbs. or 19%. This error could be from an under estimate of M_{\max} which can change because of the variability of wood's mechanical properties and/or the fastener characteristics.

A hypothesis was developed to explain this under-prediction. This was that the slower rate of loading, 0.015 inches per minute in the joint rotation tests produced lower values for M_{\max} and R than were realistic for lateral collapse testing at 4 inches per minute. With these lower values the model would indeed under-predict H_{\max} .

A study was conducted to determine how the rate of loading influenced M_{\max} and R . Thirty matched joint rotation samples were built according to the specifications in Appendix C3 with nailing and stapling patterns as specified in Appendix C1. Each type joint was tested at 4 inches per minute and 0.015 inches per minute with four repetitions each. A load-deflection curve was plotted

during each test and from these M_{\max} and R were determined. With this data a ratio of the M_{\max} generated at 4 inches per minute to 0.015 inches per minute was computed (Table 4.2). The same procedure was performed for R (Table 4.3). Tables 4.2 and 4.3 show the average M_{\max} and R values of the joints tested in the study. Table D1.3 of the Appendix shows all of the test data. The results show a significant increase of M_{\max} and R with the rate of loading.

With this new information on hand, all values from the initial joint rotation tests were increased by multiplying them by the appropriate ratio from Tables 4.2 and 4.3. Next, the Type I designs were re-analyzed using LCPAN. The results show that the Type I model now over-predicts H_{\max} by an average of 188 lbs. or a 6% error (Table 4.4). This is obviously better than the original under-prediction.

It was concluded that the Type I model was an acceptable foundation for further investigation of lateral collapse; therefore, the next step in predicting LCP was to develop K-factors that would modify the resisting moments in a Type II pallet.

Table 4.2 Average M_{\max} Values for Modification
Factor Analysis

Fastener		M_{\max}		Ratio
		Loading Rates ¹		
Type	#	0.015	4.0	0.015/4
nail	4	908	1100	1.211
nail	3	750	1038	1.384
staple	3	582	670	1.151
staple	1	183	232	1.270

¹Rates are inches/minute

Table 4.3 Average R Values for Modification
Factor Analysis

Fastener		Rotation Modulus		Ratio
		Loading Rates ¹		
Type	#	0.015	4.0	0.015/4
nail	4	2115	2818	1.332
nail	3	1956	2261	1.156
staple	3	1396	2375	1.703
staple	1	537	804	1.497

¹Rates are inches/minute

Table 4.4 Actual H_{\max} Versus Predicted H_{\max} after
Re-analysis of Type I Tests

Specimen No.	Actual H_{\max} (lb.)	Predicted H_{\max} (lb.)
1	1188	1482
2	1200	1482
3	1525	1579
4	1563	1579
5	738	2026
6	2575	2778
7	2375	2825
8	2825	3315
9	4200	3424
10	4200	3424
11	5300	4942
12	4725	4942
13	6880	7931
Average	3022	3210

4.4 Model Verification: Type II

This section presents the methods and materials used to develop and verify the moment modification factor for Type II pallets. Because of the complexity of the combined bending-axial force actions in Type II pallets, some simplifications were necessary. Consider the stringer pallet shown in Figure 3.6. If there is significant flexure in the top deckboards then many ϕ_{ij} values will be dissimilar. The magnitude of an individual ϕ_{ij} will be a function of the actions of the vertical force causing deck flexure as well as that of the horizontal force causing collapse. Compared to a Type I pallet some of the Type II joints will have reached M_{\max} while others will still undergo elastic rotation. Hence the difference in rotation compared to the Type I pallet will lead to an erroneous prediction of H_{\max} using the Type I analog model procedure.

To develop correction factors for three and four stringer Type II pallets the structural analysis program SPACEPAL (17) was used. This program calculates the moments at each joint for a given horizontal load. Initially, one SPACEPAL model was developed for three stringer pallets and one for

four stringer pallets. These analog models are shown in Appendix B2. These models are inherently unstable and some initial horizontal force, H_{eq} , is needed to insure initial stability. Additional horizontal force will cause clockwise rotation simulating lateral collapse.

A wide range of pallet styles, from expendables to warehouse-type designs, were modeled with SPACEPAL to determine the influence of various parameters on joint moments. The three study variables were a) $E_t I_t / l^3$ of the top deckboards, b) stringer aspect ratio (d_i / w_i), and c) the joint characteristics - M_{max} and R . Appendix Tables B3.1 and B3.2 describe all 27 designs of the three and 27 designs of the four stringer, double-faced pallets, respectively. Additionally, 18 single-faced three and four stringer pallet designs specified in Tables B3.3 and B3.4 of the Appendix were also analyzed for a total of 72 computer models. Each model was submitted to SPACEPAL and analyzed with 500, 2250, and 5000 lb. unit vertical loads. All 72 designs were initially run through LCAN to determine the Type I H_{max} and M_{max} . The total horizontal load (H_{tot}) applied to each model was the Type I H_{max} from LCAN plus H_{eq} .

The resulting theoretical moments developed at each joint were recorded and individual K_{ij} were computed using equations (22) and (23). Multiple regression equations between K_{ij} and unit load, deck MOE, deck moment of inertia, stringer width and height, $M1_i$ and $M2_i$ were derived for the three stringer and four stringer pallets. The result was one different regression equation for each joint in the structure (Appendix D2). For example, twelve equations were developed for a four stringer double-faced pallet representing one for each joint. R^2 values for individual joint regressions were consistently high.

Use of the twelve regression equations provides the best possible estimate of the needed modifications for Type II behavior. However, this approach is far too cumbersome for general design use. A second set of regression equations was developed by combining all K-factors from pallets with the same number of stringers. Therefore, one regression equation was used for three stringer and one equation for four stringer pallets. The three and four stringer regressions are presented in equations (36) and (37), respectively:

$$K_3 = 0.8956 + 0.0003(V) + 0.0013(E_t)(I_t)/\ell^3 \quad (36) \\ - 1.6004(Ar) + 0.0001(M_{\max})$$

$$K_4 = 0.1306 - 0.00001(V) + 0.0494(E_t)(I_t)/l^3 \quad (37)$$

$$- 0.0569(Ar) - 0.00002(M_{\max})$$

where:

K_k = K-factor for three and four stringer pallets
and

$Ar = w_i/d_i$ of stringers (in./in.).

The R-square value for equations (36) and (37) was 0.358 and 0.579, respectively.

To evaluate this simplified approach, equations (36) and (37) were implemented into LCAN and the 72 pallet designs were re-analyzed. Although the regression equations developed for each individual joint are likely to be more accurate than the second set, the number and complexity of the equations must be reduced without a significant loss of accuracy. The output of LCAN produced two H_{\max}/V ratios - $H1_{\max}/V$ and $H2_{\max}/V$ - for each design. $H1_{\max}/V$ was computed using a unique K-factor equation for each joint and $H2_{\max}/V$ was computed with only one K-factor equation. Next, the two sets of ratios were ranked from lowest to highest. As stated previously, the $H1_{\max}/V$ order of rank was considered to be the most accurate. The $H2_{\max}/V$ rank was then compared to the $H1_{\max}/V$ rank.

The purpose of the comparison was to note where each design fell in the $H1_{\max}/V$ rank versus where it fell in the $H2_{\max}/V$ rank. For example, if in the $H1_{\max}/V$ rank a particular design was ranked 29th and the same design was ranked 34th in the $H2_{\max}/V$ rank, the difference would be -5. The differences were determined for each of the 72 pallet designs. Then, the mean and standard deviation was determined for the differences. If a low standard deviation was found then one regression equation, (36) or (37), would be used in the Type II model. This is because the one equation would do as good a job modifying the moments as would the individual equations for each joint.

The results of the three stringer case showed a mean difference of zero with a standard deviation of 5.3. Figure 4.5 illustrates that the change in rank was random and showed no bias towards any one group of $H2_{\max}/V$ ratios. Therefore, the assessment of a pallet's lateral collapse potential based on its H_{\max}/V ratio would not be significantly altered using equation (36).

In the four stringer case the mean difference was again zero with a standard deviation of 6.1. Figure 4.6 shows random and unbiased changes in ranks. Based on these

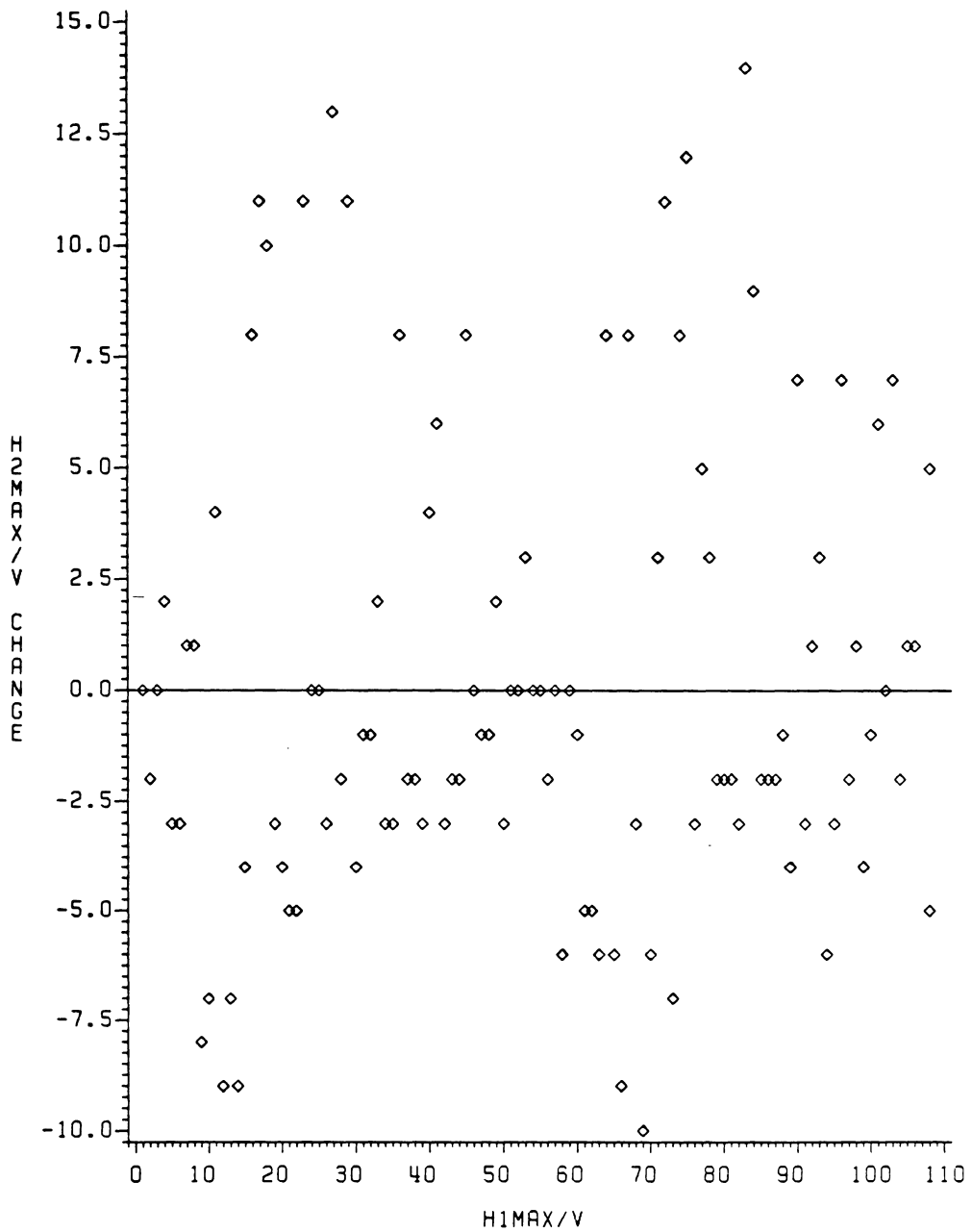


FIGURE 4.5 - THE CHANGE IN RANK OF H2MAX/V VERSUS
THE H1MAX/V RANK FOR 3 STRINGER PALLETS

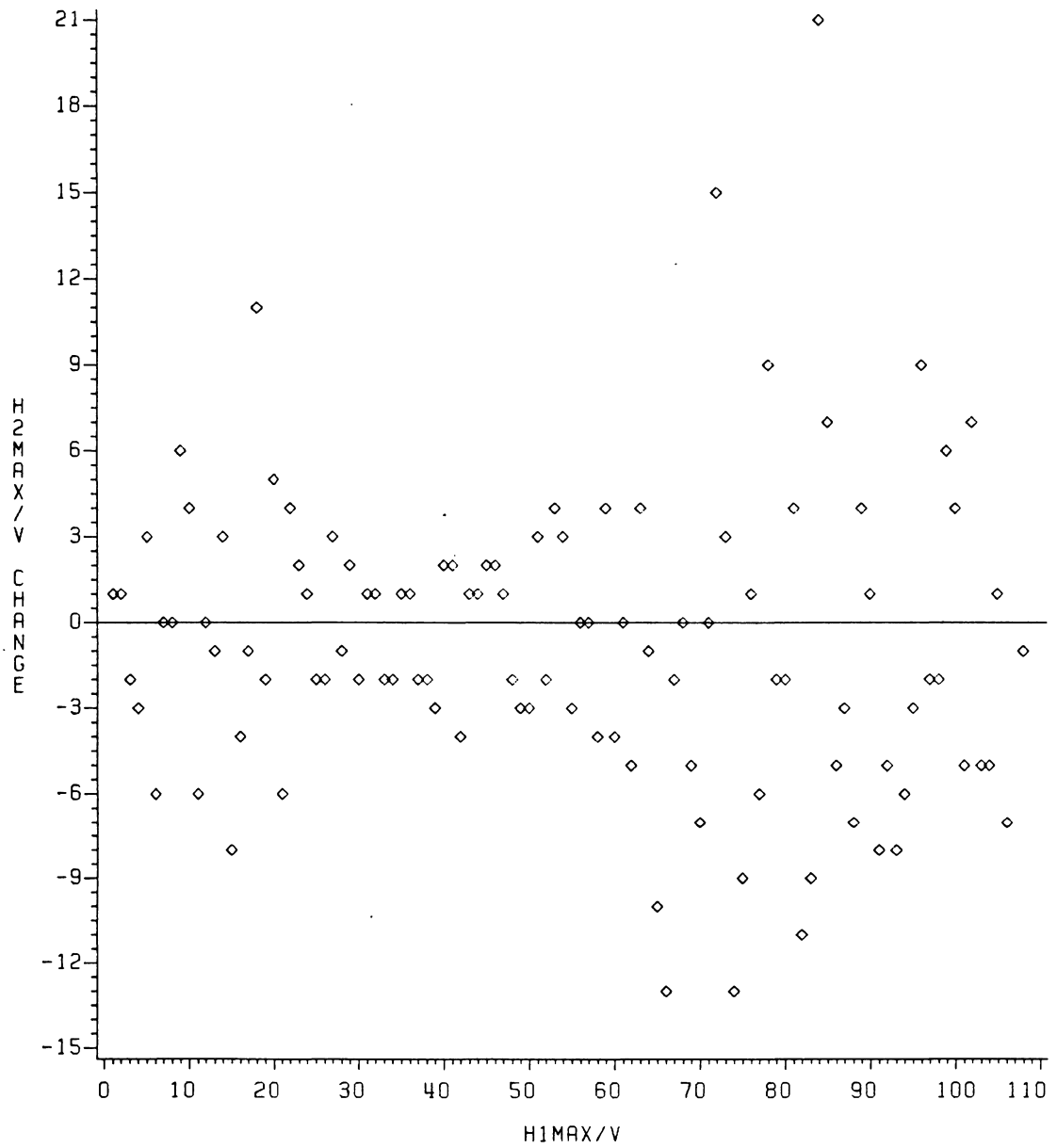


FIGURE 4.6 - THE CHANGE IN RANK OF H2MAX/V VERSUS
THE H1MAX/V RANK FOR 4 STRINGER PALLETS

analyses, it was concluded that equations (36) and (37) would provide acceptable K-factor predictions.

4.5 Experimental Verification of LCAN

A series of 18 different pallet designs were selected for an experimental verification of the lateral collapse analysis procedure. These designs were selected to represent a range of expected H_{\max}/V ratios and different geometries. Six geometries of each two, three and four stringer designs were chosen.

The pallet shook used to build the test specimens were of aspen (Populus), oak (Quercus), and yellow poplar (Liriodendron tulipifer). Each had a moisture content above 8%. The oak and poplar were used for stringer material and the oak and aspen for deckboards. The pieces were manufactured in final dimension and stored.

The fasteners used were the same helically threaded nail previously described in Chapter 4 plus a 15 gauge, 2-1/4 x 0.074 x 0.067 inches, uncoated staple. The MIBANT angle of the staple was 132 degrees as predicted by Padla (20).

To estimate the value of M_{\max} and R of stapled joints, six rotation samples with three replications, were built as specified in Appendix C2 and D1.2. Testing was conducted on the Tinius Olsen test machine with a cross-head rate of 0.015 inches per minute. A load-deflection curve was plotted during each test and from these, M_{\max} and R were determined (Appendix D1.2). After testing, MC and G of the deckboard and stringer were determined according to ASTM D-143 standards. No nail joint tests were conducted since the pallet shook (oak) used to build these specimens came from the same stack of shook that was used to build the Type I test specimens. It was assumed that the joint characteristics were similar.

The dimensions of the deckboard material used were measured to the nearest 0.001 inch. Each board received an identification number, and its E (Appendix C4) was determined by the dead-weight deflection method (21).

Knowing the deckboard dimensions, E-values, and predicted joint characteristics, LKAN was used to analyze the eighteen test geometries. These results showed that the actual test pallets had theoretical H_{\max}/V ratio's ranging from 0.3 to 2.5.

The eighteen pallets were built according to the specifications in Appendix C5 with nailing and stapling patterns as specified in Appendix C1. These pallets were tested on the lateral test machine with an approximate cross-head rate of 4 inches per minute. During each test a H versus X curve was generated. From these curves, H_{\max} was determined (Table 4.5).

After modifying R and M_{\max} for rate of loading, all of the Type II pallets were analyzed with LKAN. The results presented in Table 4.5 shows that the average difference in H_{\max} was a 269 lb. over-estimate or a 14.5% error. There was no evidence from the analysis that the model was less accurate at any one particular H_{\max}/V ratio compared to another. Material variability, accuracy in load placement during test and the use of simplified equations (36) and (37) to generate the K-factors all contributed to the error. However, for the purpose of this study this error is quite reasonable and it is concluded that the model provides an acceptable means of assessing the lateral collapse potential of a pallet.

To determine the influence of the K-factors on the computation of H_{\max} the pallets in Table 4.5 were re-

Table 4.5 Actual H_{\max} Versus Predicted H_{\max} for
Type II Tests

Specimen No.	Actual H_{\max} (lb.)	Predicted H_{\max} (lb.)
1	588	783
2	925	1060
3	1100	1210
4	1225	1271
5	1400	1580
6	1643	1739
7	1188	1450
8	1818	2072
9	1862	1962
10	1762	2146
11	2087	2200
12	2250	2195
13	2275	2439
14	2125	2693
15	2450	2733
16	2375	2999
17	2725	3372
18	3500	4238
Average	1850	2119

analyzed without using the K-factors. The results show an average 678 lb. over-estimate of the actual H_{\max} or a 37% error. From this analysis it was concluded that the K-factors significantly improve the prediction of H_{\max} and, therefore, deserve a place in the model.

CHAPTER 5

Design Procedures and Calibration

5.1 Introduction

The global objective of this investigation was to develop a design methodology that would evaluate the LCP of pallets. At this point in the investigation the model would predict H_{\max}/V ratio. For design purposes a "yardstick" must be developed to determine acceptable and unacceptable ranges of H_{\max}/V .

5.2 Field Survey and LCP Categories

For this purpose, it was necessary to locate pallets that had experienced lateral collapse. The designs collected form the basis of a definition of the transition points between LCP categories of acceptable and unacceptable. Forty manufacturers across the United States were surveyed. While fourteen of those surveyed had some type of experience with collapsing pallets, only two well documented designs

were found. Their design specifications and unit loads at the time of collapse are specified in Appendix C6. Each of the designs had three stringers with very low aspect ratios and were fastened with staples. Their H_{\max}/V ratios were determined to be 0.47 and 0.50 by LCN. A H_{\max}/V ratio of 0.50 indicates that these designs could only withstand a horizontal load no greater than one half the unit load. Adding a safety factor of 0.10 to the H_{\max}/V ratio of 0.50 equals 0.60 which was defined to be the point between high and medium LCP risk categories.

Since has been impossible to obtain field data on those pallets that are in the medium and low risk categories, 1.0 was arbitrarily selected to be the transition point between these categories. A pallet with this H_{\max}/V ratio could only withstand a maximum horizontal load equal to its unit load. In all probability, pallets in the field are going to experience a horizontal load of this magnitude. Due to this likelihood, it was felt that those pallets that have a $0.60 < H_{\max}/V < 1.00$ should be classified in the medium risk collapse category. The two LCP transition points were believed to be the best choices based on the available field data and collapse theory.

5.3 Implementation into PDS- the Pallet Design System

After verification of the design method, a condensed version of LCAN was incorporated as a subroutine in the NWPCA's PDS computer program.

Because of the limitations set on the data input, the PDS program must calculate M_{\max} using equation (38):

$$M_{\max} = (w_i/2)(\text{Separation factor}) \quad (38)$$

where:

M_{\max} = maximum moment a joint can sustain
(in.-lb.) and

Separation factor = joint withdrawal resistance
(lbs.) which is the lesser
value of equations (2), (3) or
(4).

To evaluate the accuracy of equation (38) a predicted M_{\max} was calculated for each joint rotation sample tested in this experiment (Appendix D1). A comparison between the M_{\max} calculated with equation (38) versus the actual M_{\max} is shown in Appendix D1. The tables show an under-estimate of M_{\max} averaging 63 in.-lbs. Note that in Table D1.3 some of the M_{\max} predicted values are missing. This is because these are the joints that were tested at the faster rate of

loading which equation (38) will not predict. With the limited data from this investigation this method of predicting M_{\max} was considered the best available for the PDS program.

5.4 Documented Lateral Collapse Failures

Since PDS has been in use, three pallet designs that have failed in lateral collapse have been documented. Their specifications are in Appendix Table C6 as pallets #3, #4 and #5.

Designs #3 and #4 are three stringer, single-faced pallets fastened with very low quality, helically threaded nails. During their service lives, each design was expected to sustain a maximum unit load of 2500 lbs. When the designs are run through PDS their H_{\max}/V ratios equal 0.90 and 0.87, respectively. These ratios fall within the medium collapse potential category which should indicate to a pallet designer that there is a chance of lateral collapse occurring.

Pallet #5 is a shipping pallet whose $H_{\max}/V = 0.62$ indicates a high to medium risk design. Utilizing the lateral collapse model a pallet designer might expect this design to collapse. To decrease the probability of failure this pallet's geometry, material properties, and/or its fastener characteristics should be changed.

5.5 Variable Sensitivity

After using PDS, a pallet designer should begin to sense that there are four major variables that influence a pallet's LCP. Each individual pallet designer must consider which of the four variables are the most economically feasible to change in his situation.

Figure 5.1 illustrates the effects of aspect ratio on H_{\max}/V . As this ratio increases, the pallet becomes more resistant to lateral collapse. One explanation of this change is that as the stringer height is reduced, the lever-arm distance (Y_i) of h_i is decreased, and, therefore, H_{\max} increases. Similarly, as the lever-arm distance (Z_i) of V_i is increased by increasing the stringer width, the resisting moment is increased. Thus, H_{\max} increases as well. Also,

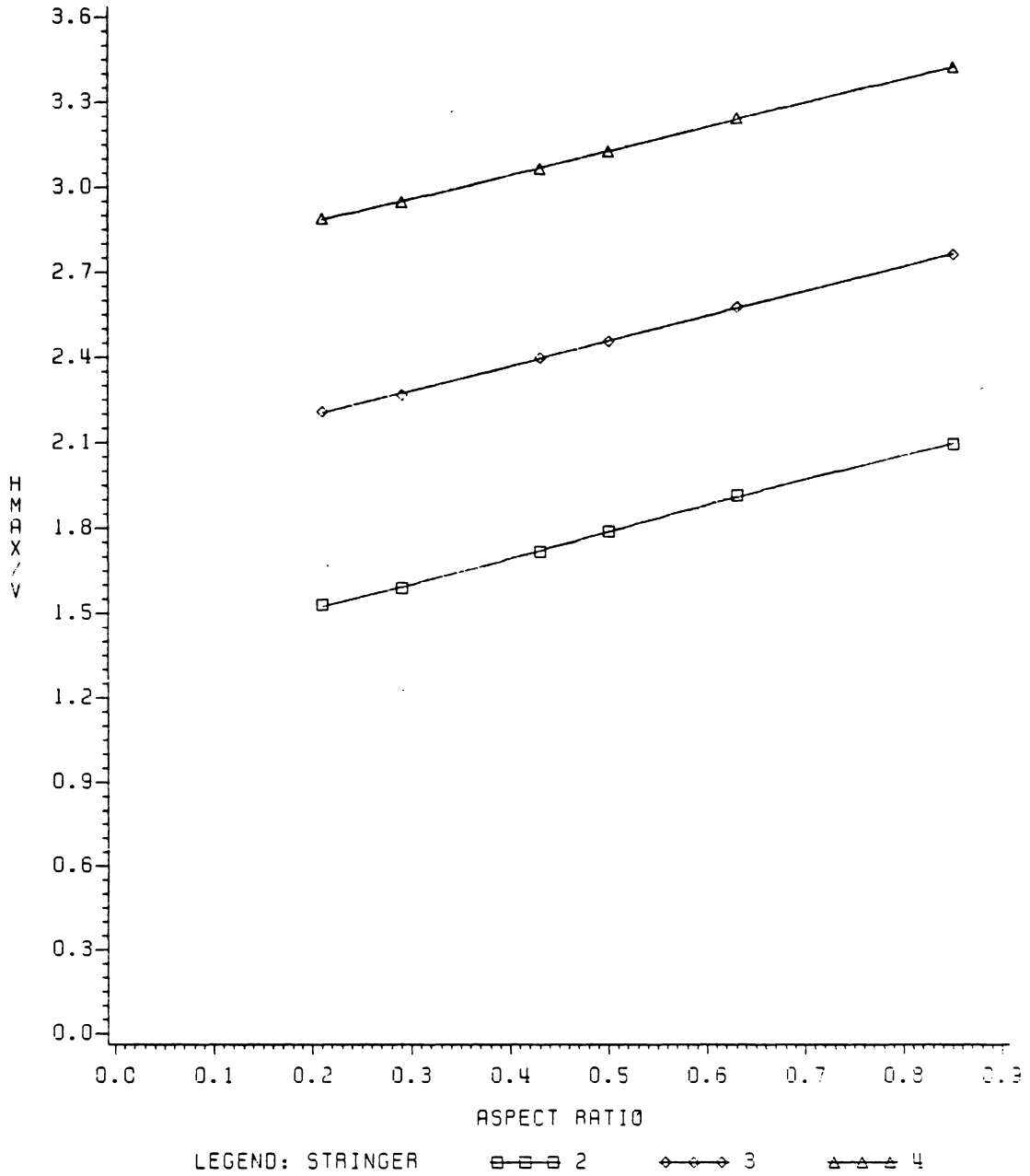


FIGURE 5.1 - THE EFFECT STRINGER ASPECT RATIO HAS ON THE HMAX/V RATIO

as the number of stringers increases, the LCP decreases. Using this information, a designer can increase the H_{\max}/V ratio of a pallet by increasing its stringer aspect ratio. This finding was expected according to Gregory's (7) stability theory.

Figure 5.2 illustrates the effect of unit load on a pallet's LCP. As the load is increased, the potential for lateral collapse is increased. More specifically, the upper deckboards will experience greater amounts of initial deflection because the larger loads will tend to open the deckboard-stringer joints. As a result, the total amount of resisting moment from the joints decreases which, in turn reduces H_{\max} . Since it is quite possible for a pallet to be subjected to a wide range of unit loads, it is important during the design process to have relative feel for the largest unit load the pallet will support.

Another variable that influences the LCP of a pallet is its $E_t I_t$ of the upper deckboards (Figure 5.3). As this variable is increased the H_{\max}/V ratio will increase up to a point where the K-factor equation predicts no deckboard bending. Beyond this point, no increase in H_{\max}/V can be accomplished. Decrease in pallet LCP might be more readily

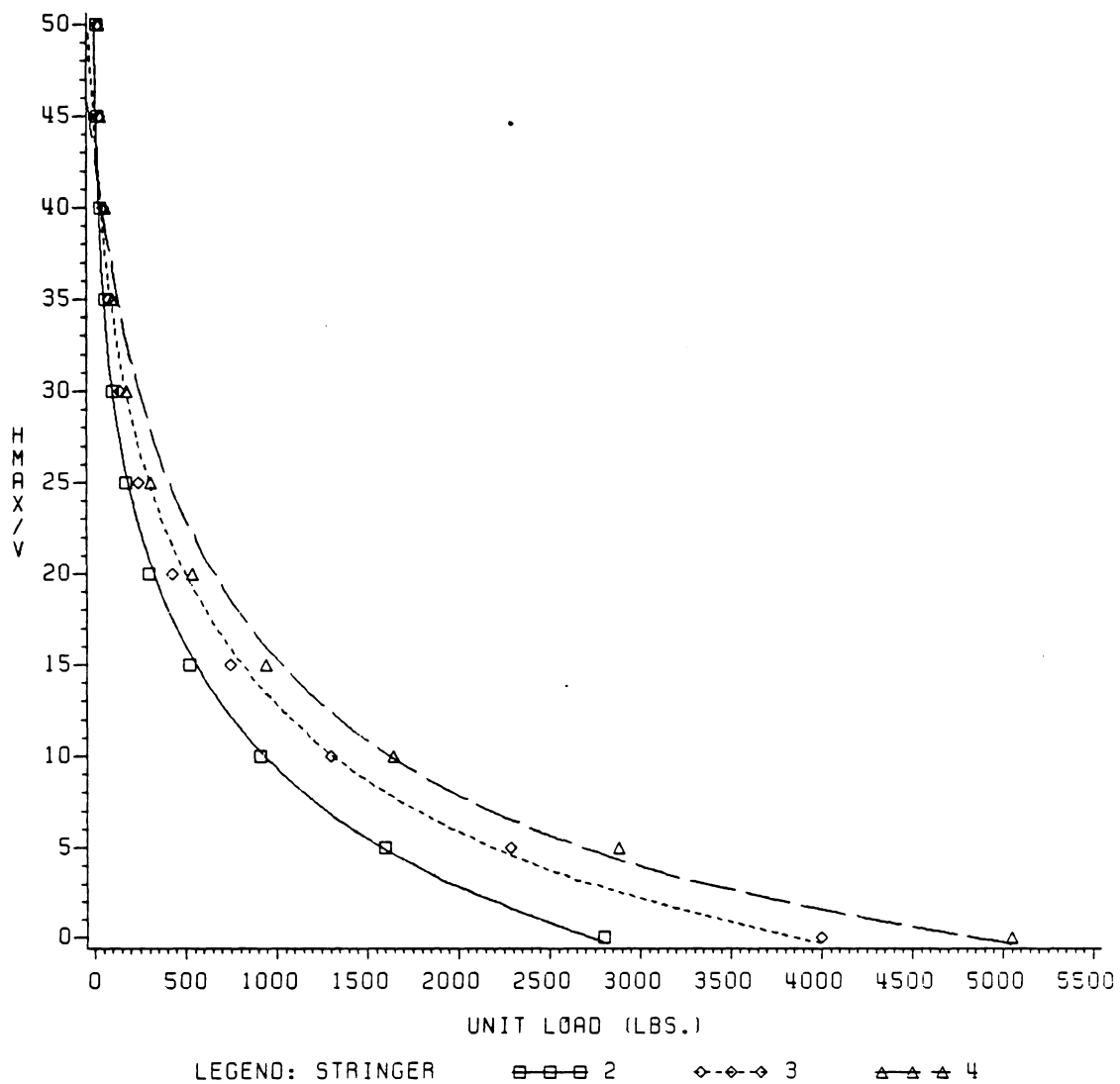


FIGURE 5.2 - THE EFFECT UNIT LOAD HAS
ON THE H_{MAX}/V RATIO

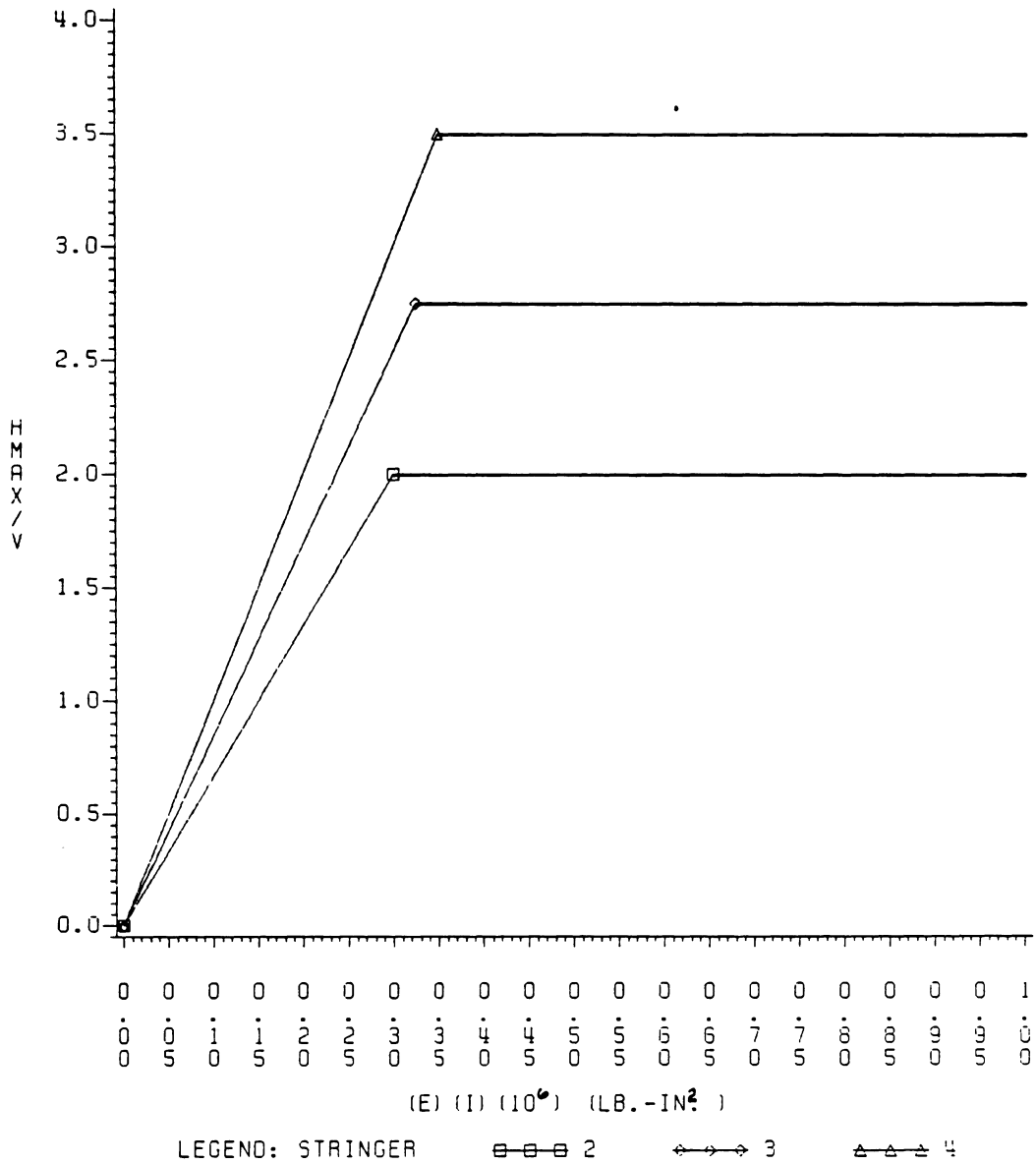


FIGURE 5.3 - THE EFFECT OF FLEXURAL RIGIDITY
ON H_{MAX}/V

and economically accomplished by changing one of the other three variables discussed in this Chapter.

The type and number of nails used in the pallet will have an effect on the M_{\max} and rotation modulus. Figure 5.4 shows that as M_{\max} increases the H_{\max}/V ratio does the same because of the greater resistance to overturning. Therefore, if it is feasible to add another nail per joint or to increase nail quality, a significant reduction in LCP will result. This is likely to be the most economically attractive means of improving resistance to lateral collapse.

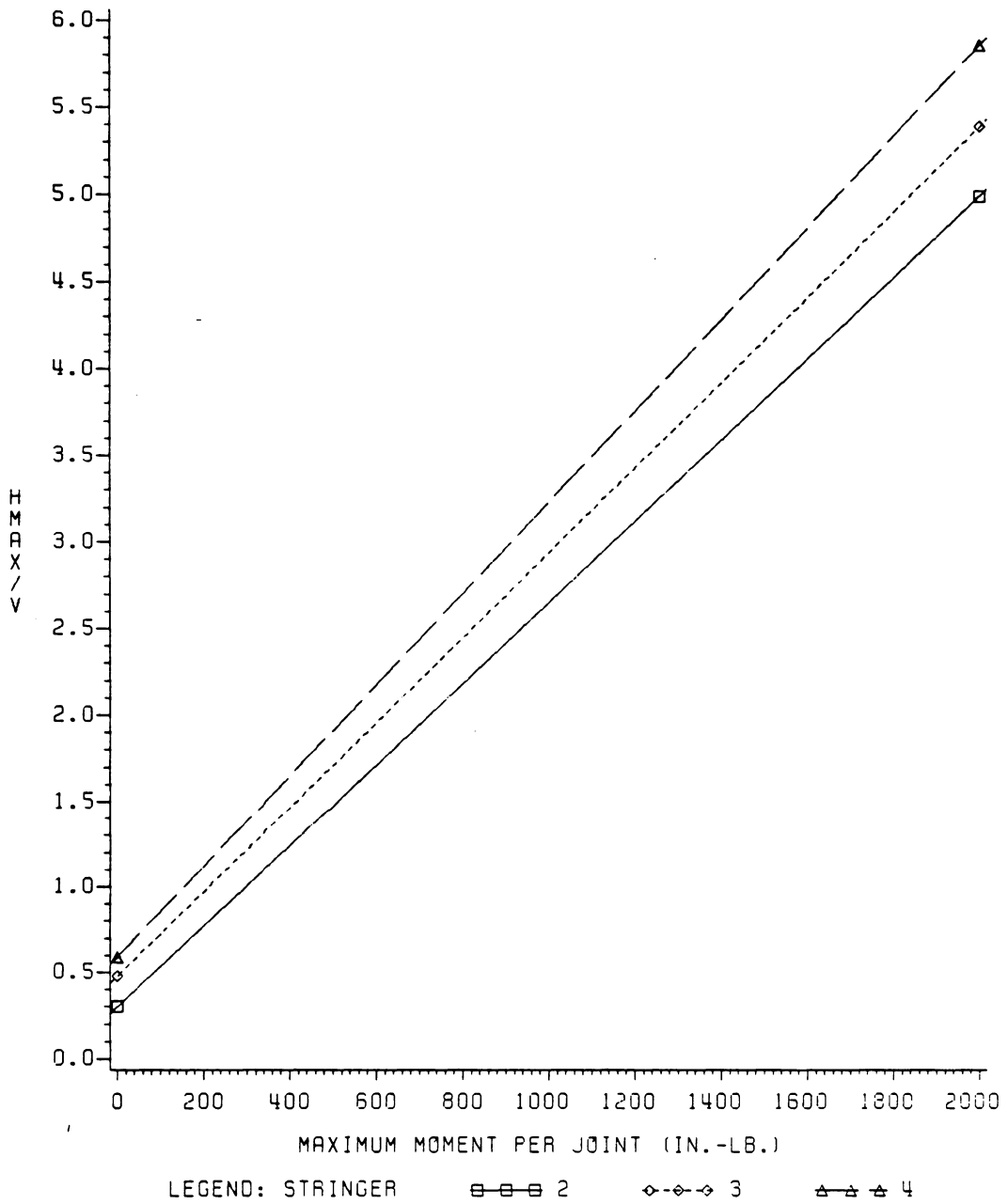


FIGURE 5.4 - THE EFFECT MAXIMUM MOMENT
PER JOINT HAS ON HMAX/V

CHAPTER 6

Conclusions

A model of static lateral collapse of wood pallets was proven to perform satisfactorily. A relative measure of lateral collapse potential was determined by the H_{\max}/V ratio. Based on limited field data, if the H_{\max}/V ratio is in the range zero to 0.60, the pallet design is in a high risk category, between 0.60 and 1.00 it is in a medium risk category, and from 1.00 to infinity it is in low risk category.

Those factors that influence the LCP are:

1) Stringer Aspect Ratio (w_1/d_1) - As this ratio is increased the collapse risk is decreased.

2) Upperdeckboard $(E_t)(I_t)/l^3$ - An increase of this property will increase the lateral collapse resistance up to a point where no deckboard bending occurs and beyond this point, LCP remains constant.

3) Joint Characteristics - The LCP of a pallet will decrease as the maximum moment and rotation modulus of the joints in the pallet are increased.

4) Unit Load - As the unit load on the pallet is increased, the risk for lateral collapse increases.

LITERATURE CITED

1. American Society for Testing Materials. 1983. Standard Methods of Testing Small Clear Specimens of Timber. ASTM Designation D143-52. Annual Book of ASTM Standards, Vol. 4.09, pp. 61-62.
2. Antonides, C.E., M.D. Vanderbilt, and J.R. Goodman. 1980. Interlayer Gap Effect on Nailed Joint Stiffness. Wood Science 13(1): 4-46.
3. Blockley, D.I. 1980. The Nature of Structural Design and Safety. John Wiley and Sons, New York.
4. Bodig, J. and B.A. Jayne. 1982. Mechanics of Wood and Composites. Van Nostrand Reinhold Co. Inc., New York. p 252.
5. Dunmire, D.E. 1966. Effects of Initial Moisture Content on Performance of Hardwood Pallets. USDA Forest Service Research Paper NC 4, June.
6. Goehring, C.B. and W.B. Wallin. A Survey of Loads, Loading Conditions for Wooden Pallets. Unpublished. Northeastern For. Expt. Station. Princeton, W.V.
7. Gregory, M.S. 1967. Elastic Instability. E. and F.N. Spon Limited, London. p 1-33.
8. Hoyle, R.J.Jr. 1978. Wood Technology in the Design of Structures. Mountain Press Publishing Co., Montana. p 31.
9. Johnston, B.G. 1976. Guide to Stability Design Criteria for Metal Structures. John Wiley and Sons, New York. p 18-80.
10. Kyokong, B. 1979. The Development of a Model of the Mechanical Behavior of Pallets. Thesis. Va. Tech, Blacksburg, Va.
11. Langhaar, H.L. and A.P. Boresi. 1959. Engineering Mechanics. McGraw-Hill Book Co., Inc. Pa.

12. Loferski, J.R. Literature Review - Design Procedures for Wooden Pallets. Unpublished. Va. Tech, Blacksburg, Va.
13. Mack, J.J. 1966. The Strength and Stiffness of Nailed Joints Under Short Duration Loading. Tech. Paper No. 40. Div. of For. Prod., C.S.I.R.O., Melbourne, Australia.
14. Mack, J.J. 1975. Contribution of Behavior of Deckboard-Stringer Joints to Pallet Performance. Wd. Res. and Wd. Construction Lab. Bull. No. 136, Va. Tech, Blacksburg, Va.
15. McCurdy, D.R. and D.W. Wildermuth. 1981. The Pallet Industry in the United States 1980. Dept. of Forestry. So. Ill. Univ. 1981.
16. Meriam, J.L. 1978. Engineering Mechanics: Statics and Dynamics. John Wiley and Sons, New York. p 190.
17. Mulheren, K. 1982. SPACEPAL. Computer program. Va. Tech, Blacksburg, Va.
18. National Forest Products Association. 1982. National Design Specifications for Wood Construction. N.F.P.A., Washington, D.C.
19. N.W.P.C.A. 1962. Specifications and Grades for Warehouse, Permanent or Returnable Pallets of West Coast Woods. N.W.P.C.A., Washington, D.C.
20. Padla, D.P. 1983. Relationships Between MIBANT Bend Angles and Selected Material Properties of Pallet Fasteners. Thesis. Va. Tech, Blacksburg, Va.
21. Percival, P.H. 1981. Portable E-tester for Selecting Structural Component Lumber. Forest Products Journal 3(2): 39-42.
22. Protective Packaging Group. 1976. Reusable Wood Pallets: Selection and Proper Design. E. For. Prod. Lab. Ottawa, Canada. For. Tech. Report 11.
23. Pugsley, A.G. 1966. The Safety of Structures. Edward Arnold (Publishers) LTD., London. p 1-53.

24. Randall, F.A.Jr. 1973. Historical Notes on Structural Safety. A.C.I. Journal Oct. p 669.
25. Stern, G.E. 1970. The MIBANT Quality Control Tool for Nails. Wd. Res. and Wd. Construction Lab. Bull. No. 100, Va. Tech, Blacksburg, Va.
26. Wallin, W.B. and E.G. Stern. 1974. Design of Pallet Joints from Different Species. N.E. For. Expt. Station.
27. Wallin, W.B. and E.G. Stern. 1974. Tentative Performance Standards for Warehouse and Exchange Pallets. For. Prod. Mktng. Lab., Princeton, W.V.
28. Wallin, W.B., E.G. Stern, and J.A. Johnson. 1976. Determination of Flexural Behavior of Stringer-type Pallets and Skids. Wd. Res. and Wd. Construction Lab. Bull. No. 146, Va. Tech, Blacksburg, Va.
29. Wallin, W.B., K.R. Whitenack. 1982. Durability Analysis for Wooden Pallets and Related Structures. N.E. Forest Experimentation Station. Princeton, WV. p 23-26.
30. West, H.H. 1980. Analysis of Structures. John Wiley and Sons, New York. p 27-29.
31. White, M.S. 1983. Personal Communications. Va. Tech, Blacksburg, Va.
32. U.S.D.A. For. Serv. 1974. Wood Handbook, For. Prod. Lab. Agri. Handbook. No. 72.

APPENDIX A

A1 - Machine Drawings

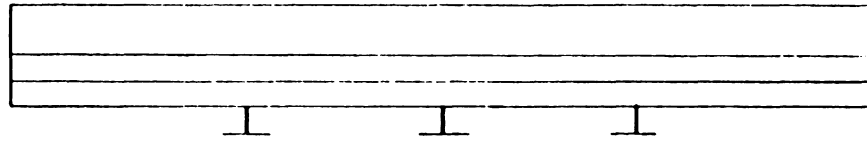
A2 - Machine Wiring

A3 - Machine Operation

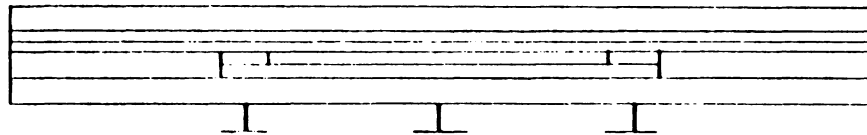
A3.1 - Pre Test Calibration Procedures

A3.2 - Typical Test Procedures

A1 - Machine Drawings



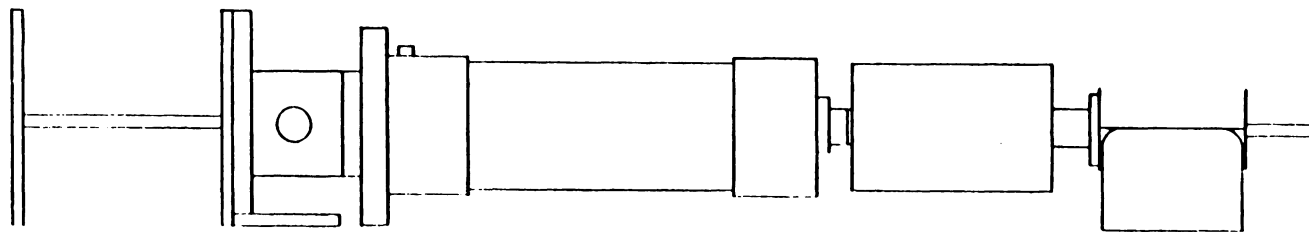
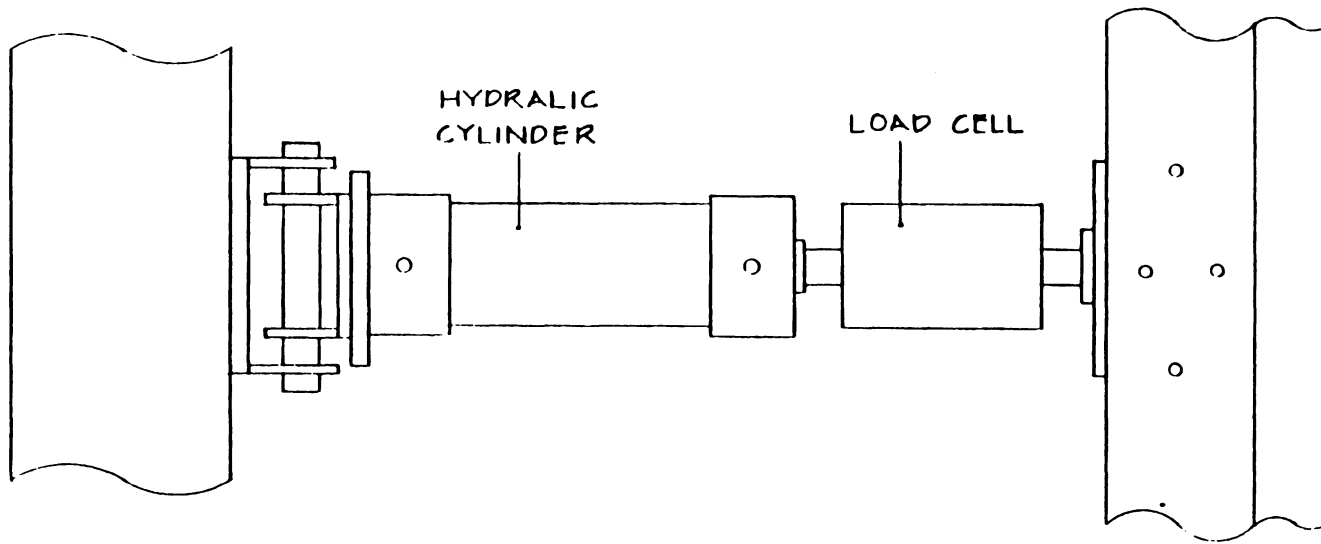
Buttress End View



Opposite End View

Scale 1" = 1'

FIGURE A1.1 - End Profile Views of Test Machine



Scale 1/4" = 1"

FIGURE A1.2 - Plan and Profile Views of Buttress-Load Head Connection

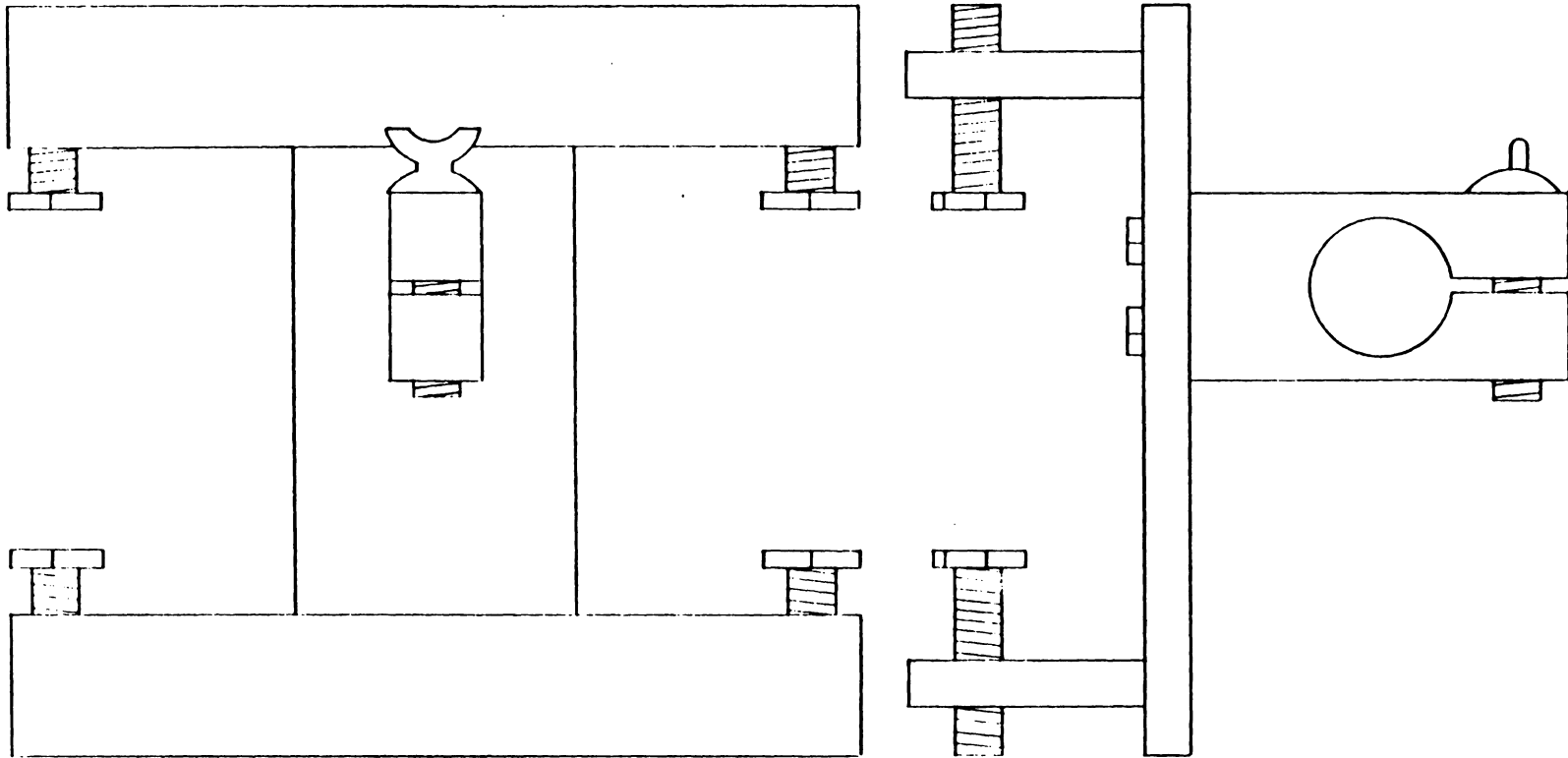


FIGURE A1.3 - Details of LVDT Bracket

A2 - Machine Wiring

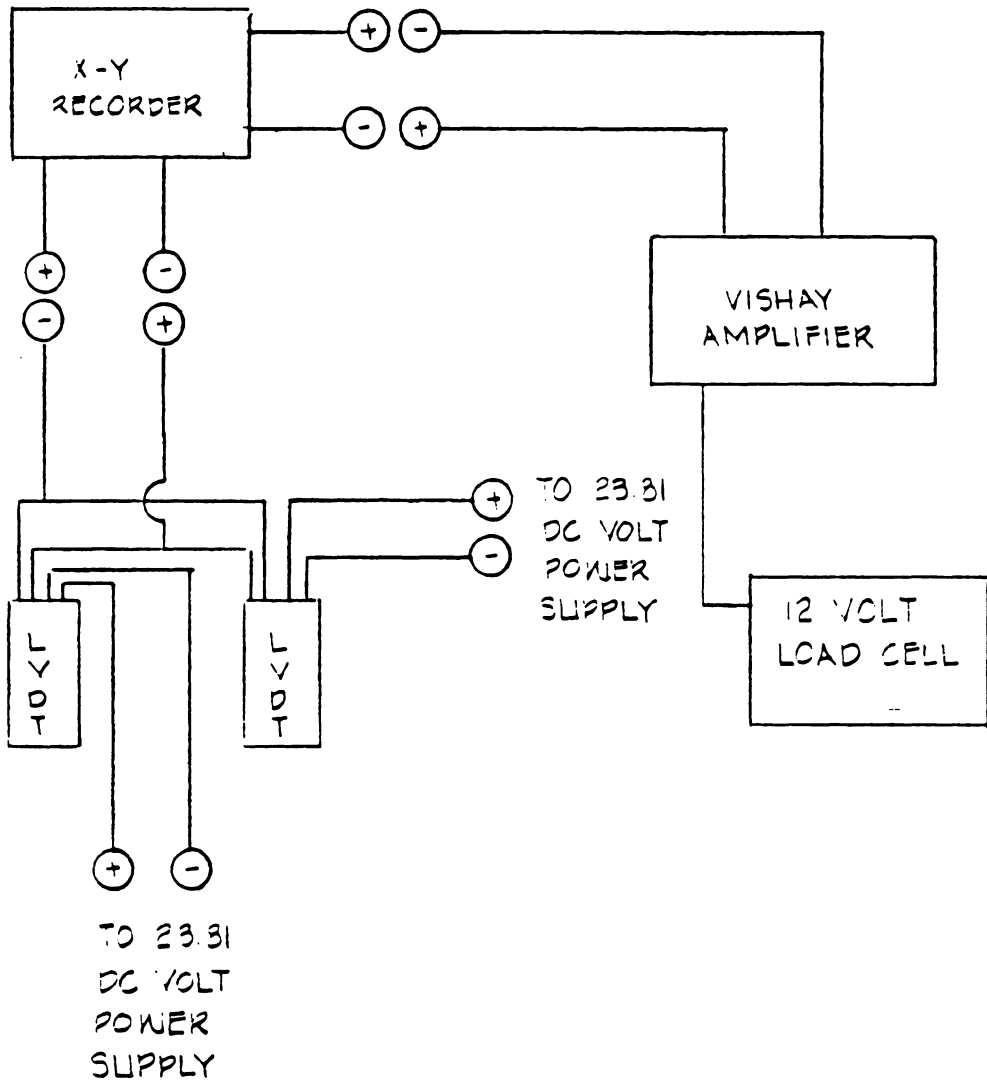


FIGURE A2.1 - Electrical Wiring Diagram of Test Machine

A3 - Machine Operation

A3.1 - Pre Test Calibration Procedures

- 1) Calibrate 10,000 lb BLH load cell according to procedures outlined in its specifications manual. Install load cell on machine.
- 2) Turn on VISHAY amplifier, Hewlet-Packard X-Y recorder and the two LVDT power supplies for a 10 minute warm-up.
- 3) Check LVDT power supplies for a 23.81 volt output.
- 4) Check bridge voltage of channel 4 which should be 12.00 volts. Adjustment is made with "BRIDGE EXCIT."
- 5) With "EXCIT" switch off, balance lights on VISHAY with the "AMP BALANCE."
- 6) Turn "EXCIT" switch on. Balance VISHAY lights with "BALANCE" knob.

A3.2 Typical Test Procedures

- 1) Place LVDT brackets in desired location along channel of base I-beams. Tighten 4 screws in each bracket.
- 2) Insert LVDTs into brackets, and tighten thumb screws.
- 3) Place test specimen on machine in desired location (about 1.5" away from retracted load head).
- 4) Adjust load head height with spacer blocks so that contact is made on upper deckboard.
- 5) If desired, slide restraining bars to appropriate positions. Tighten all bolts.
- 6) Loosely attach T-brackets on the upper deckboards so that the stem of the T is directly forward of the LVDT plunger. Slide T-bracket towards the load head causing the plunger to retract 2/3 original length. Tighten brackets.
- 7) Calibrate X-Y recorder by placing 0.015" gauge blocks between LVDT plunger and T-bracket.
- 8) Repeat step 7 for other LVDT.
- 9) Check VISHAY lights for their balance. Make necessary adjustments.
- 10) Place unit load on specimen.
- 11) Turn on hydraulic motor.
- 12) Switch the "DIRECTION" switch up on the hydraulic control box.
- 13) Bring load head forward by turning motor "SPEED" switch. Stop prior to contacting specimen.
- 14) Check the unit load's stability!
- 15) Adjust X-Y recorder pen to desired location.
- 16) Control load during test with hydraulic "SPEED" switch.

17) Once the X-Y recorder indicates maximum horizontal load, turn the "SPEED" switch to zero.

18) Move "DIRECTION" switch to the down position until load head is fully retracted.

19) Turn off hydraulic motor.

APPENIX B

- B1 - Listing of LCAN Program
- B2 - Analog Models
- B3 - Pallet Designs for Computer
 - B3.1 - Three Stringer, Double-Faced Pallets
Designed for K-Factor Development
 - B3.2 - Four Stringer, Double-Faced Pallets
Designed for K-Factor Development
 - B3.3 - Three Stringer, Single-Faced Pallets
Designed for K-Factor Development
 - B3.4 - Four Stringer, Single-Faced Pallets
Designed for K-Factor Development

B1 - Listing of LCAN Program


```

C          ZERO FOR DOUBLE-FACED PALLETS
C  NOSTR= NO. OF STRINGERS
C  JOP= TYPE OF PALLET  1) SINGLE-FACED=1
C                      2) DOUBLE-FACED=2
C
C  XJTOP1&2= # OF JOINTS ALONG THE TOP OF EA. STR.(I) WITH JOINT
C             PROP.(I)
C  XJBOT1&2= # OF JOINTS ALONG THE BOTTOM OF EACH STR.(I) WITH
C             JOINT PROP.(I)
C
C
C  IF(LEVEL.EQ.3)GO TO 70
C  WRITE (6,30)
C  FORMAT ('1', 'INPUT DATA',/)
C  WRITE (6,35) (INFO(I), I=1,80)
C  FORMAT (40A2/40A2)
C  WRITE (6,40)
C  FORMAT(//,T8, 'NJTOP(I)',T42, 'NJBOT(I)')
C  DO 45 I=1, NJP
C     WRITE (6,50)XJTOP(I),XJBOT(I)
C     FORMAT(1X,T3,F10.1,T37,F10.1)
C 45  CONTINUE
C  WRITE(6,55)
C 55  FORMAT(//,T8, 'NJP',T19, 'NINC',T31, 'XINC',T43, 'VOF',T54, 'NOSTR',
C     *T64, 'JOP')
C  WRITE (6,60)NJP,NINC,XINC,VOF,NOSTR,JOP
C 60  FORMAT (1X,T5, I5,T17, I5,T26,F10.3,T37,F10.3,T52, I5,T61, I5)
C
C
C  READ IN PALLET VARIABLES FROM DATA FILE
C
C
C  W(I),D(I)= WIDTH AND HEIGHT OF EACH STRINGER
C  V(I)= VERTICAL FORCE ONTOP OF EACH STRINGER
C  JP(I)= JOINT PROPERTY NO. OF EACH STRINGER
C          0 INDICATES 2 DIFFERENT JOINTS ALONG STR.(I)
C          1 " " 1 " " " " " "
C          2 " " 1 " " " " " (OTHER THAN 1)
C          3 " " 2 " " " " " (" " ")
C
C  OF(I)= FINAL OFFSET OF EACH STRINGER= DISTANCE FROM EDGE
C          THAT VERTICAL FORCE VECTOR ACTS AFTER SOME DEFORMATION
C          THIS DOES NOT AFFECT THE SHIFTING OF THE OFFSET WHICH
C          CHANGES WITH INCREASING X.
C
C
C
C  WRITE (6,70)
C 65  FORMAT(//,T10, 'WIDTH',T24, 'DEPTH',T34, 'J. P. ')
C 70  CONTINUE
C  READ (5,75)
C 75  FORMAT(//)
C  DO 80 I=1,NOSTR

```

```

85      READ (5,85) W(1),D(1),JP(1)
        FORMAT (2F10.3,15)
        IF (LEVEL.EQ.3)GO TO 80
        WRITE (6,90) W(1),D(1),JP(1)
90      FORMAT (1X,17,F7.2,121,F7.2,T30,15)
80      CONTINUE
C
C
C      AS THE DATA ENTERS THIS DO-LOOP, ONE OF THE NJT'S WILL BE
C      ASSIGNED FOR EACH NJP. THE ROTATION MOMENTS OF THE JOINTS
C      ARE COMPUTED BY MULTIPLYING XJTOP(I) AND XJBOT(I) WITH THE
C      FOLLOWING VALUES:
C
C      NJT=0  ONLY MAX. MOMENT KNOWN
C             RMXBI & RMXBB= MAX. MOM. JOINT CAN SUSTAIN
C
C      NJT=1  BILINEAR MOM. -THETA CURVE
C             BTOP & BBOT= INITIAL SLOPE OF MOM.-THETA CURVE
C             RMXBT & RMXBB= MAX. MOM. JOINT CAN SUSTAIN
C
C      NJT=2  TRILINEAR MOM. -THETA CURVE
C             ACRVT & ACRVB= INITIAL SLOPE OF MOM. -THETA CURVE
C             BCRVT & BCRVB= SLOPE OF SECOND LINE ON MOM. -THETA CURVE
C             RMXAT & RMXAB= MAX. MOM. OF ACRV.
C             RMXBT & RMXBB= MAX. MOM. OF BCRV.
C
C      NJT=3  POWER FUNCTION MOM. -THETA CURVE
C
C             MOM.= (ACRVT + ACRVB)*(THETA(RAD.))**(BCRVT OR BCRVB)
C             RMXAT & RMXAB= MAX. MOM. JOINT CAN SUSTAIN
C
C
C      READ (5,75)
      DO 155 I=1,NJP
        IF (LEVEL.EQ.3)GO TO 105
        WRITE(6,100)
100      FORMAT(//,T2,'NJT',T12,'Z1',T22,'Z2',T32,'Z3',T42,'Z4')
105      CONTINUE
        READ (5,110) NJT(I),Z1(I),Z2(I),Z3(I),Z4(I)
110      FORMAT (15,4F10.3)
        IF (LEVEL.EQ.3)GO TO 115
        WRITE (6,120) NJT(I),Z1(I),Z2(I),Z3(I),Z4(I)
120      FORMAT (1X,11,T7,F10.3,T17,F10.3,T27,F10.3,T37,F10.3)
115      CONTINUE
        IF (NJT(I).EQ.0) GO TO 125
        IF (NJT(I).EQ.2) GO TO 130
        IF (NJT(I).EQ.3) GO TO 135
        BTOP(I)=XJTOP(I)*Z1(I)
        BBOT(I)=XJBOT(I)*Z1(I)
        RMXBI(I)=XJTOP(I)*Z2(I)
        RMXBB(I)=XJBOT(I)*Z2(I)

```

```

IF (LEVEL.EQ.3)GO TO 140
WRITE (6,145)
145  FORMAT(1X,T10,'BTOP',T26,'BBOT',T42,'RMXT',T58,'RMXB')
WRITE(6,150) (1),BTOP(1),BBOT(1),RMXBT(1),RMXBB(1)
150  FORMAT(1X,I2,T7,F10.3,T23,F10.3,T39,F10.3,T55,F10.3)
140  CONTINUE
GO TO 155
130  ACRVT(1)= XJTOP(1)*Z1(1)
ACRVB(1)= XJBOT(1)*Z1(1)
BCRVT(1)= XJTOP(1)*Z2(1)
BCRVB(1)= XJBOT(1)*Z2(1)
RMXAT(1)= XJTOP(1)*Z3(1)
RMXAB(1)= XJBOT(1)*Z3(1)
RMXBT(1)= XJTOP(1)*Z4(1)
RMXBB(1)= XJBOT(1)*Z4(1)
IF (LEVEL.EQ.3)GO TO 160
WRITE(6,165)
165  FORMAT(1X,'(1)',T10,'ACRVT',T25,'BCRVT',T40,'RMXAT',T55,'RMXBT')
WRITE(6,170)(1),ACRVT(1),BCRVT(1),RMXAT(1),RMXBT(1)
170  FORMAT(1X,I1,T8,F10.3,T23,F10.3,T38,F10.3,T53,F10.3)
WRITE(6,175)
175  FORMAT(1X,T10,'ACRVB',T25,'BCRVB',T40,'RMXAB',T55,'RMXBB')
WRITE(6,170)(1),ACRVB(1),BCRVB(1),RMXAB(1),RMXBB(1)
160  CONTINUE
GO TO 155
C
135  ACRVT(1)= XJTOP(1)*Z1(1)
ACRVB(1)= XJBOT(1)*Z1(1)
BCRVT(1)= Z2(1)
BCRVB(1)= Z2(1)
RMXAT(1)= XJTOP(1)*Z3(1)
RMXAB(1)= XJBOT(1)*Z3(1)
IF (LEVEL.EQ.3)GO TO 155
WRITE(6,180)
180  FORMAT(1X,'(1)',T8,'ACRVT',T21,'BCRVT',T31,'RMXAT',T42,'ACRVB',T
* 4,'BCRVB',T66,'RMXAB')
WRITE (6,185)(1),ACRVT(1),BCRVT(1),RMXAT(1),ACRVB(1),BCRVB(1),
* RMXAB(1)
185  FORMAT(1X,I1,T4,F10.3,T16,F10.3,T27,F10.3,T38,F10.3,T49,F10.3,
* T62,F10.3)
GO TO 155
125  RMXBT(1)=XJTOP(1)*Z2(1)
RMXBB(1)=XJBOT(1)*Z2(1)
IF (LEVEL.EQ.3) GO TO 155
WRITE(6,190)
190  FORMAT (1X,T10,'RMXT',T20,'RMXB')
WRITE(6,195)(1),RMXBT(1),RMXBB(1)
195  FORMAT(1X,I2,T7,F10.3,T17,F10.3)
C
155  CONTINUE
C

```

```

C
C READ IN THE NUMBER AND DIMENSIONS OF THE UPPER DECKBOARDS
C TO COMPUTE THE AVERAGE MOE AND TOTAL MOMENT OF INERTIA
C
C
200 READ (5,200) NODKBD
   FORMAT(T30,12)
C
   LY=2
   LP=1
   IL=1
   EAVG=0.0
   ETOT=0.0
   TERTIA=0.0
   TOTDKS=0.0
   IF(LEVEL.EQ.3)GO TO 205
   WRITE (6,210)
210  FORMAT(//,14,'MOE',T20,'BASE',T30,'DEPTH',T45,'# OF BDS',T63
   *,'INERTIA')
205  CONTINUE
C
   READ (5,75)
   DO 215 I=1,NODKBD
220   READ (5,220)E(I),B1(I),D1(I),NOBDS(I)
      FORMAT (T4,F10.1,T32,F5.3,T50,F5.3,T70,12)
      ERTIA=0.0
      ERTIA=((B1(I)*(D1(I)**3))/12)*FLOAT(NOBDS(I))
      TERTIA=ERTIA+TERTIA
      ETOT=E(I)*FLOAT(NOBDS(I))+ETOT
      TOTDKS=TOTDKS+FLOAT(NOBDS(I))
      IF(LEVEL.EQ.3)GO TO 215
      WRITE (6,225) E(I),B1(I),D1(I),NOBDS(I),ERTIA
225  FORMAT (1X,F10.1,T20,F5.3,T30,F5.3,T49,12,T61,F10.5)
215  CONTINUE
C
   FAVG=ETOT/TOTDKS
   IF(LEVEL.EQ.3)GO TO 230
   WRITE(6,235) EAVG,TERTIA
235  FORMAT(//,'AVG. MOE= ',T11,F10.1,T22,'PSI',T30,'TOT. MOMENT OF INE
   *RTIA= ',F10.5,T67,'IN**3')
230  CONTINUE
C
C
C THE FOLLOWING ROUTINE BREAKS DOWN THE UNIT LOAD INTO CERTAIN
C PERCENTAGES, ACCORDING TO THE NUMBER OF STRINGERS, AND ALLOCATES
C THEM TO A STRINGER
C
C
240 READ (5,240)NOUNIT
   FORMAT(//,17X,12,/)

```

```

IF(LEVEL.EQ.3)GO TO 245
WRITE (6,250)NOUNIT
250  FORMAT(1X,'# OF LOAD CASES= ',T18,12)
245  CONTINUE
C
C
C   THIS DO-LOOP COMPUTES THE HMAX FOR VARIOUS UNIT LOADS
C
C
DO 255 IN=1,NOUNIT
  HMAX=0.0
  XM=0.0
  HLN(IN)=0.0
  Z(IN)=0.0
  Y(IN)=0.0
  RMOM1(IN)=0.0
  RMOM2(IN)=0.0
  RMAX1(IN)=0.0
  RMAX2(IN)=0.0
  RMX1(IN)=0.0
  RMXB(IN)=0.0
  JCT=0
  READ (5,260) UNIT,SPACE,DKL,OHG
260  FORMAT(4F10.2)
      IF(LEVEL.EQ.3)GO TO 265
      WRITE(6,270)IN,UNIT
270  FORMAT(/,'LOAD CASE # =',T14,12,T30,'UNIT LOAD= ',T42,F10.3)
      C
      WRITE(6,275)SPACE,DKL,OHG
275  *  FORMAT(1X,'SPACING =',T11,F5.2,T20,'DECK LENGTH =',T33,F5.2,
          T45,'OVERHANG =',T55,F5.2)
265  CONTINUE
C
C
C   COMPUTE THE AMOUNT OF UNIT LOAD DISTRIBUTED TO EACH STRINGER
C
C
M1= 0
M= 0
IF (NOSTR.EQ.3) GO TO 280
IF (NOSTR.EQ.2) GO TO 285
PB1=0.0
PB2=0.0
PB3=0.0
PB4=0.0
PB1=SPACE/DKL
PB2=PB1
PB3=((DKL-2*SPACE)/2)/DKL
PB4=PB3
M1= NOSTR/4
M=M1

```

```

DO 290 I=1,M
  V(I)= UNIT*PB1
290 CONTINUE
  M1=M+1
  M=M+M1
  DO 295 I=M1,M
    V(I)=UNIT*PB3
295 CONTINUE
    M1=M+1
    M=M+M1
    DO 300 I=M1,M
      V(I)=UNIT*PB4
300 CONTINUE
      M1=M+1
      M=M+M1
      DO 305 I=M1,M
        V(I)=UNIT*PB2
305 CONTINUE
        GO TO 310
280 M1=NOSTR/3
      M=M1
      DO 315 I=1,M
        V(I)=UNIT*0.25
315 CONTINUE
        M1=M+1
        M=M+M1
        DO 320 I=M1,M
          V(I)=UNIT*0.5
320 CONTINUE
          M1=M+1
          M=M+M1
          DO 325 I=M1,M
            V(I)=UNIT*0.25
325 CONTINUE
            GO TO 310
C
285 DO 330 I=1,2
      V(I)=0.5*UNIT
330 CONTINUE
C
310 CONTINUE
C
  IF (LEVEL.EQ.3)GO TO 335
  WRITE(6,340)DKL
340 FORMAT(/, 'DECKBOARD(S) LENGTH = ', F4.1, T28, ' IN. ')
  WRITE (6,345)
345 FORMAT(1X, 'STRINGER', T25, 'APPLIED LOAD')
  DO 335 I=1, NOSTR
    WRITE (6,350)I, V(I)
350 FORMAT(1X, T4, I2, T26, F10.3)
335 CONTINUE

```

C
C
C
C
C

VARIABLES FOR K-FACTOR REGRESSION EQUATIONS

X1=0.0
X5=0.0
X6=0.0
X7=0.0
X8=0.0
X10=0.0
IF (NOSTR.EQ.4) GO TO 355
X1=UNIT
X8=SPACE**3
X7=TERTIA*EAVG
X5=(W(1)+W(2)+W(3))/3.
X6=D(1)
GO TO 360

C
355

X1=UNIT
X8=((DKL-SPACE)/2)**3
X10=TERTIA*EAVG
X6=D(1)
X7=(W(1)+W(2)+W(3)+W(4))/4.

C
C
C
C
C
C
C

ESTABLISH INITIAL PARAMETERS..INCLUDING FRICTION RESISTANCE FOR
SINGLE-FACED PALLETS IN 'HINIT'

360

CONTINUE
FRICT= 0.55
H101= 0.00
HLAG= 0
HINIT= 0.00

C

IF (JOP.EQ.1) GO TO 365
DO 370 I=1,NOSTR
HINIT= HINIT + V(I)*W(I)/(2.0*D(I))

370

CONTINUE
GO TO 375

365

DO 380 I=1,NOSTR
HINIT= HINIT + V(I)*W(I)/(2.0*D(I))

380

CONTINUE

C

DO 385 I=1,NOSTR
HINIT= HINIT + FRICT*V(I)*VOF/(D(I)-VOF)

385

CONTINUE

C

375

CONTINUE

C
C
C
C
C
C

THIS SECTION PRODUCES A PICTURE OF THE PALLET DESIGN WITH
THE UNIT LOAD AND HINIT APPLIED

```
      IF (LEVEL.GT.0) GO TO 390
      WRITE (6,395) UNIT
395  *  FORMAT (/T50,'UNIT LOAD =',1X,F10.2,1X,'LBS'/T45,32(1H|)/T45,32(
      *  1HV))
      WRITE (6,400)HINIT
400  *  FORMAT (/,'INITIAL HORZ. FORCE =',1X,F7.1,1X,'LBS',T37,
      *  7(1H-),1)T45,32(1H*))
      IF (NOSTR.EQ.4) GO TO 405
      IF(NOSTR.EQ.2)GO TO 410
      WRITE(6,415)
415  *  FORMAT (T45,'*',T61,'*',T76,'*')
      WRITE(6,415)
      WRITE(6,415)
      GO TO 420
405  *  WRITE(6,425)
425  *  FORMAT(T45,'*',T55,'*',T66,'*',T76,'*')
      WRITE (6,425)
      WRITE (6,425)
      GO TO 420
410  *  CONTINUE
430  *  FORMAT(T45,'*',T76,'*')
      WRITE(6,430)
      WRITE (6,430)
420  *  IF (JOP.EQ.1)GO TO 435
      WRITE(6,440)
440  *  FORMAT(T45,32(1H*))
      GO TO 445
435  *  IF (NOSTR.EQ.4) GO TO 450
      IF(NOSTR.EQ.2) GO TO 455
      WRITE (6,415)
      GO TO 390
450  *  WRITE (6,425)
445  *  IF(NOSTR.EQ.3) GO TO 390
      WRITE (6,460)
460  *  FORMAT(T55,'|',T66,'|')
      WRITE (6,465)SPACE
465  *  FORMAT(T55,'SPACING = ',F5.2,T71,'IN.')
```

GO TO 390
C
C
C
C
C

COMPUTE VALUES AT EACH INCREMENT

```

390      X= 0.0
        PSI=0.0
        THETA = 0.0
        THETA2=0.0
        ALPHA=0.0
        ALPHA2=0.0
        PSI2=0.0
        MNUM=0
        NJPM=0
        ENICPT=0.0

C
C
C      IN THIS DO-LOOP HTOT IS COMPUTED AT EACH XINC
C
C
C      DO 470 J=1,NINC
        X= X+ XINC
        HTOT= 0.0

C
C
C      IN THIS DO-LOOP H IS COMPUTED FOR EACH STRINGER AT EACH XINC
C
C
C      DO 475 K=1,NOSTR
        R1=0.0
        R2=0.0
        YM=0.0
        PSI =(ATAN(D(K)/W(K)))*57.296
        HLN(K)=SQRT(D(K)**2+W(K)**2)
        Z(K)=W(K)-X
        YM=SQRT(HLN(K)**2-Z(K)**2)
        ALPHA=(ARSIN(YM/HLN(K)))*57.296
        THETA=ALPHA-PSI
        PSI2=90.0-PSI
        ALPHA2=90.0-ALPHA
        THETA2=PSI2-ALPHA2
        TN=0.0
        TN=W(K)-VOF*TAN(THETA2/57.296)
        IF (X.GE.TN)GO TO 485
        GO TO 480
485      Z(K)=W(K)-X
        YM=SQRT(HLN(K)**2-Z(K)**2)
        ALPHA=90.0+90.0-((ARSIN(YM/HLN(K)))*57.296)
        THETA=ALPHA-PSI
        THETA2=THETA
        ALPHA2=0.0
480      IF(JP(K).NE.0) GO TO 490
        MNUM=1
        NJPM=2
490      IF(JP(K).NE.1) GO TO 495
        MNUM=1

```

```

NJPM=1
495   IF (JP(K).NE.2) GO TO 500
      MNUM=2
      NJPM=2
500   IF (JP(K).NE.3) GO TO 505
      MNUM=3
      NJPM=4

C
C
C   IN THIS DO-LOOP THE TOTAL ROTATION MODULUS FOR THE TOP AND
C   BOTTOM JOINT ALONG A SIRINGER IS COMPUTED
C
505   DO 510 M=MNUM,NJPM
      THTCR1=0.0
      THTCR2=0.0
      ENTCPT=0.0
      THETCR=0.0
      IF (NJT(M).EQ.1)GO TO 515
      IF (NJT(M).EQ.3)GO TO 520
      THTCR1=(RMXAT(M)+RMXAB(M))*57.296/(ACRVT(M)+ACRVB(M))
      ENTCPT=(RMXAT(M)+RMXAB(M))/((BCRVT(M)+BCRVB(M))*
*      (THTCR1/57.296))
*      THTCR2=57.296*((RMXBT(M)+RMXBB(M))-ENTCPT)/(BCRVT(M)
      +BCRVB(M))
      GO TO 525
520   THETCR=((RMXAT(M)+RMXAB(M))/(ACRVT(M)+ACRVB(M)))
*      ** (1.0/(BCRVT(M)))*57.296
      GO TO 525
515   THETCR=(RMXBT(M)+RMXBB(M))*57.296/(BTOP(M)+BBOT(M))
525   IF (NJT(M).EQ.3)GO TO 530
      IF (NJT(M).EQ.1)GO TO 535
      IF (THETA.LE.THETCR1)GO TO 540
      IF (THETA.LE.THETCR2)GO TO 545
      RMOM1(M)=RMXBT(M)
      RMOM2(M)=RMXBB(M)
      GO TO 550
545   RMOM1(M)=(BCRVT(M)*THETA/57.296)+ENTCPT
      RMOM2(M)=(BCRVB(M)*THETA/57.296)+ENTCPT
      GO TO 550
540   RMOM1(M)=ACRVT(M)*THETA/57.296
      RMOM2(M)=ACRVB(M)*THETA/57.296
      GO TO 550
535   RMOM1(M)=BTOP(M)*THETA/57.296
      RMOM2(M)=BBOT(M)*THETA/57.296
      IF (THETA.GE.THETCR)RMOM1(M)=RMXBT(M)
      IF (THETA.GE.THETCR)RMOM2(M)=RMXBB(M)
      GO TO 550
530   RMOM1(M)=ACRVT(M)*(THETA/57.296)**BCRVT(M)
      RMOM2(M)=ACRVB(M)*(THETA/57.296)**BCRVB(M)
      IF (THETA.GE.THETCR)RMOM1(M)=RMXAT(M)

```

```

      IF (THETA.GE.THETCR)RMOM2(M)=RMXAB(M)
C
C
550      R1=R1+RMOM1(M)
      R2=R2+RMOM2(M)
      IF (LEVEL.GT.0) GO TO 510
      WRITE(6,555)R1,R2,(M)
555      IFORMAT(1X,2F10.3,T30,11)
510      CONTINUE
C
C
      RMAX1(K)=R1
      RMAX2(K)=R2
C
      IF (LEVEL.GT.0) GO TO 560
      WRITE (6,565)ALPHA,ALPIA2,PS12,YM,Z(K),THTCR1
565      FORMAT (1X,6F13.6)
      WRITE (6,565) THETCR,PS1,THETA,THETA2,ENCPT,THTCR2
      WRITE(6,570)RMAX1(K),RMAX2(K)
570      FORMAT(1X,2F15.3)
C
560      CA=0.0
      CR=0.0
      IF (NOSTR.EQ.2) GO TO 575
      IF (NOSTR.EQ.3) GO TO 580
C
C
C      FOUR STRINGER REGRESSION EQUATION
C
C
*      CA=0.13057599-0.00001176*X1+0.04938176*X10/X8-
      0.05689698*X7/X6-0.00002484*(RMXBT(1)+RMXBB(1))
      GO TO 585
C
C
C      THREE STRINGER REGRESSION EQUATION
C
C
580      CA=0.89561928+0.0003172*X1+0.00130390*X7/X8-1.60039455*X5/X6
*      +.00006912*(RMXBB(1)+RMXBT(1))
      GO TO 585
C
C
C      TWO STRINGER EQUATIONS
C
C
575      RY=0.0
      RW=0.0
      RY=((UNIT/(SPACE+2*OHG))*(SPACE**3))/(24*EAVG*TERTIA)
      RW=((UNI1/(SPACE+2*OHG))*OHG**2*SPACE)/(4*EAVG*TERTIA)
      ALPHA=ALPIIA/57.296

```

```

      CA=(ALPHA-RY+RW)/ALPHA
      CR=(ALPHA+RY-RW)/ALPHA
      IF (K.EQ.1) CUR=CA
      IF (K.EQ.2) CUR=CR
      IF (CUR.GT.1.0) CUR=1.0
      IF (CUR.LE.0.0) CUR=0.0
      HTOT=HTOT+((V(K)*(TN-X))+CUR*RMAX1(K)+RMAX2(K)-(.55*V(K)*VOF
*)
      ))/(YM-VOF)
      GO TO 475

C
C
585      IF (CA.GT.1.0) CA=1.0
      IF (CA.LE.0.0) CA=0.0
      HTOT=HTOT+((V(K)*(TN-X))+CA*(RMAX1(K)+RMAX2(K))-(.55*V(K)*VO
*)
      ))/(YM-VOF)

C
C
      IF (LEVEL.GT.0) GO TO 475
      WRITE(6,590)X,K,HTOT
590      FORMAT(1X,F6.4,I11,F21.3)
475      CONTINUE

C
C
C      IN THE NEXT 18 LINES HMAX, AND THE CORRESPONDING ROTATION MODULI
C      AND XINC ARE FILED
C
      HHS(J)= HTOT
      XS(J)= X
      IF (HTOT.LE.HMAX) GO TO 593
      HMAX= HTOT
      XH= X
      DO 600 L=1,NOSTR
          RMXT(L)=RMAX1(L)
          RMXB(L)=RMAX2(L)
600      CONTINUE
      GO TO 470
593      JCT= JCT+1
      IF (JCT.EQ.20) GO TO 595

C
C
470      CONTINUE

C
C      COMPUTE H/V RATIO
C
595      HII=0.0
      VII=0.0
      HII=HMAX/UNIT

C

```

```

C
C THIS SECTION PRODUCES A PICTURE WITH THE UNIT LOAD ON
C A DISPLACED PALLET. ALSO, THE H/V RATIO
C
C
        IF (LEVEL.EQ.3) GO TO 255
        WRITE (6,605) UNIT
605      FORMAT(/T41, 'UNIT LOAD =', 1X, F10.2, 1X, 'LBS'/T39, 32(1H|)/T39, 32(1
*      HV))
        WRITE (6,610) HMAX
610      FORMAT (/, T5, 'HMAX =', 1X, F7.1, 1X, 'LBS', 5X, 10(1H-), ')', T39, 32(1H*
*      ))
        IF (NOSTR.EQ.4) GO TO 615
        IF (NOSTR.EQ.2) GO TO 620
        WRITE (6,625)
625      FORMAT (T36, '*', T52, '*', T68, '*')
        GO TO 627
615      WRITE (6,630)
630      FORMAT (T36, '*', T46, '*', T58, '*', T68, '*')
        GO TO 627
620      WRITE(6,635)
635      FORMAT(1X, T36, '*', T68, '*')
        GO TO 627
627      IF (JOP.EQ.1) GO TO 650
        WRITE (6,640)
640      FORMAT (T33, 33(1H*))
        GO TO 645
650      IF (NOSTR.EQ.4) GO TO 655
        IF (NOSTR.EQ.2) GO TO 660
        WRITE (6,665)
665      FORMAT (T33, '*', T49, '*', T65, '*')
        GO TO 645
655      WRITE (6,670)
670      FORMAT (T33, '*', T43, '*', T55, '*', T65, '*')
        GO TO 645
660      WRITE(6,675)
675      FORMAT(1X, T33, '*', T65, '*')
        IF (NOSTR.NE.4) GO TO 645
        WRITE(6,680)
680      FORMAT(1X, T46, '|', T58, '|')
        WRITE(6,685) SPACE
685      FORMAT(146, 'SPACING =', F5.2, T71, 'IN')
645      WRITE (6,690)
690      FORMAT (165, '|', T70, '|')
        WRITE (6,695) XM
695      FORMAT (T67, 'XM =', 1X, F5.3, 1X, 'IN')
        WRITE (6,700) HU
700      FORMAT(1X, 'HMAX/UNIT = ', T14, F8.5)
C
C
C OUTPUT MOMENTS GENERATED ALONG EACH STRINGER

```

```

C
C
705 WRITE(6,705)
    FORMAT(//,'VALUES OF MOMENTS AT XMAX')
    IF (JOP.EQ.2) GO TO 710
    WRITE (6,715)
715 FORMAT (1X,15,'STRINGER #',T25,'TOP MOMENT')
    GO TO 720
710 WRITE (6,725)
725 FORMAT (1X,T5,'STRINGER #',T25,'TOP MOMENT',T45,'BOTTOM MOMENT')
    DO 730 I=1,NOSTR
        WRITE (6,735) (I),RMAX1(I),RMAX2(I)
735 FORMAT (1X,T10,I1,T25,F10.3,T45,F10.3)
730 CONTINUE
    GO TO 740
720 DO 745 I=1,NOSTR
        WRITE (6,750) (I),RMXT(I)
750 FORMAT (1X,T10,I1,T25,F10.3)
745 CONTINUE
740 CONTINUE

```

```

C
C
C
C
C

```

CALCULATION OF WORK UP TO HMAX. WORK IS THE AREA UNDER THE X-HTOT CURVE

```

755 WRITE(6,755)
    FORMAT(//,'VALUES OF WORK TOTAL UP TO XMAX')
    WRITE(6,760)
760 FORMAT(1X,T2,'XINC',T23,'WORK')
    XMAXN=0.0
    XR=0.0
    AREA1=0.0
    AREA2=0.0
    XR1=0.0
    AR1=0.0
    AR2=0.0
    AR3=0.0
    NMAX=(XM/XINC)+1
    XR=HS(1)-HINIT
    AREA1=(XR*XINC)/2
    AREA2=HINIT*XINC
    AR3=AREA1+AREA2

```

```

C

```

```

    DO 765 I=2,NMAX
        XR1=HS(I)-HS(I-1)
        AR1=(XR1*XINC)/2
        AR2=HS(I-1)*XINC
        AR3=AR1+AR2+AR3
    WRITE (6,770)XS(I),AR3
770 FORMAT (1X,F10.5,F20.3)

```

765 CONTINUE

C

255 CONTINUE

C

C

STOP

DEBUG UNIT(6), SUBCHK, SUBTRACE

END

B2 - Analog Models

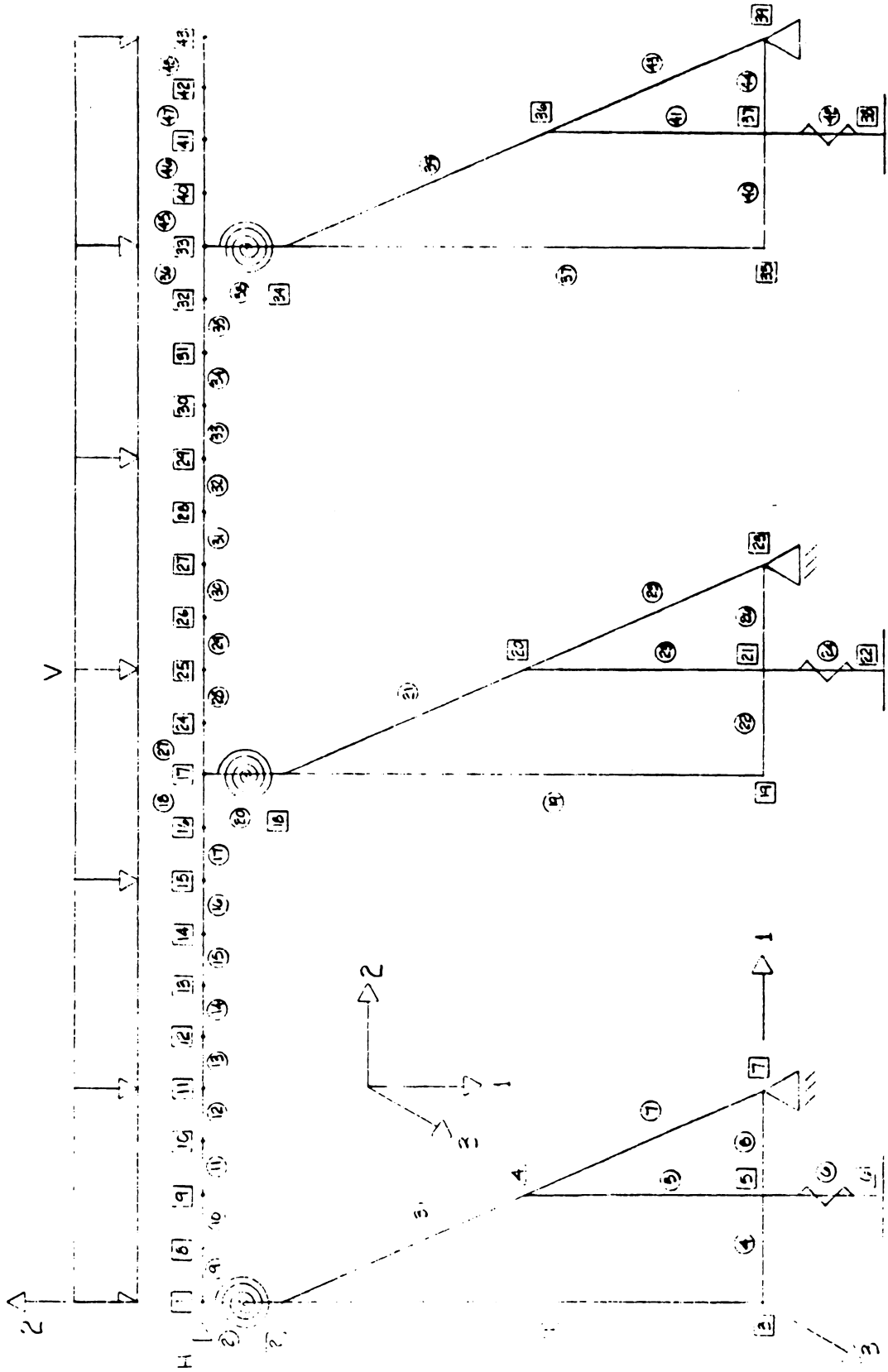


FIGURE B2.1 - Three Stringer Analog Model

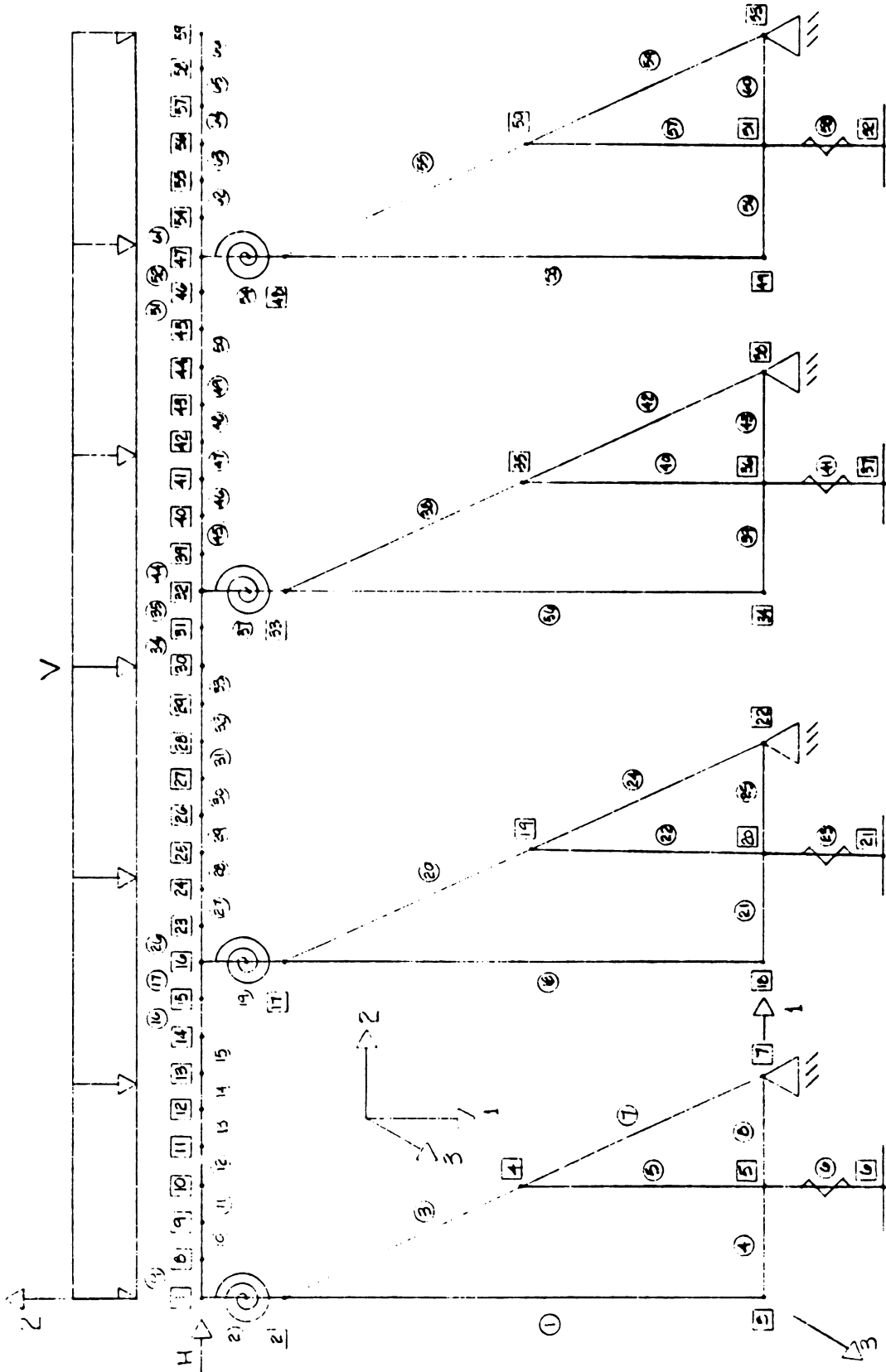


FIGURE B2.2 - Four Stringer Analog Model

B3 - Pallet Designs for Computer

Table B3.1. Three Stringer, Double-Faced Pallets
Designed for K-Factor Development

EI/L ³ (lb./in.)	Stringer Aspect Ratio (in./in.)	Joint Characteristics ¹	
		M _{max}	R
1675.0	0.27	100	1000
167.9	0.27	100	1000
9.9	0.27	100	1000
1675.0	0.43	100	1000
167.9	0.43	100	1000
9.9	0.43	100	1000
1675.0	0.58	100	1000
167.9	0.58	100	1000
9.9	0.58	100	1000
1675.0	0.27	250	5500
167.9	0.27	250	5500
9.9	0.27	250	5500
1675.0	0.43	250	5500
167.9	0.43	250	5500
9.9	0.43	250	5500
1675.0	0.58	250	5500
167.9	0.58	250	5500
9.9	0.58	250	5500
1675.0	0.27	400	10000
167.9	0.27	400	10000
9.9	0.27	400	10000
1675.0	0.43	400	10000
167.9	0.43	400	10000
9.9	0.43	400	10000
1675.0	0.58	400	10000
167.9	0.58	400	10000
9.9	0.58	400	10000

¹Characteristics given are 1. M_{max} (in.-lb.)
2. R (in.-lb./radian)

Table B3.2. Four Stringer, Double-Faced Pallets
Designed for K-Factor Development

EI/L ³ (lb./in.)	Stringer Aspect Ratio (in./in.)	Joint Characteristics ¹	
		M _{max}	R
631.0	0.27	100	1000
85.9	0.27	100	1000
6.6	0.27	100	1000
631.0	0.43	100	1000
85.9	0.43	100	1000
6.6	0.43	100	1000
631.0	0.58	100	1000
85.9	0.58	100	1000
6.6	0.58	100	1000
631.0	0.27	250	5500
85.9	0.27	250	5500
6.6	0.27	250	5500
631.0	0.43	250	5500
85.9	0.43	250	5500
6.6	0.43	250	5500
631.0	0.58	250	5500
85.9	0.58	250	5500
6.6	0.58	250	5500
631.0	0.27	400	10000
85.9	0.27	400	10000
6.6	0.27	400	10000
631.0	0.43	400	10000
85.9	0.43	400	10000
6.6	0.43	400	10000
631.0	0.58	400	10000
85.9	0.58	400	10000
6.6	0.58	400	10000

¹Characteristics given are 1. M_{max} (in.-lb.)
2. R (in.-lb./radian)

Table B3.3. Three Stringer, Single-Faced Pallets
Designed for K-Factor Development

EI/L ³ (lb./in.)	Stringer Aspect Ratio (in./in.)	Joint Characteristics ¹	
		M _{max}	R
1675.0	0.58	400	10000
1675.0	0.43	400	10000
1675.0	0.27	400	10000
1675.0	0.58	250	5500
1675.0	0.58	100	1000
167.9	0.43	400	10000
167.9	0.58	250	5500
9.9	0.58	250	10000

¹Characteristics given are 1. M_{max} (in.-lb.)
2. R (in.-lb./radian)

Table B3.4. Four Stringer, Single-Faced Pallets
Designed for K-Factor Development

EI/L ³ (lb./in.)	Stringer Aspect Ratio (in./in.)	Joint Characteristics ¹	
		M _{max}	R
631.0	0.58	400	10000
631.0	0.43	400	10000
631.0	0.27	400	10000
631.0	0.58	250	5500
631.0	0.58	100	1000
8.6	0.43	400	10000
8.6	0.58	250	5500
6.6	0.58	250	10000

¹Characteristics given are 1. M_{max} (in.-lb.)
2. R (in.-lb./radian)

APPENDIX C

- C1 - Fastener Patterns
- C2 - Construction Specifications and Unit Load for Type I Pallets
- C3 - Construction Specifications for Joint Rotation Samples
 - C3.1 - Specification of Joint Rotation Samples Fastened with Nails
 - C3.2 - Specification of Joint Rotation Samples Fastened with Staples
 - C3.3 - Specification of Joint Rotation Samples for Rate of Loading Study
- C4 - Upper Deckboard MOE by Pallet
- C5 - Construction Specifications and Unit Load for Type II Pallets
- C6 - Construction Specifications and Unit Load for Field Pallets

C1 - Fastener Patterns

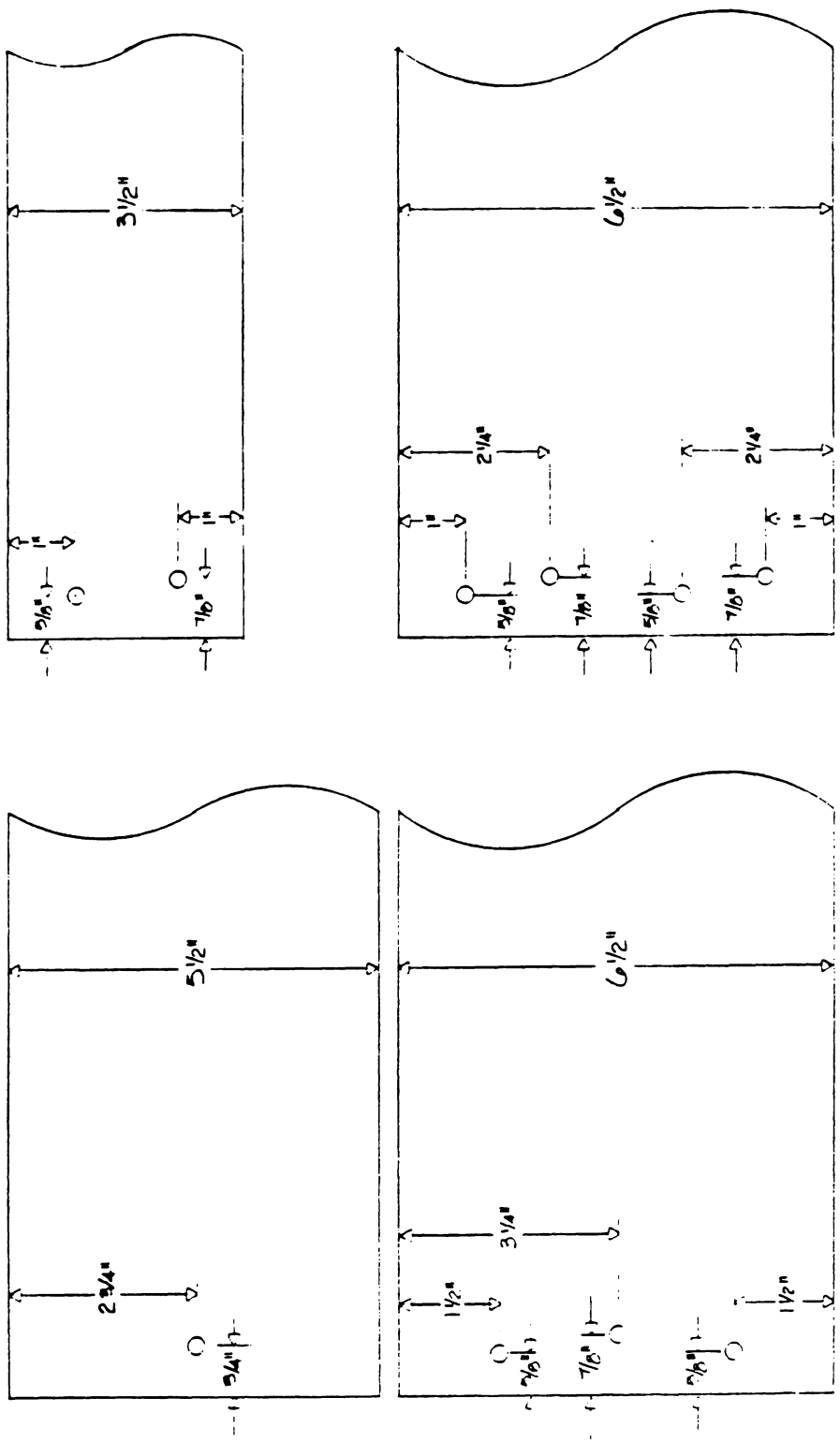


FIGURE C1.1 - Nail Patterns

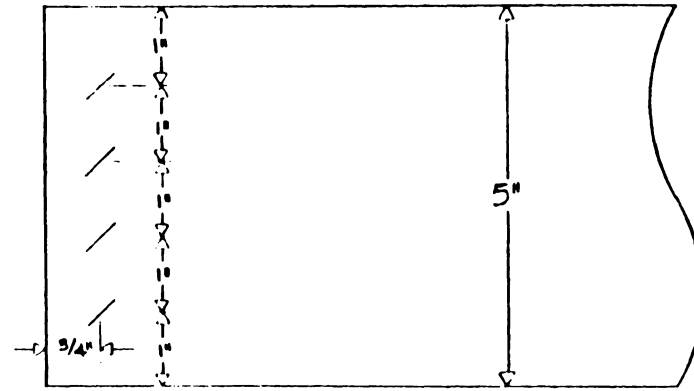
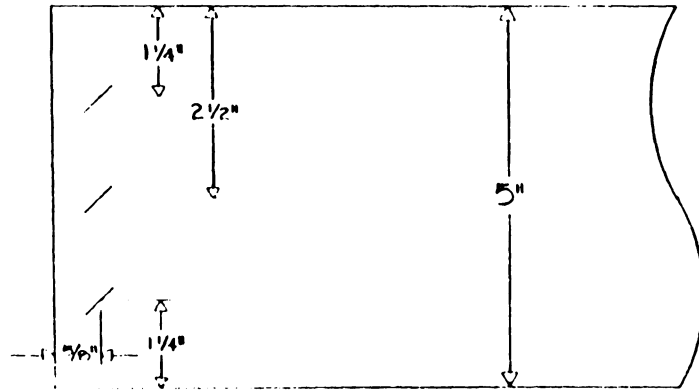
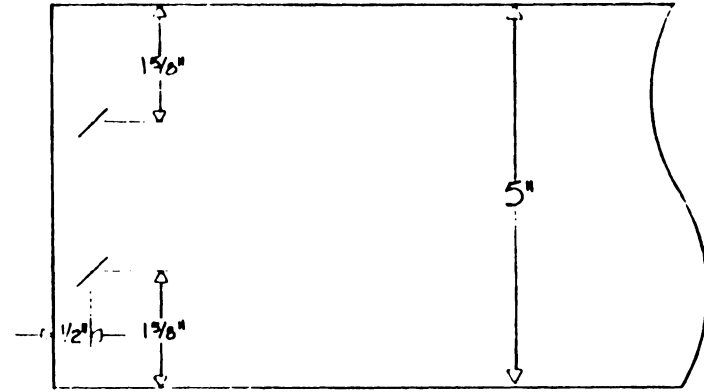
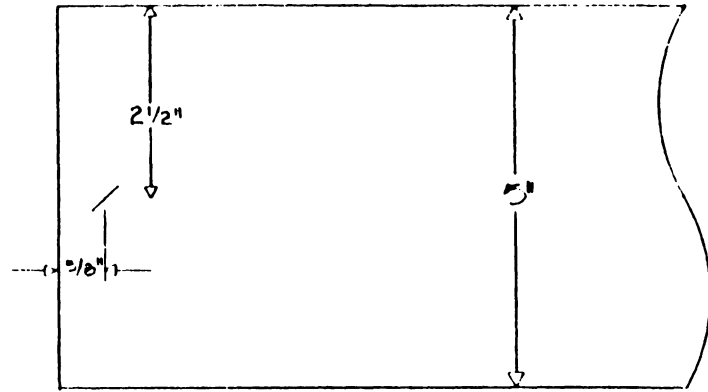


FIGURE C1.2 - Staple Patterns

C2 - Construction Specifications and Unit Load for Type I
Pallets

Table C2. Construction Specifications and Unit Loads Applied During Type I Testing

Pallet No. (1)	Size	Deckboards				Stringers			Fasteners		Unit Load (lbs)
		# Top	# Bot.	Width	Thickness	#	Width	Height	Type	#/Joint	
1	12 x 40	1	1	6.5	0.5	3	1.5	3.5	Nail	3	400
2	12 x 40	1	1	6.5	0.5	3	1.5	3.5	Nail	3	400
3	12 x 40	1	1	6.5	0.5	3	1.5	3.5	Nail	4	400
4	12 x 40	1	1	6.5	0.5	3	1.5	3.5	Nail	4	400
5	24 x 40	3	0	6.5	0.5	3	1.5	3.5	Nail	4	300
6	24 x 40	3	0	6.5	0.5	3	1.5	3.5	Nail	4	2000
7	24 x 40	3	2	6.5	0.5	3	1.5	3.5	Nail	3	700
8	24 x 40	3	2	6.5	0.5	3	1.5	3.5	Nail	3	750
9	24 x 40	3	2	6.5	0.5	3	1.5	3.5	Nail	4	1000
10	24 x 40	3	2	6.5	0.5	3	1.5	3.5	Nail	4	1000
11	40 x 40	3	3	6.5	0.5	3	1.5	3.5	Nail	3	2000
12	40 x 40	3	3	6.5	0.5	3	1.5	3.5	Nail	4	2000
13	40 x 48	9	0	6.5	0.5	3	1.5	3.5	Nail	4	5000

(1) All dimension in inches

C3 - Construction Specifications for Joint Rotation Samples

Table C3.1 Specifications of Joint Rotation Samples Fastened with Nails¹

Specimen No.	Deckboard		Stringer		Fastener	
	Width	Thickness	Width	Height	#	Type
1	6.5	0.5	1.5	3.5	4	Nail
2	6.5	0.5	1.5	3.5	4	Nail
3	6.5	0.5	1.5	3.5	4	Nail
4	6.5	0.5	1.5	3.5	3	Nail
5	6.5	0.5	1.5	3.5	3	Nail
6	6.5	0.5	1.5	3.5	3	Nail
7	3.5	0.375	1.5	3.5	2	Nail
8	3.5	0.375	1.5	3.5	2	Nail
9	3.5	0.375	1.5	3.5	2	Nail
10	5.5	0.5	1.5	3.5	1	Nail
11	5.5	0.5	1.5	3.5	1	Nail
12	5.5	0.5	1.5	3.5	1	Nail

¹ All dimensions in inches

Table C3.2 Specifications of Joint Rotation Samples Fastened with Staples¹

Specimen No.	Deckboard		Stringer		Fastener	
	Width	Thickness	Width	Height	#	Type
1	5.0	0.5	1.5	3.5	4	Staple
2	5.0	0.5	1.5	3.5	4	Staple
3	5.0	0.5	1.5	3.5	4	Staple
4	5.0	0.5	1.37	3.5	3	Staple
5	5.0	0.5	1.37	3.5	3	Staple
6	5.0	0.5	1.37	3.5	3	Staple
7	5.0	0.5	1.13	3.5	2	Staple
8	5.0	0.5	1.13	3.5	2	Staple
9	5.0	0.5	1.13	3.5	2	Staple
10	5.0	0.5	1.37	3.5	1	Staple
11	5.0	0.5	1.37	3.5	1	Staple
12	5.0	0.5	1.37	3.5	1	Staple

¹ All dimensions in inches

Table C3.3 Specifications of Joint Rotation Samples
For Rate of Loading Study¹

Specimen No.	Deckboard		Stringer		Fastener	
	Width	Thickness	Width	Height	#	Type
1	6.5	0.5	1.5	3.5	4	Nail
2	6.5	0.5	1.5	3.5	4	Nail
3	6.5	0.5	1.5	3.5	4	Nail
4	6.5	0.5	1.5	3.5	4	Nail
5	6.5	0.5	1.5	3.5	4	Nail
6	6.5	0.5	1.5	3.5	4	Nail
7	6.5	0.5	1.5	3.5	4	Nail
8	6.5	0.5	1.5	3.5	4	Nail
9	6.5	0.5	1.5	3.5	3	Nail
10	6.5	0.5	1.5	3.5	3	Nail
11	6.5	0.5	1.5	3.5	3	Nail
12	6.5	0.5	1.5	3.5	3	Nail
13	6.5	0.5	1.5	3.5	3	Nail
14	6.5	0.5	1.5	3.5	3	Nail
15	6.5	0.5	1.5	3.5	3	Nail
16	6.5	0.5	1.5	3.5	3	Nail
17	5.0	0.5	1.37	3.5	3	Staple
18	5.0	0.5	1.37	3.5	3	Staple
19	5.0	0.5	1.37	3.5	3	Staple
20	5.0	0.5	1.37	3.5	3	Staple
21	5.0	0.5	1.37	3.5	3	Staple
22	5.0	0.5	1.37	3.5	3	Staple
23	5.0	0.5	1.37	3.5	3	Staple
24	5.0	0.5	1.37	3.5	3	Staple
25	5.0	0.5	1.37	3.5	1	Staple
26	5.0	0.5	1.37	3.5	1	Staple
27	5.0	0.5	1.37	3.5	1	Staple
28	5.0	0.5	1.37	3.5	1	Staple
29	5.0	0.5	1.37	3.5	1	Staple
30	5.0	0.5	1.37	3.5	1	Staple
31	5.0	0.5	1.37	3.5	1	Staple
32	5.0	0.5	1.37	3.5	1	Staple

¹ All dimensions in inches

C4 - Upper Deckboard MOE by Pallet

Table C4. Upper Deckboard MOE by Pallet

Pallet No.	Species	MOE PSI $\times 10^6$	Average MOE PSI $\times 10^6$
1	Aspen	1.10	1.17
		1.14	
		1.15	
		1.18	
		1.16	
		1.28	
2	Aspen	1.34	1.33
		1.30	
		1.30	
		1.32	
		1.33	
		1.40	
3	Aspen	1.16	1.18
		1.16	
		1.17	
		1.18	
		1.18	
		1.22	
4	Aspen	1.20	1.23
		1.23	
		1.30	
		1.22	
5	Aspen	1.13	1.09
		1.05	
		0.98	
		0.99	
		1.10	
		1.10	
		1.04	
		1.35	
6	Aspen	0.98	0.99
		0.99	
		0.98	
		0.99	

Table C4. Upper Deckboard MOE by Pallet, Continued

Pallet No.	Species	MOE PSI $\times 10^6$	Average MOE PSI $\times 10^6$
7	Oak	0.93	0.94
		0.94	
		0.94	
		0.94	
8	Aspen	0.95	0.97
		1.03	
		0.97	
		0.93	
9	Aspen	1.31	1.37
		1.38	
		1.40	
		1.36	
		1.39	
		1.37	
		1.41	
10	Oak	1.45	1.47
		1.48	
		1.50	
		1.46	
		1.43	
		1.50	
11	Oak	1.00	0.98
		0.96	
		0.99	
		0.98	
		0.98	
		0.98	
12	Oak	1.53	1.55
		1.56	
		1.60	
		1.54	
		1.55	
		1.53	
		1.53	
		1.52	

Table C4. Upper Deckboard MOE by Pallet, Continued

Pallet No.	Species	MOE PSI $\times 10^6$	Average MOE PSI $\times 10^6$
13	Oak	1.58	1.48
		1.41	
		1.48	
		1.50	
		1.41	
		1.49	
14	Aspen	1.23	1.26
		1.28	
		1.18	
		1.31	
		1.26	
		1.29	
15	Oak	1.40	1.39
		1.41	
		1.37	
		1.39	
		1.37	
		1.39	
16	Oak	1.36	1.38
		1.40	
		1.38	
		1.33	
		1.33	
		1.31	
		1.41	
		1.51	
17	Oak	1.06	1.10
		1.10	
		1.07	
		1.10	
		1.15	
18	Oak	1.20	1.24
		1.25	
		1.24	
		1.23	
		1.27	

C5 - Construction Specifications and Unit Load for Type II
Pallets

Table C5. Construction Specifications and Unit Loads Applied During Type II Testing

Pallet No. (1)	Size	Deckboards				Stringers			Fasteners		Unit Load (lbs)
		# Top	# Bot.	Width	Thickness	#	Width	Height	Type	#/Joint	
1	48 x 48	4	0	3.50	0.375	4	1.13	3.75	Staple	2	2600
2	36 x 36	6	0	3.50	0.375	2	1.50	3.50	Staple	4	1000
3	36 x 36	6	0	5.50	0.875	2	1.50	3.50	Staple	4	1000
4	36 x 36	4	0	3.50	0.500	2	1.25	3.75	Nail	1	3000
5	40 x 40	4	3	3.50	0.300	4	1.37	3.63	Staple	3	2800
6	48 x 48	6	0	3.30	0.375	3	1.00	3.75	Nail	1	2400
7	40 x 40	4	3	3.50	0.300	4	1.20	3.63	Staple	3	2800
8	40 x 48	5	3	3.95	0.375	4	1.20	3.50	Nail	1	1850
9	40 x 40	7	0	4.84	0.500	2	1.50	3.63	Staple	3	4000
10	40 x 48	5	3	3.50	0.375	4	1.50	3.60	Nail	1	1850
11	40 x 40	7	0	5.00	0.500	2	1.50	3.63	Staple	4	4000
12	48 x 40	8	0	5.50	0.500	3	1.38	3.75	Staple	1	5000
13	48 x 40	6	3	5.03	0.500	3	1.13	3.75	Staple	3	4800
14	36 x 36	6	6	5.50	0.500	2	1.75	3.38	Nail	1	1125
15	40 x 40	6	3	5.00	0.500	3	1.37	3.75	Staple	3	4800
16	40 x 48	6	0	3.50	0.375	3	1.00	3.75	Nail	2	2400
17	48 x 40	8	0	5.50	0.500	3	1.75	3.00	Nail	1	1500
18	48 x 36	8	0	6.00	0.875	4	1.75	3.00	Nail	1	1700

(1) All dimensions in inches

C6 - Construction Specifications and Unit Load for Field
Pallets

Table C6. Specifications of Designs Found During Field Survey

Pallet No. (1,2)	Size	Deckboards				Stringers			Fasteners	Unit Load (lbs)	
		# Top	# Bot.	Width	Thickness	#	Width	Height			
1	42 x 42	5	0	3.5	0.75	3	1.5	3.5	Type Length Wire Dia- meter MIBANT Angle # Top # Bottom	Staple 2.5" 0.07" 70 degr. 30 0	3000
2	48 x 40	6	3	3.5	0.375	3	1.06	3.75	Type Length Wire Dia- meter MIBANT Angle # Top # Bottom	Staple 1.5" 0.07" 70 degr. 36 18	1200
3	48 x 40	1 2 2 1	0 0 0 0	8.25 6.25 6.125 5.875	0.875 0.875 0.875 0.875	2 1	1.375 1.4375	3.5 3.5	Type Length Wire Dia- meter MIBANT Angle # Top # Bottom	Nail 2.25" 0.098" 89 degr. 60 0	600 - 2500

(1) Includes all available information
(2) All dimensions in inches

Table C6. Specifications of Designs Found During Field Survey (continued)

Pallet No. (1,2)	Size	Deckboards				Stringers			Fasteners	Unit Load (lbs)
		# Top	# Bot.	Width	Thickness	#	Width	Height		
4	52 x 36	3	0	4.75	0.875	2	1.375	3.625	Type Nail Length 2.25" Wire Dia- meter 0.098" MIBANT Angle 89 degr. # Top 60 # Bottom 0	600 - 2500
		6	0	4.0	0.875	1	1.4375	3.625		
5	35 x 42	5	3	3.5	0.50	3	1.5	3.5	Type Nail Length 1.75" Wire Dia- meter 0.099" MIBANT Angle 75 degr. # Top 30 # Bottom 18	1000

(1) Includes all available information
(2) All dimensions in inches

APPENDIX D

D1 - Result of Joint Rotation Tests

D1.1 - Test Results of Joint Rotation Samples for Nails

D1.2 - Test Results of Joint Rotation Samples for
Staples

D1.3 - Test Results of Joint Rotation Samples for Rate
of Loading Study

D2 - Regression Equations for Individual Joints

D2.1 - K-factor Regression Equations and Corresponding
R-Square Values for 3 Stringer Single-faced
Pallets

D2.2 - K-factor Regression Equations and Corresponding
R-Square Values for 3 Stringer Double-faced
Pallets

D2.3 - K-factor Regression Equations and Corresponding
R-Square Values for 4 Stringer Single-faced
Pallets

D2.4 - K-factor Regression Equations and Corresponding
R-Square Values for 4 Stringer Double-faced
Pallets

D1 - Result of Joint Rotation Tests

Table D1.1 Test Results of Joint Rotation Samples for Nails

Joint No.	Deckboard		Stringer		Rotation Modulus (in-lb/radian)	Mmax Actual (in-lb)	Mmax Predicted (in-lb)
	MC (%)	G	MC (%)	G			
1	31	.71	31	.69	4650	660	643
2	28	.69	30	.66	5575	785	543
3	30	.65	30	.63	4775	655	543
4	31	.63	32	.64	4870	555	350
5	30	.63	29	.61	5210	630	350
6	30	.62	33	.65	4920	765	420
7	33	.69	34	.63	9870	343	378
8	36	.63	35	.62	11210	515	295
9	34	.64	34	.64	8900	342	284
10	32	.64	30	.60	4995	175	260
11	32	.67	37	.65	6210	248	247
12	35	.66	36	.66	5295	327	263

Table D1.2 Test Results of Joint Rotation Samples for Staples

Joint No.	Deckboard		Stringer		Rotation Modulus (in-lb/radian)	Mmax Actual (in-lb)	Mmax Predicted (in-lb)
	MC (%)	G	MC (%)	G			
1	31	.38	11	.41	2704	256	187
2	37	.32	12	.34	2910	210	218
3	30	.35	13	.39	2790	197	133
4	40	.30	12	.42	1874	125	117
5	40	.36	13	.36	2190	165	186
6	32	.31	11	.38	1936	175	210
7	36	.40	12	.40	845	64	52
8	40	.30	12	.42	1250	92	117
9	30	.35	13	.39	905	144	133
10	40	.35	16	.37	2400	45	61
11	44	.38	14	.43	2505	83	50
12	41	.41	15	.35	2465	67	58

Table D1.3 Test Results of Joint Rotation Samples for Rate of Loading Study

Joint No.	Deckboard		Stringer		Rotation Modulus (in-lb/radian)	Mmax Actual (in-lb)	Mmax Predicted (in-lb)
	MC (%)	G	MC (%)	G			
1	45	.68	12	.53	5526	335	
2	40	.66	14	.52	2812	290	
3	43	.62	11	.41	2889	325	
4	41	.66	13	.47	1461	210	
5	45	.71	15	.50	2571	225	184
6	40	.64	11	.62	2629	230	200
7	49	.69	9	.67	2423	265	213
8	43	.81	11	.45	1455	215	171
9	29	.65	35	.47	2586	300	
10	37	.64	27	.63	1448	230	
11	29	.62	34	.41	1395	225	
12	29	.69	29	.37	2393	255	
13	26	.72	27	.48	3556	215	101
14	28	.68	31	.47	2079	190	80
15	32	.76	33	.81	2305	170	128
16	33	.69	37	.78	1722	170	122
17	20	.72	26	.69	1849	182	
18	24	.54	23	.78	1280	160	
19	32	.69	25	.48	1280	180	
20	33	.48	23	.64	1517	161	
21	22	.64	25	.40	2647	156	84
22	25	.74	21	.56	3122	152	102
23	33	.74	22	.42	2057	160	87
24	32	.78	21	.54	1982	128	122
25	37	.66	17	.66	545	198	
26	38	.77	17	.66	520	240	
27	39	.59	19	.35	558	240	
28	35	.79	16	.60	525	243	
29	35	.57	18	.56	816	203	104
30	41	.78	15	.66	837	196	115
31	35	.64	18	.54	796	178	103
32	38	.63	15	.76	767	155	127

D2 - Regression Equations for Individual Joints

TABLE D2.1. K-Factor Regression Equations and Corresponding R-Square Values for 3 Stringer Single-Faced Pallets

K-Factor Equations (1)	R-Square
$Ks31 = 5.68635132 - 0.00002889(V) - 0.00009837(L^3) - 0.00000072(E) + 0.17502467(I) - 0.39947025(W) - 0.79014411(D) - 0.00018179(M)$	0.738
$Ks32 = 5.66669504 - 0.00002389(V) - 0.00010992(L^3) - 0.00000067(E) - 0.41079192(W) - 0.77619802(D) - 0.00014175(M)$	0.848
$Ks33 = 250.7705817 - 0.0008093(V) + 0.0000383(E) - 16.4948666(I) - 55.7927888(W) - 58.8150714(D) - 0.0065595(M)$	0.762

(1) Symbol Definition:

- L = clear span distance between stringers
- V = unit load
- E = MOE of top deckboards
- I = moment of inertia of top deckboards combined
- W = average width of stringers
- D = stringer height
- M = average total Mmax along one stringer

TABLE D2.2. K-Factor Regression Equations and Corresponding R-Square Values for 3 Stringer Double-Faced Pallets

K-Factor Equations (1)	R-Square
$Ks31 = 2.43228515 - 0.00006528(L^3) - 0.0000011(E) + 0.7814489(I) - 0.21001454(W) - 0.00004962(M)$	0.783
$Ks32 = 61.24254207 + 0.00172063(V) - 0.00067536(L^3) - 0.0000115(E) + 1.37425331(I) - 11.73232568(W) - 9.31846199(D) + 0.00115825(M)$	0.702
$Ks33 = 4.07106448 - 0.00008382(L^3) - 0.00000046(E) + 0.33723721(I) - 0.89071147(W) - 0.29950822(D) - 0.00005554(M)$	0.212
$Ks34 = -5.93345235 + 0.00001408(V) + 0.00009903(L^3) + 0.00000148(E) - 1.06035888(I) + 1.06580506(W) + 0.40450276(D) + 0.00009852(M)$	0.656
$Ks35 = 197.9453275 - 0.0011024(V) - 0.0005403(L^3) - 0.0000144(E) + 14.4007571(I) - 19.5586775(W) - 39.9635269(D) - 0.0031941(M)$	0.693
$Ks36 = -2.61288313 + 0.00004959(L^3) + 0.00000035(E) - 0.26715823(I) + 0.5579279(W) + 0.19528509(D) + 0.00004583(M)$	0.060

(1) Symbol Definition:

- L = clear span distance between stringers
- V = unit load
- E = MOE of top deckboards
- I = moment of inertia of top deckboards combined
- W = average width of stringers
- D = stringer height
- M = average total Mmax along one stringer

TABLE D2.3. K-Factor Regression Equations and Corresponding R-Square Values for 4 Stringer Single-Faced Pallets

K-Factor Equations (1)	R-Square
$Ks41 = 5.0032253 - 1.20504034(D) - 0.52384469(W) - 0.00196144(L^3) + 0.00000022(E)(I) - 0.00035932(M)$	0.953
$Ks42 = 15.10242161 - 3.14771579(D) - 2.50884051(W) + 0.00184796(L^3) - 0.00000036(E)(I) - 0.00042289(M)$	0.904
$Ks43 = 10.5117218 - 2.32754501(D) - 1.20354758(W) + 0.00167631(L^3) + 0.00000022(E)(I) - 0.00058701(M)$	0.935
$Ks44 = -80.50777616 + 14.71527213(D) + 22.43734744(W) + 0.00105292(L^3) - 0.00000017(E)(I) - 0.0013589(M)$	0.748

(1) Symbol Definition:

- L = clear span distance between the outer and its adjacent stringer
- V = unit load
- E = MOE of top deckboards
- I = moment of inertia of top deckboards combined
- W = average width of stringers
- D = stringer height
- M = average total Mmax along one stringer

TABLE D2.4. K-Factor Regression Equations and Corresponding R-Square Values for 4 Stringer Double-Faced Pallets

K-Factor Equations (1)	R-Square
$Ks41 = 1.4137509 - 0.32359308(D) - 0.6602909(W) + 0.00221648(L^3) - 0.00004882(M)$	0.782
$Ks42 = 0.44967133 - 0.0006568(V) - 5.41929666(D) + 0.04637274(L^3) + 0.00000912(E)(I)$	0.302
$Ks43 = -1.14055642 - 0.0000537(V) + 0.35941114(W) - 0.00156753(L^3) + 0.00000023(E)(I) - 0.00001479(M)$	0.780
$Ks44 = -2.86183775 + 0.3980167(D) + 1.07234489(W) - 0.00086422(L^3) - 0.0000006(E)(I) + 0.00006394(M)$	0.320
$Ks45 = -2.51106256 + 0.30114723(D) + 1.37424857(W) - 0.00170584(L^3) - 0.00000013(E)(I) + 0.00009622(M)$	0.693
$Ks46 = -16.50237272 + 0.0001487(V) + 5.72319906(W) + 0.01554779(L^3) + 0.00000271(E)(I)$	0.584
$Ks47 = 32.96264373 - 8.50611181(D) - 2.76068946(W) + 0.00224858(L^3) + 0.00000028(E)(I) - 0.00056211(M)$	0.732
$Ks48 = 4.55671798 - 0.93221829(D) - 1.05516907(W) + 0.00140221(L^3) + 0.0000007(E)(I) - 0.0001293(M)$	0.486

(1) Symbol Definition:

L = clear span distance between the outer and its adjacent stringer
V = unit load
E = MOE of top deckboards
I = moment of inertia of top deckboards combined
W = average width of stringers
D = stringer height
M = average total Mmax along one stringer

**The vita has been removed from
the scanned document**